Far-Infrared and Infrared Spectroscopy of Transient Molecules of Astronomical Interest

Thesis for the Degree of Doctor of Science
Submitted to Department of Astronomical Science,
School of Mathematical and Physical Science,
The Graduate University for Advance Studies

by Isamu Morino

in 1995

CONTENTS

Chapter 1. Introduction

1 - 1. Interstellar Molecules

The first molecules discovered in interstellar space were the diatomic radicals CH and CN, and the positive ion CH^+. These molecules were detected with optical absorption observations in diffuse clouds (Dunham and Adams, 1937; Swings and Rosefeld, 1937; Douglas and Herzberg, 1941).

In 1960's many interstellar molecules have been found with the radioastronomical observations in wide frequency range: OH (Weinreb *et al.* 1963), NH_3 (Cheung *et al.* 1968), H_2O (Cheung *et al.* 1969), H_2CO (Palmer *et al.* 1969), CO (Wilson, Jefferts, and Penzias, 1970), and so on. These identifications are mainly based on measurements in laboratory, especially by microwave spectroscopic techniques developed from 1950's. Recently, many transient molecules such as radicals and ions and metal-bearing molecules are studied in laboratory and detected in interstellar space. In total, more than 100 molecules have been discovered in interstellar space through observations in various wave length regions, as listed in Table 1 - 1. In radio region, most of lines are observed as emission, and some are observed as absorption of background radiation. These molecules have been detected in several different regions in interstellar space: HII regions in which H atom is ionized, diffuse molecular clouds, dense cold dark clouds such as Taurus Molecular Cloud-1 (TMC-1), star-forming regions such as Orion Molecular Cloud-1 (OMC-1) and Sagittarius B2 (Sgr B2) and circumstellar envelopes of late type stars such as IRC+10216.

The discovery of many interstellar molecules expands a new field of chemistry and physics in interstellar space. Existence of molecular species in interstellar space indicates that various chemical processes occur in extreme physical conditions of temperature and density and in long time scale. These condition and time scale are very different from the

terrestrial condition. The molecules are used as probe of physical conditions of interstellar space. In radio astronomical observations of spectral lines, the velocity shifts provide information about motion of object. Observed line intensities of molecules such as NH_3 are used for estimation of temperature of interstellar objects. Distributions of molecules such as CO are used as density prove of interstellar matter using an empirical conversion factor with respect to H_2.

1 - 2. Formation Mechanism of Interstellar Molecules

The chemistry in interstellar space is studied by molecular spectral line observations in radiofrequency region. It is found that the chemical reactions in interstellar space are very different from those under the terrestrial conditions in the points of density and temperature. Rapid exothermic and two body reactions are thought to be important for molecular formation, and cosmic ray and ultra-violet ionization processes are also considered. Ion-molecules reactions and neutral-neutral reactions with no activation energy barriers are proposed in gas phase. The gas phase rate coefficients measured in laboratory are summarized, for example, by Huntress (1977). Suzuki (1979) constructed a chemical network including 2884 gas-phase reactions, and calculated the time dependent abundances of 234 molecules up to 10^9 yr in dark cloud with conditions of $n(H) = 10^5$ cm^{-3}, T = 30 K. The gas-phase chemical model calculation including about 600 reactions has been carried out by Herbst and Leung (1989) to predict abundances of observed complex molecules in dense interstellar clouds with $n(H_2) = 2 \times 10^3$ cm^{-3}, T = 10 K, and $\tau_V = 500$ at 10^5 yr. Millar *et al.* (1991) compiled the rate coefficients of 2880 gas-phase reactions among 313 molecules and calculated fractional abundances with respect to H_2 abundances at early time (3.162×10^5 yr) and steady state (10^8 yr) in dark cloud with $n(H_2) = 10^4$ cm^{-3}, T = 10 K and Av = 10 mag. These model calculations explained abundances of observed simple molecules.

However, there are several observational results which are not explained by gas-phase reactions, such as radiative association reactions, ion-molecule reactions,

dissociateve recombination reactions, and neutral-neutral reactions. Other processes such as grain surface reactions, high temperature reaction induced by shock wave seem to have important roles in some molecular synthesis.

Dust grain process was included in chemical model calculations by Hasegawa and Herbst (1993). They calculated the abundance of molecules with three phase model, that is, gas, grain surface and mantle in dense interstellar clouds with $n(H + H_2) = 2 \times 10^4$ cm^{-3} and T = 10 K at 10^6 yr. Dust mantle is made of core with main composition of silicon compounds, and solid H_2O, CO, CH_4 and so on. The surface reactions have important roles for formation of the H_2 molecule and other molecules which are evaporated from surface by ultra-violet radiation and/or shock wave. However, Hasegawa and Herbst (1993) did not include surface reaction and the effect of sock wave explicitly, and the dust was considered as a reservoir of molecules produced in gas phase. Some observed abundances are not explained.

Although some molecules such as hydrides is very important to understand chemistry in interstellar space, it have not been detected in radio astronomical observation, because they have rotational transitions in submillimeter wave and far-infrared regions. Observations in these regions are limited because of atmospheric absorption and technical problems, but observation techniques in these regions are greatly developing recently. Spectroscopic data of hydrides are limited in laboratory. In the later Sections, some examples of interstellar chemistry are described.

1 - 3. Hydrogen Sulfide Chemistry

Hydrogen sulfide (H_2S) in interstellar space was first detected via the rotational transition 1_{10} - 1_{01} (168.763 GHz) toward several giant molecular clouds(GMCs) by Thaddeus *et al.* (1972). Dickel, Dickel, and Wilson (1981) observed the same transition using the NRAO 11 m radio telescope toward the OMC-1, DR21, W51, W3, NGC 2264, NGC 7358, and Sgr B2. Recently, Minh, Irvine, and Ziurys (1989), and Minh *et al.* (1990, 1991) have carried out new observations toward cold dark clouds, L134N and

TMC-1, and star forming region, OMC-1, Sgr B2, W3, W49, and W51 using the FCRAO 14 m telescope. They determined the fractional abundance of H_2S relative to H_2 to be $f(H_2S) \sim 10^{-9}$ toward the dark clouds. On other hand, they found the abundance of $f(H_2S) \sim 10^{-6}$ toward Orion-KL which was factor 1000 larger than those in dark clouds. It is suggested that these differences in H_2S abundance are caused by formation mechanisms of H_2S, that is, in star forming region the abundance may increase by grain related process. In order to clarify the reason more clearly, the author proposes the search for the SH radical.

Both S and S^+ do not react with H_2 in usual interstellar condition, which is much different from the case of O and O^+. That is, the following reactions,

$$S^+ + H_2 \rightarrow SH^+ + H + 0.87 \text{ eV}, \quad (1)$$

$$SH^+ + H_2 \rightarrow SH_2^+ + H + 0.6 \text{ eV}, \quad (2)$$

$$SH_2^+ + H_2 \rightarrow SH_3^+ + H + 0.35 \text{ eV}, \quad (3)$$

are all endothermic (Adams, Smith, and Millar, 1984), and do not occur in normal interstellar conditions. In gas phase the H_2S formation in quiescent clouds is thought to be due to the following reaction (Prasad and Huntress, 1982),

$$S + H_3^+ \rightarrow SH^+ + H_2 - 2.4 \text{ eV}, \quad (4)$$

$$SH^+ + H_2 \rightarrow SH_3^+ + h\nu, \quad (5)$$

$$SH_3^+ + e^- \rightarrow H_2S + H, \quad (6a)$$

$$SH + H_2, \quad (6b)$$

Reaction (4) is exoergic ion-molecule reaction, reaction (5) radiative association reaction, and reactions (6a) and (6b) dissociative recombination reactions, which produce SH and H_2S with a branching ratio of 0.5. In reaction (4), H_3^+ is formed from reaction H_2^+ with H_2 as follows,

$$H_2^+ + H_2 \rightarrow H_3^+ + H, \quad (7)$$

and H_2^+ is produced by cosmic ray ionization process, as follows,

$$H_2 + \text{cosmic ray} \rightarrow H_2^+ + e^- + \text{cosmic ray}. \quad (8)$$

Other reactions are omitted in this case due to small contribution.

On the other hand, it is proposed that H_2S may be produced by dust surface reaction, and evaporated from grain surface to gas phase by shock wave from young star. Tielens and Hagen (1982) proposed the following reactions:

$$H + S \rightarrow HS, \quad (9)$$

$$HS + H \rightarrow H_2S, \quad (10)$$

$$H_2S + H \rightarrow HS + H_2, \quad (11)$$

where reaction (11) has an activation energy barrier of approximately 900 K. Figure 1 - 1 shows SH_n production mechanism.

It is assumed that H_2S formation in quiescent clouds such as TMC-1 is due to only gas phase process, and in star-forming region such as OMC-1 dust grain process seems to give larger contribution for H_2S production than gas phase process. The above assumptions are only qualitative explanation. If H_2S and SH are produced by gas-phase reactions, only H_2S observation may not be enough for the understanding of the formation mechanism.

The chemical network calculations including gas, grain surface, and grain mantle processes by Hasegawa and Herbst (1993) predict the almost same abundances of H_2S and SH in gas phase and the [SH]/[H_2S] ratio ~ 10^{-5} in grain surface, where the fractional abundances of H_2S and SH relative H_2 at 10^5 yr are estimated to be 7.0×10^{-10} and 5.6×10^{-15}, respectively. If evaporation of a large quantity of H_2S from grain surface by the effect of shock wave is included in their calculation, the predicted abundance of H_2S may agree with the observational one in OMC-1.

The SH radical is thought to be produced with the same branching ratio as H_2S in gas-phase reaction. If SH is detected, it proves the gas-phase reactions, and if not detected, H_2S is mainly coming from grain surface.

The SH radical is one of the most simple sulfur-bearing molecules, but still not detected. Searches of SH using the Λ-type doubling transitions (111 MHz) were carried out by Meeks, Gordon and Litvak (1969), and Heiles and Turner (1971) using the 1000-ft Arecibo antenna. The detection limit on T_A^* was 27 K toward W49. The upper limit of the column density was estimated to be 5.6×10^{12} cm^{-2} where the abundance ratio

[S]/[O] of 1/40 and the column density of OH of 2.2 x 10^{14} cm^{-2} were used. The reasons of non detection may be due to the weak line strength and small beam filling factor (beam width of about 50 arc min). The searches using the rotational transitions in the submillimeter wave region are more suitable, because of the large transition moment. However, submillimeter wave and far-infrared frequencies of SH have not been measured directly in laboratory because of technical difficulties. In the present study, the author successfully measured these frequencies and determined precise molecular constants, which is described in Chapter 3, and estimated the upper limit from observed data in 850 GHz region, which is described in Chapter 5.

1 - 4. Ammonia Chemistry

Ammonia was the first polyatomic molecule detected in interstellar space through the transitions between the inversion splitting around 23 GHz (Cheung *et al.* 1968). Since NH_3 is one of ubiquitous interstellar molecules and has many transitions in relatively narrow frequency range, it is known to be an important molecule for determination of kinetic temperature. In fact, NH_3 is detected in quiescent dark clouds such as L134N and TMC-1 (Ho, Martin, and Barrett, 1978; Little *et al.* 1979; Ungerechts *et al.* 1980), star forming regions such as OMC-1 and Sgr B2(Batrla *et al.* 1983; Keene, Blake, and Phillips, 1983), circumstellar envelopes such as IRC+10216, IRC+10420, and VY CMa (Betz, McLaren, and Spears, 1979; McLaren and Betz, 1980), external galaxies (Martin and Ho, 1979; Martin, Ho, and Ruf, 1982), and so on.

The formation mechanism of ammonia in cold dense clouds is shown in Figure 1 - 2. The first step of the ion-molecule reactions is

$$N^+ + H_2 \rightarrow NH^+ + H, \qquad (12)$$

The reaction (12) is slightly endothermic(~7 meV). N^+ is formed mainly by a dissociative charge transfer reaction:

$$N_2 + He^+ \rightarrow N^+ + N + He, \qquad (13)$$

which produces translationally hot N^+ ion, where He^+ is produced by cosmic ray ionization process. By a measurement of Adams, Smith, and Millar (1984), reaction (13) supplies N^+ with sufficient energy to overcome the endothemisity of reaction (12). The following ion molecule reaction:

$$N + H_3^+ \rightarrow NH_2^+ + H, \qquad (14)$$

is somewhat unusual, since H_3^+ usually transfers a proton to more abundant neutral partner. A series of reactions of NH^+ with H_2 leads to NH_2^+, NH_3^+, and NH_4^+, which can recombine with electron to form NH, NH_2, NH_3.

On other hand, it is proposed that NH_3 may be produced on dust surface, and evaporated from grain surface to gas phase by shock wave in star formation regions.

It is important to detect NH and NH_2 in interstellar space in order to understand the ammonia formation mechanisms.

Recently, the NH radical was detected toward diffuse clouds through absorption lines in the ultra-violet region by Meyer and Roth (1991). More recently, the 15 absorption lines of the NH_2 radical were very strongly detected for the first time in interstellar clouds, Sgr B2(N) and Sgr B2(M) using a 10.4 m telescope of Caltech Submillimeter Observatory (CSO) (van Dishoeck *et al.* 1993). Sgr B2(N) and (M) have hot and dense core (T_{kin} ~ 150 - 200 K, $n(H_2) > 10^6$ cm^{-3}), surrounding low density very hot envelope (T_{kin} ~ 900 K, $n(H_2) < 10^4$ cm^{-3}), and shock wave from those core exists (Wilson *et al.* 1982). van Dishoeck *et al.* (1993) determined the column density of NH_2 to be 5 x 10^{15} cm^{-2}, and the fractional abundance relative to H_2 to be $f(NH_3) = 1 \sim 3 \times 10^{-8}$, and estimated the abundance ratio $[NH_2]/[NH_3] = 0.5$ in the envelope. However no NH_2 emission was observed from the dense core. Although the $[NH_2]/[NH_3]$ ratio is close to that in chemical model calculations including gas, grain surface, and grain mantle process by Hasegawa and Herbst (1993), it is not clear whether the observed abundance of NH_2 is explained by direct gas phase ion-molecule reaction process or photodissociation of NH_3 produced on dust surface. It is necessary to do further observations using other lines in other objects.

The abundance ratio $[NH_2D]/[NH_3]$ is expected to be $\sim 10^{-5}$ from the cosmic abundance ratio of H and D, but is recently found to be very high in the hot, dense cores of the molecular clouds, and not explained by gas-phase process. For example, the abundance ratio $[NH_2D]/[NH_3]$ is 6.2×10^{-2} in the compact ridge component of Orion-KL (Turner, 1990) and 1.7×10^{-2} in the core of Sgr B2 (Turner *et al.* 1978). The isotopic species NHD has not been detected, but the detection may be useful to discriminate dust-grain contribution from the gas-phase reaction, because the radical is mainly produced by gas phase reactions including ion-molecule reactions and photodissociation. The abundance of NHD is expected to be 8.5×10^{13} cm^{-2} in Sgr B2, if the NH_2 abundance is 5×10^{15} cm^{-2} (van Dishoeck *et al.* 1993), and the abundance ratio $[NH_2]/[NHD]$ is assumed to be equal to $[NH_2D]/[NH_3] = 1.7 \times 10^{-2}$ (Turner *et al.* 1978).

In this study, the author measured the pure rotational spectra of NH_2, NHD, and ND_2 and determined precise molecular constants, which is described in Chapter 3. The author compared the laboratory data with spectral line survey observations of Orion-KL and Sgr B2, which is described in Chapter 5.

1 - 5. Vibrational Transition Moment of Interstellar Molecules

More than 20 species of interstellar molecules were detected in absorption through vibration rotation transitions using ground based infrared telescopes. Not only stable molecules such as CO (Wiedmann *et al.* 1991), HCN (Ridgeway, Carbon, and Hall, 1978; Wiedemann *et al.* 1991), NH_3 (McLaren and Betz, 1980), CH_4 (Hall and Ridgway, 1978; Lacy *et al.* 1991), and C_2H_2 (Ridgway *et al.* 1976), but also transient molecules such as CN (Wiedmann *et al.* 1991), CCC (Hinkle, Keady, and Bernath, 1988) and C_5 (Bernath, Hinkle, and Keady, 1988), were discovered in mainly IRC+10216 and/or OMC-1. These observations were carried out by using 3 - 4 m class telescopes combined with a Fourier transform spectrometer. Now, large telescopes with 8 - 10 m diameter such as SUBARU are constructing (Kaifu, 1995) and by infrared

observation many interstellar molecules will be identified in near future. They will provide deeper understanding of chemistry and physics in relatively warmer interstellar space. The vibrational transition moments of molecules are indispensable in order to derive abundance of interstellar molecules from the observed line intensities. However, it is very difficult to determine the vibrational transition moment of transient species by usual experimental technique, because concentration of transient molecule is not known in laboratory.

The anomalous intensity distribution in vibration-rotation spectra are reported for many molecules, and explained by Herman-Wallis effect, which is caused by the mixing of the permanent dipole transition moment with the vibrational transition moment through centrifugal distortion effect. The intensity of each vibration rotation line is not explained by a simple vibrational transition moment (Hönl-London factor). The intensity discrepancy from the Hönl-London factor is first studied by Herman and Wallis (1955). When the intensity difference in each vibration-rotation line is obtained, the vibrational transition moment can be determined by the intensity analysis.

The Herman-Wallis effect for a diatomic molecule in the $^1\Sigma$ state is explained by considering the mixing of wavefunctions. The vibration-rotation Hamiltonian is written by

$$\boldsymbol{H}_{\mathrm{vr}} = B\mathbf{J}^2 + \frac{1}{2}\omega\left(p^2 + q^2\right), \tag{15}$$

where the first term denotes the rotational term, and the second the molecular vibration. Here, the author uses relations $B = 1/(8\pi^2 \mathrm{I})$ and $\mathrm{I}^{-1} = \mathrm{I_e}^{-1}(1 - \beta)$ (Kroto, 1975) in order to consider the vibration rotation interaction in Eq. (15), where I is the moment of inertia, $\beta = \gamma q$, and $\gamma = (8B_e/\omega_e)^{1/2}$. Eq. (15) can be rewritten as follows,

$$\boldsymbol{H}_{\mathrm{vr}} = B_e\mathbf{J}^2 - B_e\gamma q\mathbf{J}^2 + \frac{1}{2}\omega_e\left(p^2 + q^2\right), \tag{16}$$

where the second term denotes the vibration rotation interaction, and B_e and ω_e are the rotational constant and vibrational frequency at equilibrium configuration. The second term of Eq. (16) mixes the wavefunctions in different vibrational states and the wavefunction is expressed as follows,

$$|\mathrm{v},J\rangle = |\mathrm{v},J\rangle - \frac{\sqrt{\mathrm{v}+1}}{\sqrt{2}}\frac{1}{\omega_e}(-B_e\gamma)J(J+1)|\mathrm{v}+1,J\rangle + \frac{\sqrt{\mathrm{v}}}{\sqrt{2}}\frac{1}{\omega_e}(-B_e\gamma)J(J+1)|\mathrm{v}-1,J\rangle \quad . (17)$$

In the case of *R*-branch transition of the v = 1 - 0 band, the intensity is expressed as follows,

$$\mathrm{I} \propto \left|\langle \mathrm{v}=1,J+1|\mathrm{M}_1|\mathrm{v}=0,J\rangle\right|^2 \{1-8(B_e/\omega_e)^{3/2}(J+1)\frac{\langle \mathrm{v}=0,J+1|\mathrm{M}_0|\mathrm{v}=0,J\rangle}{\langle \mathrm{v}=1,J+1|\mathrm{M}_1|\mathrm{v}=0,J\rangle}\}, \quad (18)$$

where, $\langle \mathrm{v}=0,J+1|\mathrm{M}_0|\mathrm{v}=0,J\rangle$ is assumed to be equal to $\langle \mathrm{v}=1,J+1|\mathrm{M}_0|\mathrm{v}=1,J\rangle$, and M_0 and M_1 the coefficients of the dipole moment function in the expression $\mathrm{M} = \mathrm{M}_0 + \mathrm{M}_1\frac{r-r_e}{r_e} + \cdots$. The author assumes also the rotational level dependence of the permanent dipole moment is small. Setting $\mu_0 = \langle \mathrm{v}=0,J+1|\mathrm{M}_0|\mathrm{v}=0,J\rangle$ and $\mu_{10} = \langle \mathrm{v}=1,J+1|\mathrm{M}_0|\mathrm{v}=0,J\rangle$, Eq. (18) can be expressed as follows,

$$\mathrm{I} \propto \mu_{10}^2\{1-8(B_e/\omega_e)^{3/2}(J+1)\frac{\mu_0}{\mu_{10}}\} \qquad (\mathrm{v}=1\rightarrow 0,\ J=J''+1\rightarrow J'',\ R\text{-branch}). \quad (19)$$

On the other hand, the intensity for *P*-branch transition can be given by follows,

$$\mathrm{I} \propto \mu_{10}^2\{1+8(B_e/\omega_e)^{3/2}J\frac{\mu_0}{\mu_{10}}\} \qquad (\mathrm{v}=1\rightarrow 0,\ J=J''-1\rightarrow J'',\ P\text{-branch}). \quad (20)$$

The vibrational transition moment is usually in range of 10^{-1}~$^{-3}$ Debye, and the magnitude of permanent dipole moment is a few Debye. Therefore, the second terms in Eqs. (19) and (20) have non-negligible effect in vibration rotation transition intensities. When both the dipole moment and the vibrational transition moment are positive, it is expected that the *P*- and *R*-branch transitions become stronger and weaker, respectively. The intensity analysis of *R*- and *P*-branch transitions gives the transition moment μ_{10} uniquely, if the value of μ_0 is determined from other methods. In the Π electronic state, *Q*-branch is also allowed, but the Herman-Wallis effect dose not appear in the *Q*-branch transition. If Herman-Wallis effect is very large, the higher order term is necessary. The whole formulation for infrared intensity in absorption is described in Section 5 - 2. Recently, the theoretical studies and experimental applications for more complicated molecules such as linear, symmetric-top, and asymmetric-top molecules are reported by Watson (1987, 1992), Johns and Noël (1992), Lafferty *et al.* (1992), Errera *et al.* (1995), and Maki, Quapp, and Klee (1995).

In the present study, the vibrational transition moment of CH is determined by intensity analysis using the Herman-Wallis effect, which is described in Chapter 4, and using this value, the column density of CH is determined from the infrared observational spectrum of a late-type cool star, which is described in Chapter 5. The anomalous intensity in the vibration rotation spectrum of ^{18}OH is compared with those of ^{16}OH in order to confirm Herman-Wallis effect.

1 - 6. Outline of this Thesis

In the next Chapter, spectrometers in far-infrared region are reviewed and the spectrometer and the cell used in the present experiment are described. Chapter 3 reports far-infrared absorption spectroscopy of SH, NH_2, NHD, ND_2, and NH_2OH. The observation of the pure rotational spectrum of SH is the first application of far-infrared Fourier transform spectroscopy to transient molecules. The pure rotational transitions of NH_2, NHD, and ND_2 and the vibration-rotation transitions of NH_2OH are systematically observed. In Chapter 4, infrared emission spectroscopy of CD and ^{18}OH is described. The molecular constants in vibrationally excited states are determined from the analysis of the observed emission spectra of CD and ^{18}OH. The anomalous intensity for CH and ^{18}OH are discussed and the vibrational transition moment of CH is determined from the intensity analysis for the first time. In Chapter 5, results of laboratory spectroscopy are applied to astronomical observational results. The upper limit of the column density of SH is estimated from the submillimeter wave emission spectrum in Orion-KL. The column density of CH is determined from the infrared absorption spectrum in late-type star, TX Psc. The spectral line survey observation data in Orion-KL and Sgr B2 are compared with the calculated frequencies of NHD using molecular constants in the present study, and the upper limit of column density in Sgr B2 is estimated.

References

Adams, N. G., Smith, D., and Millar, T. J. 1984, Mon. Not. R. Astron. Soc. **211,** 857.

Batrla, W., Wilson, T. L., Bastien, P., and Ruf, K. 1983, Astron. Astrophys. **128,** 279.

Bernath, P. F., Hinkle, K. H., and Keady, J. J. 1988, Science, **244,** 562.

Betz, A. L., McLaren, R. A., and Spears, D. L. 1979, Astrophys. J. **229,** L97.

Chung, A. C., Rank, D. M., Townes, C. H., Thornton, D. D., and Welch, W. J. 1968, Phys. Rev. Lett. **21,** 1701.

_____. 1969, Nature, **221,** 626.

Dickel, H. R., Dickel, J. R., and Wilson, W. J. 1981, Astrophys. J. **250,** L43.

Douglas, A. E. and Herzberg, G. 1941, Astrophys. J. **94,** 381.

Dunham, Jr., T. 1937, Pub. Astron. Soc. Pacific. **49,** 26.

Errera. Q., Auwera, J. V., Belafhal, A., and Fayt, A. 1995, J. Mol. Spectrosc. **173,** 347.

Hall, D. N. B. and Ridgway, S. T. 1978, Nature, **273,** 281.

Hasegawa, t. I. and Herbst. E. 1993, Mon. not. R. Astron. Soc. **263,** 589.

Heiles. C .E. and Turner, B. E. 1971, Astrophys. Lett. **8,** 89-91.

Herbst. E. and Leung, C. M. 1989, Astrophys. J. Suppl. **69,** 271.

Herman, R. and Wallis, R. F. 1955, J. Chem. Phys. **23,** 637.

Hinkle, K. W., Keady, J. J., and Bernath, P. F. 1988, Science, **241,** 1319.

Ho, P. T., Martin, R. N., and Barrett, A. H. 1978, Astrophys. J. **221,** L117.

Kaifu, N. 1995, "*Scientific and Engineering Frontiers for 8 - 10 m Telescopes,*" Universal Academic Press, Inc. P. 21.

Johns, J. W. C. and M. Noël, M. 1992, J. Mol. Spectrosc. **156,** 403.

Keene, J., Blake, G. A., and Phillips, T. G. 1983, Astrophys. J. **271,** L27.

Kroto, 1975, "*Molecular Rotation spectra,*" John Wiley & Sons, Ltd.

Lacy, J. H., Carr, J. S., Evans II, N. J., Baas, F., Achtermann, J. M., and Arens, J. F. 1991, Astrophys. J. **376,** 556.

Lafferty, W. J., Fraser, G. T., Pine, A. S., Flaud, J. -M., Camy-Peyret, C., Dana, V., Mandin, J. -Y., Barbe, A., Plateaux, J. J., and Bouazza, S. 1992, J. Mol. Spectrosc. **154,** 51.

Little, L. T., Macdonald, G. H., Riley, P. W., and Matheson D. N. 1979, Mon. Not. R. Astron. Soc. **189,** 539.

Maki, A., Quapp, W., and Klee, S. 1995, J. Mol. Spectrosc. **171,** 420.

Martin, R. N. and Ho, P. T. P. 1979, Astron. Astrophys. **74,** L7.

Martin, R. N., Ho; T. P. and Ruf, K. 1982, Nature, **296,** 632.

McLaren, R. A. and Betz, A. L. 1980, Astrophys. J. **240,** L159.

Meeks, M. L., Gordon, M. A., and Litvak. M. M. 1969, Science **163,** 173.

Millar, T. J., Rawlings, J. M. C., Bennett, A., Brown, P. B., and Charnley, 1991, Astron. Astrophys. Suppl. Ser. **87,** 585.

Minh, Y. C., Irvine, W. M., and Ziurys, L. M. 1989, Astrophys. J. **345,** L63.

Minh, Y. C., Ziurys, L. M., Irvine, W. M., and McGonagle, D. 1990, Astrophys. J. **360,** 136.

_____. 1991, Astrophys. J. **366,** 192.

Meyer, D. M. and Roth, K. 1991, Astrophys. J. **376,** L49.

Palmer, P., Zuckerman, B., Buhl, D., and Snyder, L. E. 1969, Astrophys. J. **156,** L147.

Prasad, S. S. and Huntress, Jr. 1982, W. T. Astrophys. J. **260,** 590.

Ridgeway, S. T., Carbon, D. F., and Hall, D. N. B. 1978, Astrophys. J. **225,** 138.

Ridgeway, S. T., Hall, D. N. B., Kleinmann, S. G., Weinberger, D. A., and Wojslaw, R. S. 1976, Nature, **264,** 345.

Suzuki, H. 1979, Prog. Theor. Phys. **62,** 18.

Swings, P. and Rosefeld, L. 1937, Astrophys. J. **86,** 483.

Thaddeus, P., Kutner, m. L., Penzias, A. A., Wilson, R. W., and Jefferts, K. B. 1972, Astrophys. J. **176,** L73.

Tielens, A. G. G. and Hagen, W, 1982, Astron. Astrophys. **114,** 245.

Turner, B. E. 1990, Astrophys. J. **362,** L29.

Turner, B. E., Zuckerman, B, Morris, M., and Palmer, P. 1978, Astrophys. J. **219,** L43.

Ungerechts, H., Walmsley, C. M., and G. Winnewisser, 1980, Astron. Astrophys. **88,** 259.

van Dishoeck, E. F., Jansen, D. J., Schilke, P., and Phillips, T. G. 1993, Astrophys. J. **416,** L83.

Watson, J. K. G., 1987. J. Mol. Spectrosc. **125,** 428.

_____. 1992, J. Mol. Spectrosc. **153,** 211.

Weinreb, S., Barret, A. H., Meeks, M. L., and Henry, J. C. 1963, Nature, **200,** 829.

Wiedmann, G. R., Hinkle, K. H., Keady, J. J., Deming, D., and Jennings, D. E. 1991, Astrophys. J. **382,** 321.

Wilson, R. W., Jefferts, K. B., and Penzias, a. A. 1970, Astrophys. J. **161,** L43.

Wilson, T. L., Ruf, K., Walmsley, C. M., Martin, R. N., Pauls, T. A., and Batrla, W. 1982, Astron. Astrophys. **115,** 185.

Table 1 - 1

Molecules detected in interstellar space(1995)

linear molecules

$^1\Sigma$ H_2, CH^+, HCl, CC, CO, CS, SiO, PN, HCN, HNC, N_2O, HCCCN, HC_5N, HC_7N, HC_9N, $HC_{11}N$, HCCNC, HCO^+, HN_2^+, $HCNH^+$, $HCCCNH^+$, HCS^+, OCS, CCC, C_5, CCCO, CCCS, C_4Si, NaCl, AlCl, KCl, AlF

$^2\Sigma$ CN, CO^+, CCH, C_4H, CCCN, CP, SiN, MgCN, MgNC

$^2\Pi$ OH, CH, C_3H, C_5H, C_6H, NO, NS, SO^+

$^3\Sigma$ NH, SO, CCO, CCS, HCCN

$^3\Pi$ SiC

Spherical top molecules

$^1A_1$ CH_4, SiH_4

Symmetric top molecules

$^1A_1$ NH_3, CH_3CN, CH_3NC, CH_3CCH, CH_3C_4H, CH_3CCCN, CH_3C_5N

Asymmetric molecules

$^1A_1$ H_2O, H_2S, H_2CO, H_2CCO, H_2CS, H_2CCC, H_2CCCC, cyclic-C_3H_2, SO_2, SiC_2

^1A_g C_2H_4

$^2B_1$ NH_2, H_2CCN, cyclic-C_3H

$^1A'$ HNO, HNCO, HNCS, NaCN, $HOCO^+$, HCOOH, CH_2NH, NH_2CN, C_2H_5OH, HNCCC, C_2H_3CN, C_2H_5CN, HC_2CHO

$^2A'$ HCO

molecules with internal rotation

CH_3NH_2, CH_3OH, CH_3SH, CH_3CHO, $HCOOCH_3$, CH_3OCH_3, CH_3COCH_3

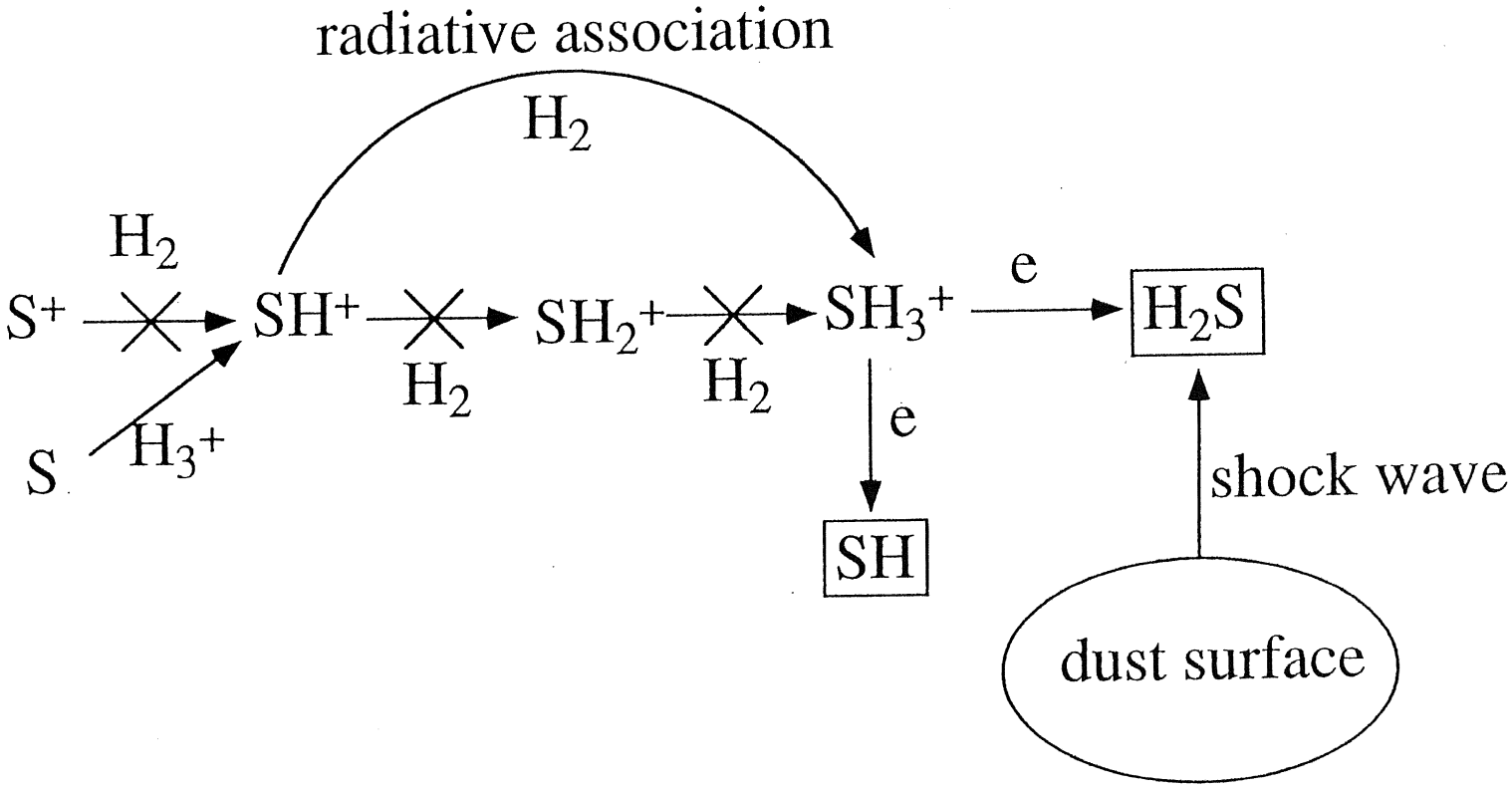

Figure 1 - 1. Simple schematic illustration for the formation of the hydrogen sulfide.

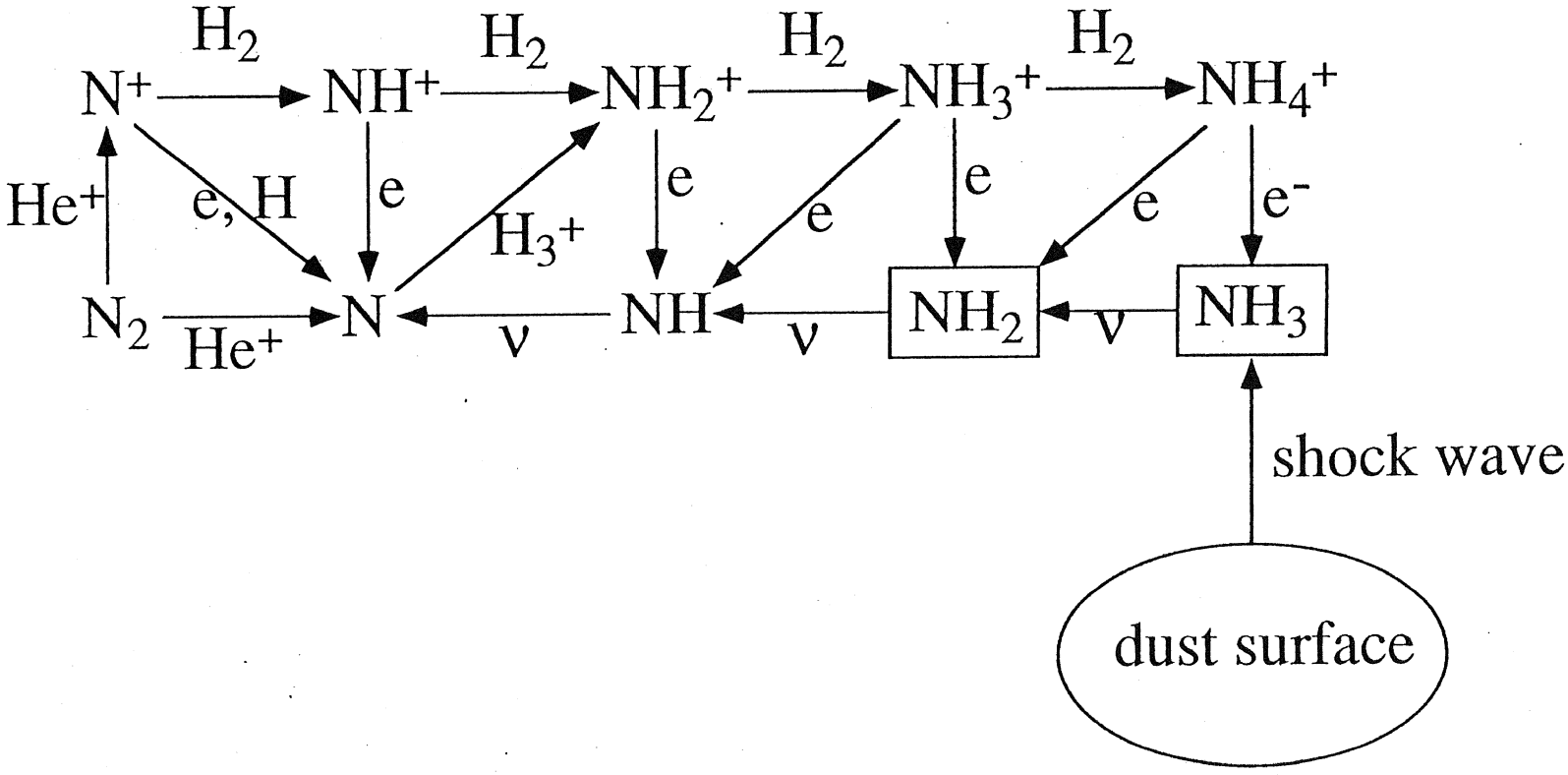

Figure 1 - 2. Simple schematic illustration of the formation of ammonia.

Chapter 2. High-Resolution Spectrometers in Far-Infrared and Infrared Regions

Abstract

Far-infrared spectroscopic methods for transient molecules are shortly reviewed. In this study, far-infrared and infrared spectra were measured using a high-resolution Fourier transform spectrometer (Bruker IFS 120 HR) at Nobeyama Radio Observatory. The author constructed an absorption cell for far-infrared Fourier transform spectroscopy of short-lived species and an emission cell for mid-infrared spectroscopy. The far-infrared absorption cell was combined with White-type multi-reflection system to increase an effective optical path length. By this optical arrangement, the far-infrared observations of transient molecules using a Fourier transform spectrometer became possible.

2 - 1. Spectrometers

The most sensitive spectrometer in far-infrared region is a laser magnetic resonance (LMR) spectrometer, which use non-tunable far-infrared optically pumped molecular laser and magnetic field for tuning molecular transition frequencies by Zeeman effect. The far-infrared LMR spectrometer has a tuning range of about 20 GHz. It is a very high sensitive method, but not applicable to molecules with small Zeeman effect, and have frequency measurement uncertainty of a few MHz originating from indirect determination of zero-field frequencies. The detail of the LMR spectrometer is reviewed by Evenson *et al.* (1980). The highest accuracy in determination of transition frequency is available by tunable far-infrared spectrometer, which is used a far-infrared source generated by a mixing of two stabilized CO_2 lasers and microwave radiation on metal-insulator-metal (MIM) diode. The accuracy is about 35 kHz, but one disadvantage is in small radiation power (a few hundred nW). The detail is described by Evenson, Jennings, and Petersen (1984) and Nolt *et al.* (1987). The far-infrared laser spectrometer is mainly applied to observe the pure rotational transitions of molecules such as hydride.

The submillimeter spectrometer (microwave spectrometer) using multiplied millimeter wave source from klystron or Gunn oscillator is recently reviewed in detail by Ziurys *et al.* (1994). The resolution is about 50 kHz. Since the highest frequency is about 650 GHz, the spectrometer is mainly applied to the observation of pure rotational transitions of not so light molecules.

Submillimeter spectroscopy using a backward wave oscillator (BWO) was recently developed (Winnewisser *et al.* 1994) with phase-looked system. It covers up to 1.3 THz and supplies a power of several mW, and the resolution is the same as the microwave spectrometer. More recently, this technique was applied for transient molecules of astronomical interest, such as SH (Klisch *et al.* 1995).

A Fourier transform (FT) spectrometer is equivalent to two beam interferometers like as Michelson interferometer. An interferogram is recorded by mixing of the two beams at beam splitter, and spectrum is obtained from the interferogram by performing

the Fourier transformation. This method is applied for laboratory and astronomical observations in far-infrared, infrared, visible, and ultra-violet regions. Since in far-infrared region usually source power is small, the sensitivity of FT spectrometer is low compared with the method using a monochromatic source. Therefore, this method is applied for spectroscopy of stable molecules in far-infrared region so far. However, in the frequency region between 200 and 400 cm^{-1}, FT spectrometer is only available as a high-resolution spectrometer. The author applied FT spectroscopy for short-lived species for the first time. An absorption cell was newly constructed and used in the observations of the pure rotational spectra of SH, NH_2, NHD, and ND_2 and the vibration-rotation spectrum of NH_2OH.

In infrared region, high-resolution spectroscopy is carried out by using a tunable laser sources (diode laser, difference frequency laser) and FT spectrometer. Fourier transform spectrometer is also applicable to emission measurement, and the emission method is more sensitive than absorption method. The author constructed the positive column discharge emission cell, which is described in Section 3 and observed the vibration-rotation emission spectra of CD, CH, and ^{18}OH.

Both far-infrared absorption and infrared emission spectra were recorded using a high-resolution FT spectrometer (Bruker IFS 120 HR) at Nobeyama Radio Observatory. It covers from 50 to 10,000 cm^{-1}, and the highest resolution is 0.002 cm^{-1}. Optical arrangement of spectrometer is shown in Figure 2 - 1.

2 - 2. Construction of an Absorption Cell for Short-Lived Species in Far-Infrared Region

Figure 2 - 2 shows the absorption cell used in the present experiment. The far-infrared beam (Hg lamp) from a FT spectrometer, was focused on the window of the absorption cell by a concave mirror with 1500 mm focal length. A 60 μm thick polypropylene sheet was used as the windows for the cell. The transmittance of the window material was 80-90 % in the 50 - 700 cm^{-1} region as shown in Figure 2 - 3. The use of transparent sheet in optical region made it easy to do alignment of a multi-path cell.

The author measured the transmittance of other materials by the FT spectrometer, with a Mylar 6 μm beamsplitter. Figure 2 - 4 shows the transmission spectrum of a 0.5 mm thick Teflon sheet, which is usable up to 200 cm^{-1} with about 70 % transmittance. Figure 2 - 5 shows the transmission spectrum of a 180 μm thick black polyethylene sheet, which is usable up to 700 cm^{-1}, but the transmittance is not good in all region. Results of theses measurement indicate that the polypropylene sheet is the best as far-infrared window.

The effective optical path length was set to about 24 m by White-type multi-reflection arrangement. The output beam from the cell was focused on a liquid-helium cooled Si composite bolometer. Inside the dewar, a filter transmitting radiation below 600 cm^{-1} was mounted. Dry nitrogen gas flow was used to decrease water vapor absorption along the optical path between the absorption cell and detector. The total length of the cell was 1.5 m. The central part was made of a Pyrex glass tube with inner diameter of 103 mm and both ends were made of glass tubes with 142 mm inner diameter. Two electrodes made of 0.1 mm thick stainless steel plate with water cooling system were attached to the absorption cell as side arms, as shown in Figure 2 - 2. The surface of the electrodes was exposed only to rare and/or clean gas flow, and reactant gas was introduced into the cell through a nozzle. This arrangement made it possible to maintain a long-term stable discharge by keeping the electrode surface clean.

The author observed the pure rotational spectrum of the OH radical as a test measurement. The result was successful with more than 30 % absorption, as shown in Figure 2 - 6. In this experiment, the partial pressures of H_2O and He are 50 and 100 mTorr, respectively. The dc discharge current was 500 mA. The 6 μm Mylar beamsplitter was used, and frequency coverage was 0 - 700 cm^{-1} with 0.01 cm^{-1} resolution. The integration time was about 1 hr for 12 scans.

2 - 3. Construction of an Emission Cell in Infrared Region

Fourier transform spectroscopy of infrared emission spectra is grown recently by using a high temperature cell, and the following species are studied so far, SeO (Fink *et al.* 1987), AlH (White, Dulick, Bernath, 1993), HBr (Braun and Bernath, 1994), InH (White, Dulick, and Bernath, 1995) and BiN (Breidohr *et al.* 1994). The chemiluminesence spectra of metal compounds were also observed in diatomic molecules such as TeH (Fink *et al.* 1989), TeF, TeCl (Ziebarth, Setzer, and Fink, 1995). A hollow cathode lamp is used for the observations of electronic spectra of hydrides, NH (Brazier, Ram, and Bernath, 1986),YD (Ram and Bernath, 1995a) and CrD (Ram and Bernath, 1995b).

In the present study, the author produced radicals in a positive column discharge emission cell shown in Figure 2 - 7. The cell is made of a 50 cm long (1.2 cm inner diameter) Pyrex tube with a water-cooled jacket. The anode and cathode are made of 27 cm long stainless steel sheets with 0.1 mm thickness and mounted inside the water-cooled glass tube with 4 cm inner diameter. The rare gas was introduced from the both ends of electrodes. The reactant gas was introduced from both ends of the cell. The reaction products were continuously pumped out by a rotary pump from the central part of the cell. In this system, it is possible to maintain a long-term stable discharge by keeping the surface of the electrode and the CaF_2 window clean.

The infrared emission from the cell was focused onto the input iris of the Fourier transform spectrometer by a CaF_2 lens with 75 mm focal length. The incident beam from the iris was introduced into the Michelson interferometer, and detected by an InSb detector through a low-pass filter ($< 4000\ cm^{-1}$).

In observation of the infrared emission spectrum of the ^{18}OH radical, a different discharge cell was used, as shown Section 4 - 2.

References

Braun, V and Bernath, P. F. 1994, J. Mol. Spectrosc. **167,** 282.

Brazier, C. R., Ram, R. S., and Bernath, P. F. 1986, J. Mol. Spectrosc. **120,** 381.

Breidohr, R., Setzer, K. D., Shestakov, O. Fink, E. H., and Zyrnicki, W. 1994, J. Mol. Spectrosc. **166,** 471.

Evenson, K. M., Saykally, R. J., Jennings, D. A., Curl, Jr., R. F., and Brown, J. M. 1980, "*Chemical and Biochemical Applications of Lasers,*" Academic Press, New York, P.95.

Evenson, K. M., Jennings, D. A., and Petersen, F. R. 1984, Appl. Phys. Lett. **44,** 576.

Fink, E. H., Setzer, K. D, Ramsay, D. A. and Vervloet, M. 1987, J. Mol. Spectrosc. **125,** 66.

_____. 1989, J. Mol. Spectrosc. **138,** 19.

Klisch, E., Klaus, Th, Belov, S. P., Winnewisser, G., and Herbest, E. 1995, in preparation.

Nolt, I. G. Radostitz, J. V., Dilonardo, G., Evenson, K. M., Jennings, D. A., Leopold, K. R., Vanek, M. D., Zink, L. R., Hinz, A., and Chance, K. V. 1987, J. Mol. Spectrosc. **125,** 274.

Ram. R. S. and Bernath, P. F. 1995a, J. Mol. Spectrosc. **171,** 169.

_____. 1995b, J. Mol. Spectrosc. **172,** 91.

White, J. B., Dulick, M., and Bernath, P. F. 1993, J. Chem. Phys. **99,** 8371.

_____. 1995, J. Mol. Spectrosc. **169,** 410.

Winnewisser, G., Krupnov, A. F., Tretyakov, M. Yu., Liedtke, M., Lewen. F., Saleck, A. H., Schieder, R., Shkaev, A. P., and Volokhov, S. V. 1994, J. Mol. Spectrosc. **165,** 294.

Ziebarth, K., Setzer, K. D., and Fink, E. H. 1995, J. Mol. Spectrosc. **173,** 488.

Ziurys, L. M., Barclay, W. L., Anderson, m. A., Fletcher, D. A., and Lamb, J. W. 1994, Rev. Sci. Instrum. **65,** 1517.

S1-S3 Sources
AC Aperture Changer
FC Filter Changer
BS BeamSplitter
MS Mirror Scanner
RM Retroreflector Mirror
D1-D6 Detectors

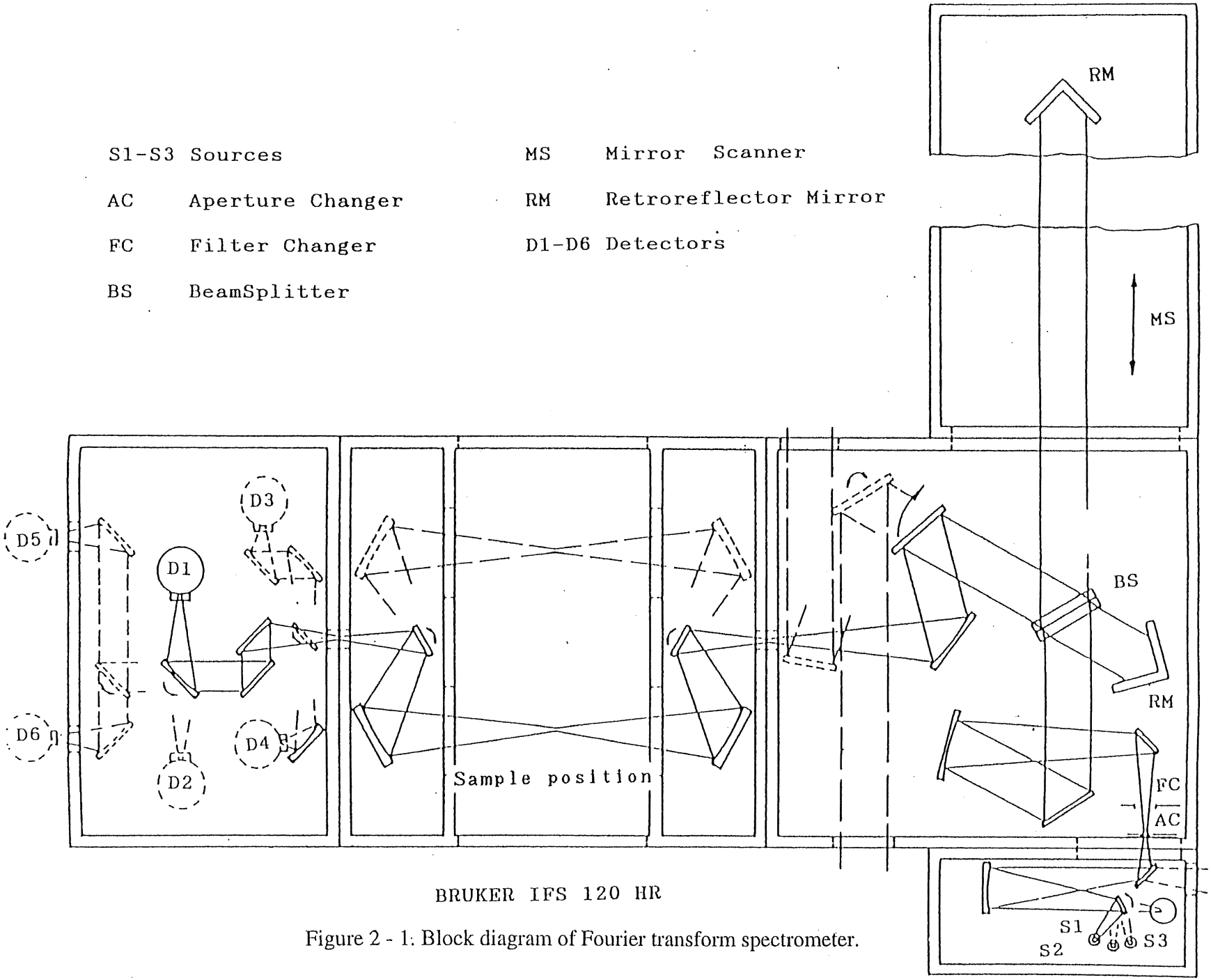

Figure 2 - 1. Block diagram of Fourier transform spectrometer.

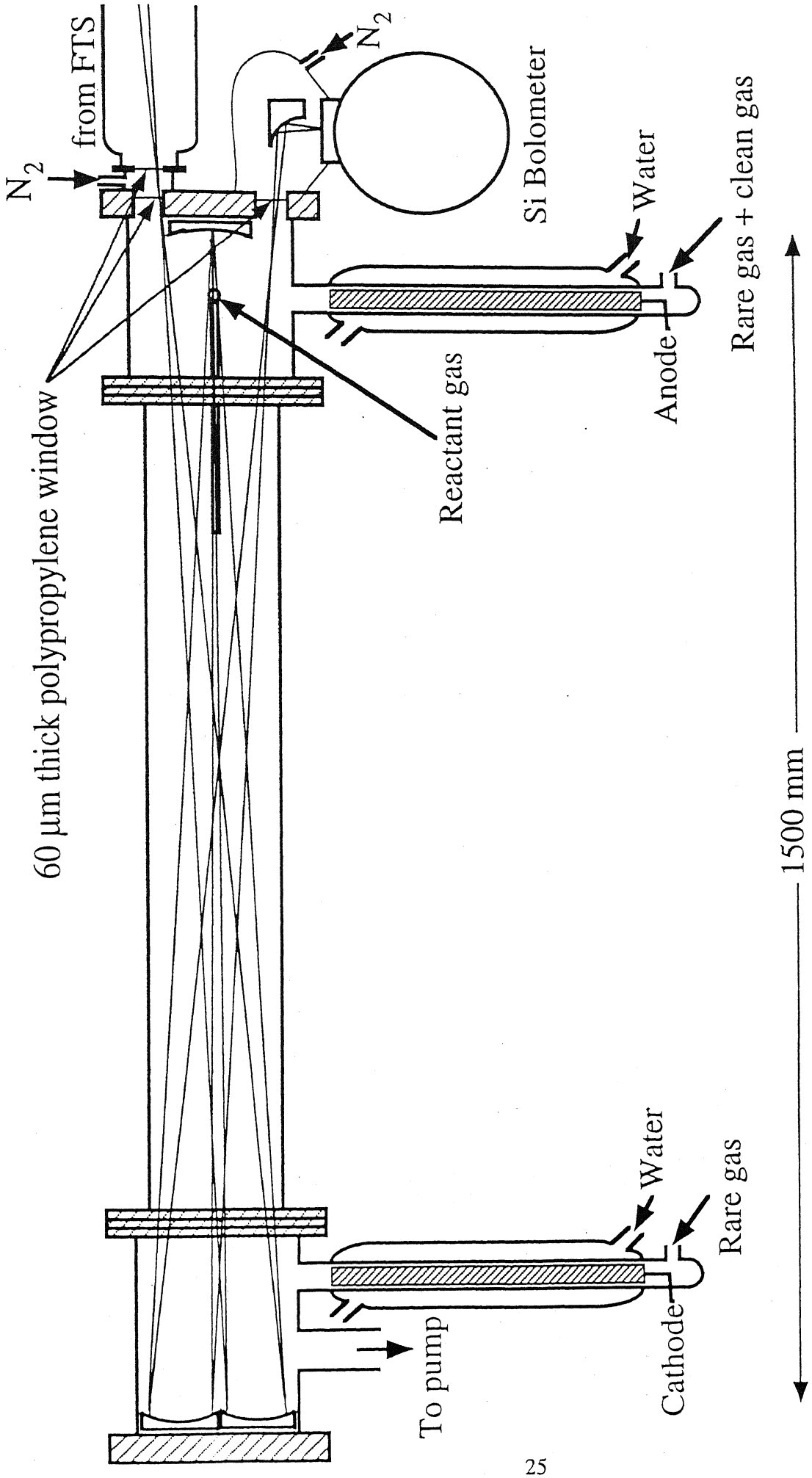

Figure 2 - 2. Schematic diagram of multipath discharge cell for absorption spectroscopy.

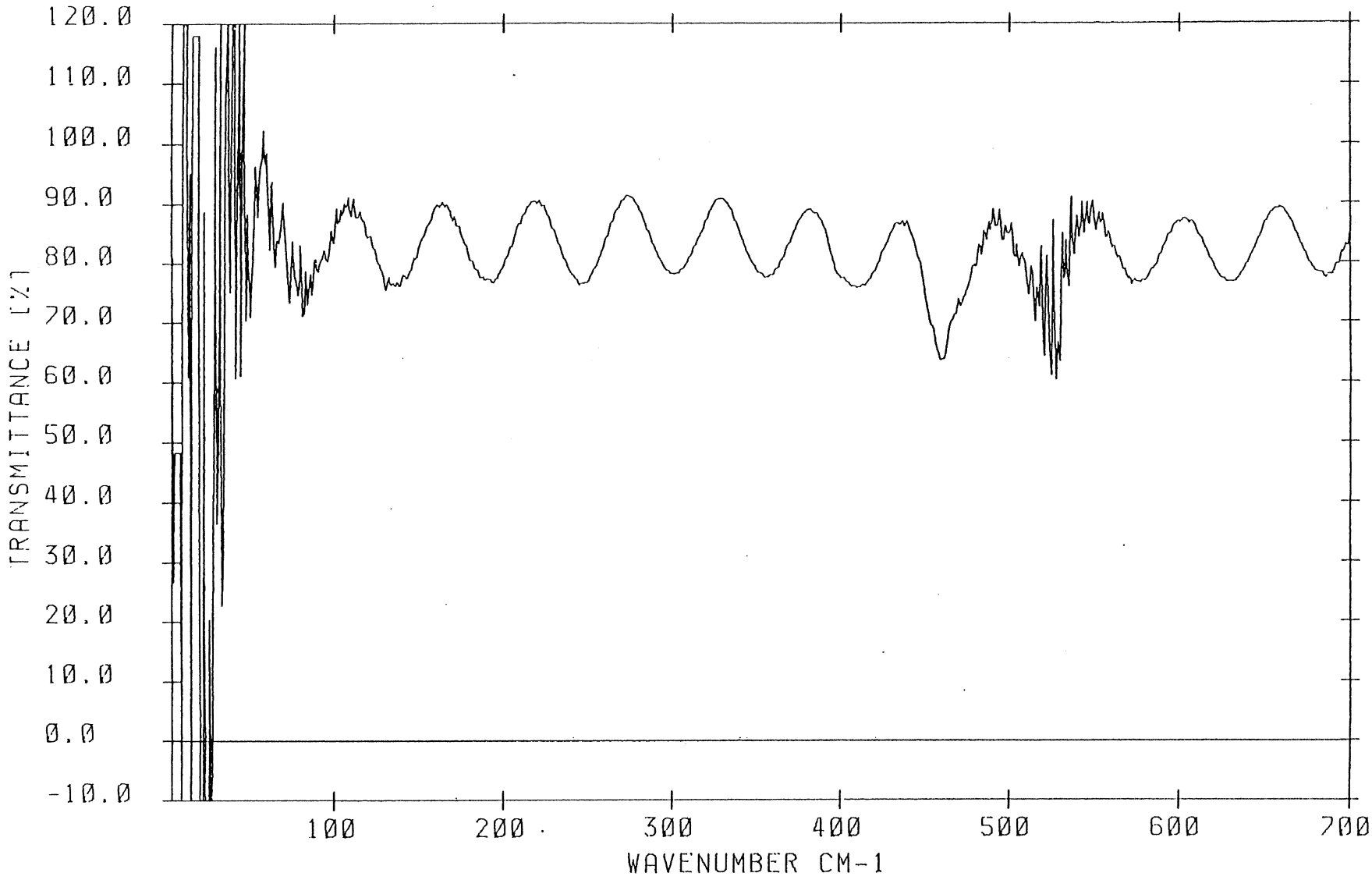

Figure 2 - 3. Observed transmission spectrum of a 60 μm thick polypropylene sheet. Below 50 cm^{-1} region, the noise level is increased because of a low source power and low transmittance of the beamsplitter. A sinusoidal wave with a cycle of about 50 cm^{-1} is due to interference of this sheet itself.

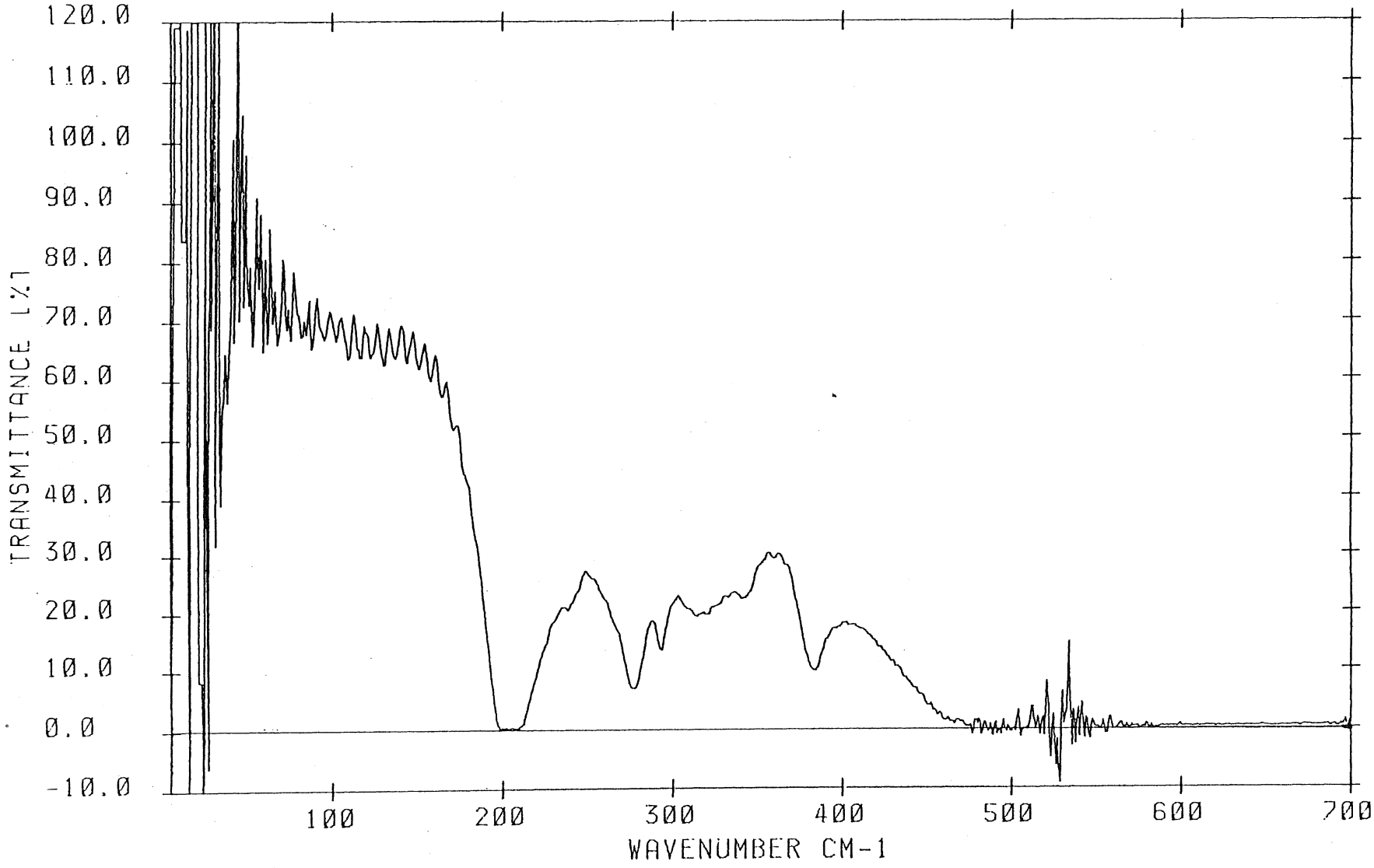

Figure 2 - 4. Observed transmission spectrum of a 0.5 mm thick Teflon sheet.

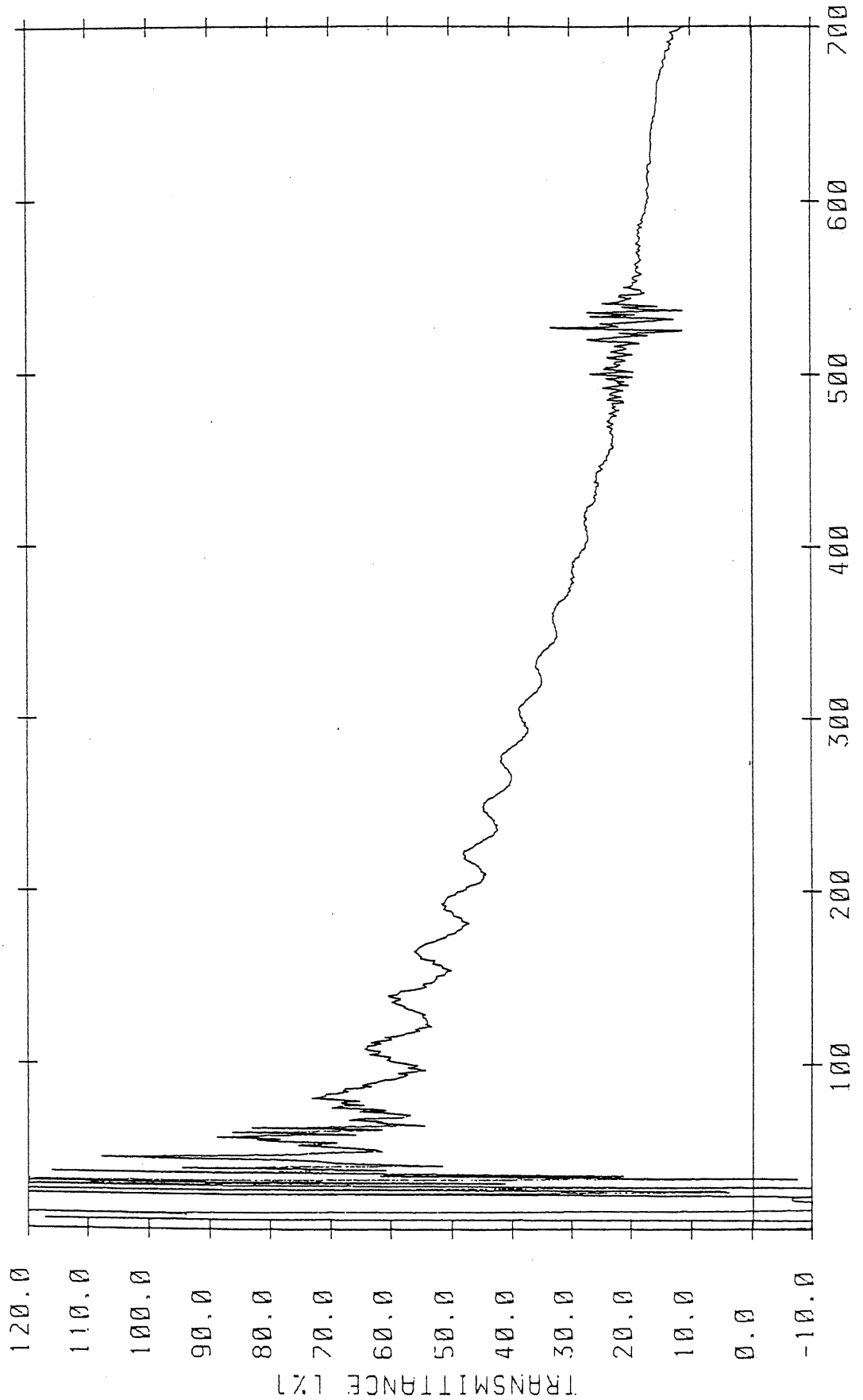

Figure 2 - 5. Observed transmission spectrum of a 180 µm thick black polyethylene sheet.

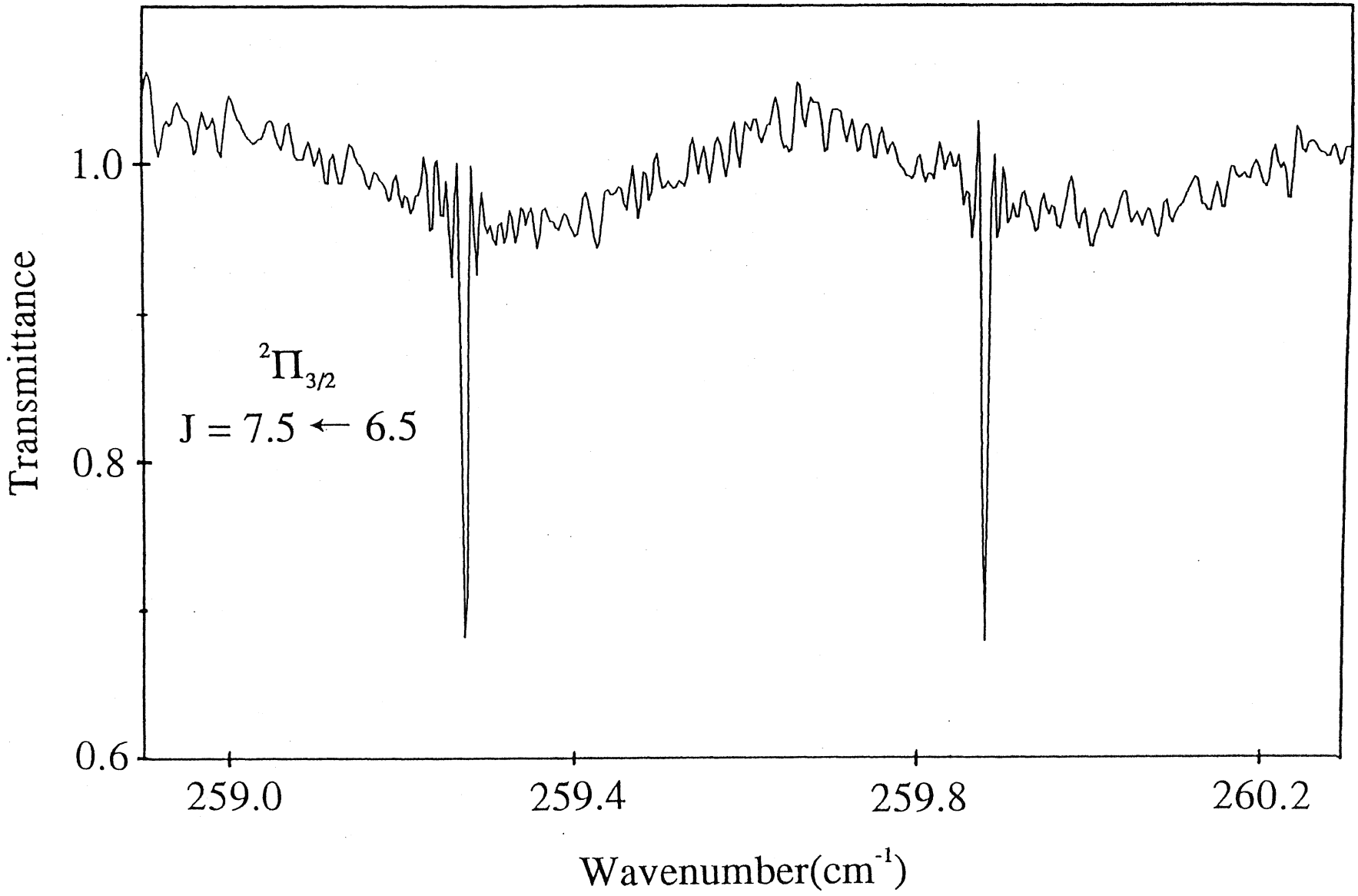

Figure 2 - 6. Observed spectrum of the $J = 7.5 - 6.5$ transition in the $^2\Pi_{3/2}$ state of the OH radical.

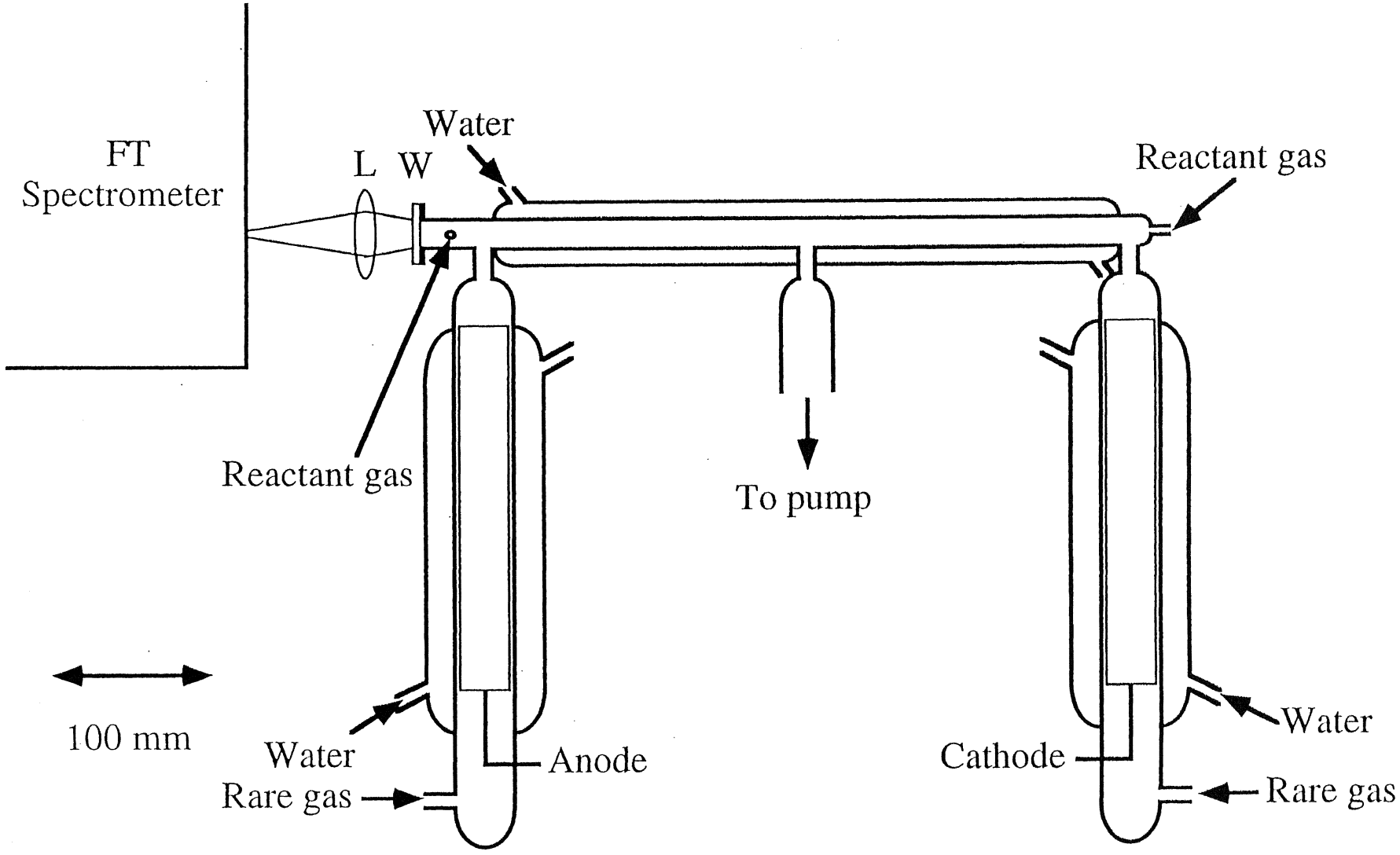

Figure 2 - 7. Schematic diagram of the positive column dc discharge cell in order to observe infrared emission spectra. W is a CaF_2 window, and L is CaF2 lens.

Chapter 3. Fourier Transform Far-Infrared Spectroscopy of Short-Lived Molecules

3 - 1. Pure Rotational Spectrum of the SH Radical

Abstract

The pure rotational absorption spectrum of the SH radical in the ground $^2\Pi$ state was observed by a high-resolution Fourier transform spectrometer. The radical was generated by a dc discharge in an H_2S, H_2, and He mixture. Rotational transitions in the $^2\Pi_{1/2}$ components were directly observed for the first time. The observed 31 absorption lines, together with Λ-type doubling transitions measured by Meerts and Dymanus (1974, 1975) were analyzed by a least-squares method, to determine the rotational, centrifugal, spin-rotation coupling, and Λ-type doubling constants in the ground state.

3 - 1 - 1. Introduction

So far 14 species of sulfur-bearing molecules, CS, SO, SO^+, SiS, NS, HCS^+, CCS, H_2S, SO_2, OCS, C_3S, H_2CS, HNCS, and CH_3SH have been detected in interstellar space. However, the simplest sulfur compound SH has not been detected in spite of radioastronomical searches using the Λ-type doubling transitions (Meeks, Gordon and Litvak, 1969; Heiles and Turner, 1971). The failure in the detection may be due to the weak line strength around 111 MHz frequency region. Pure rotational transitions in the far-infrared region are more suitable for searches in interstellar space due to the larger intensities. The detection in space may contribute to understanding of sulfur chemistry, especially production and reaction mechanism of SH_n, which are already described in Chapter 1.

Laboratory high-resolution spectroscopic studies of SH by electron paramagnetic resonance (EPR) technique has been applied to the ground $^2\Pi_{3/2}$ state by Radford and Linzer (1963), McDonald (1963), Uehara and Morino (1970), Brown and Thistlethwaite (1972), and Tanimoto and Uehara (1973). The Λ-type doublet transitions in the $^2\Pi_{3/2}$ and $^2\Pi_{1/2}$ states were observed by Meerts and Dymanus (1974) who used molecular beam electronic resonance (MBER) technique and determined accurate hyperfine coupling constants and the dipole moment to be 0.7580(1) D.

The pure rotational transition $J = 3.5 - 2.5$ in the SH $^2\Pi_{3/2}$ v=0 state has been observed with far-infrared laser magnetic resonance (FIR LMR) by Davies *et al.* (1978). Later, Ashworth and Brown (1992) extended the FIR LMR measurements to the first three rotational transitions in the $^2\Pi_{3/2}$ component and determined an improved set of molecular constants by a simultaneous analysis of the LMR data and selected data from previous studies. The vibration-rotation transitions were observed by Bernath, Amano, and Wong (1983) using a difference frequency laser spectrometer. Winkel and Davis (1984) applied Fourier transform emission spectroscopy to observe v = 3 - 2, 2 - 1, and 1 - 0 bands and determine Λ-type doubling constants. Benidar *et al.* (1991) also observed the same band as Winkel and Davis (1984) to carry out intensity measurements of

rovibrational transitions in order to study the Herman-Wallis effect. Recently, Ram *et al.* (1995) also observed the infrared emission spectrum of v = 4 - 3, 3 - 2, 2 - 1, and 1 - 0 bands using a Fourier transform spectrometer. The electronic spectrum of the $A^2\Sigma^+$ - $X^2\Pi$ system was observed and analyzed by Porter (1950), Ramsay (1952), and Johns and Ramsay (1961).

Since the Hund's case (a) limit is nearly applicable to the ground state of the SH radical due to the large magnitude of the spin-orbit interaction constant, the Zeeman effect in the $^2\Pi_{1/2}$ components becomes small. Therefore, the pure rotational transitions in the $^2\Pi_{1/2}$ state have not been observed by the FIR LMR experiments. In this section, the application of Fourier transform(FT) spectroscopy to observe directly the pure rotational transitions of SH is reported. A set of molecular constants was determined precisely by an analysis together with the accurate Λ-type doubling frequencies of Meerts and Dymanus (1974, 1975).

3 - 1- 2. Experimental

Detail of the absorption cell in this study was already described in Chapter 2. In short, the far-infrared beam from a FT spectrometer equipped with a Mylar beamsplitter of 23 μm thickness was focused on the window of the absorption cell. The output beam from the cell after passing White-type multireflection arrangement was focused on a liquid-helium cooled Si composite bolometer. Two electrodes made of stainless steel plate with water cooling system were attached to the absorption cell as side arms. The surface of the electrodes was exposed only to He and H_2 gas or He gas flow, and H_2S was introduced into the cell through a nozzle.

The SH radical was produced by a dc discharge in a H_2S, H_2, and He mixture with partial pressures of 10, 20, and 400 mTorr, respectively. The reaction products were pumped out continuously with a mechanical booster pump followed by a rotary pump. The optimum production occurred with a 400 mA discharge current. The frequency region of 0-700 cm^{-1} was observed with a 0.0075 cm^{-1} resolution. The integration time

was about 24.3 hr with 394 scans, and the noise level corresponded to 0.5 % absorption typically. The observed wavenumbers were calibrated against the rotational lines of H_2O in the 65 - 200 cm^{-1} region (Guelachvili and Narahari Rao, 1986).

3 - 1 - 3. Observed Spectrum and Analysis

The absorption spectrum of SH was observed in 60 - 120 and 160 - 250 cm^{-1} region. The observation in the spectral lines below 60 cm^{-1} and between 120 and 160 cm^{-1} was impossible, because of the transmittance of the 23 μm Mylar beamsplitter. Figures 3 - 1 - 1 and 3 - 1 - 2 show the typical observed spectra of SH in the $^2\Pi_{1/2}$ and $^2\Pi_{3/2}$ states, respectively. There were also many absorption lines due to the parent and discharge product molecules in the observed region. The SH lines were easily found by their characteristic doublet structure due to the Λ-type doubling, and also confirmed by comparison with a spectrum observed without discharge. The observed lines, listed in Table 3 - 1 - 1, were assigned using the molecular constants reported in the previous work (Ashworth and Brown, 1992).

The observed 31 spectral lines were analyzed with a least squares fitting procedure. The effective Hamiltonian used corresponds to a Hund's case (a) parity-conserving basis set expressed in the N^2-formalism (Brown *et al.* 1979).

The effective Hamiltonian for the $^2\Pi$ electronic state is considered as follows,

$$\boldsymbol{H}_{\text{eff}} = \boldsymbol{H}_{\text{rot}} + \boldsymbol{H}_{\text{cd}} + \boldsymbol{H}_{\text{so}} + \boldsymbol{H}_{\text{sr}} + \boldsymbol{H}_{\Lambda}, \tag{1}$$

where, $\boldsymbol{H}_{\text{rot}}$ is the rotational energy term, $\boldsymbol{H}_{\text{cd}}$ the centrifugal distortion term of the rotational energy, $\boldsymbol{H}_{\text{so}}$ the spin-orbit interaction, which represents the electron spin coupling to the magnetic field by the electron orbital angular momentum, $\boldsymbol{H}_{\text{sr}}$ spin-rotation interaction, which arises from the electron spin coupling to the rotation of the molecules, and $\boldsymbol{H}_{\Lambda}$ Λ-type doubling term, which represents an interaction between the rotation of the molecule and its electronic orbital angular momentum. The $\boldsymbol{H}_{\Lambda}$ term breaks the twofold degeneracy of the ± (or *e* and *f*) levels, where levels with parity $+(-1)^{J-\frac{1}{2}}$ are called *e* levels, and levels with parity $-(-1)^{J-\frac{1}{2}}$ are called *f* levels. In this Section, in order

to describe these sub-levels, parity ± was used. For the CD and ^{18}OH radicals in the following Sections, *e* and *f* level notation was used.

Hyperfine splittings due to hydrogen nucleus were not observed. The magnitude of the splitting was calculated to be less than 5 MHz(< 0.0002 cm^{-1}) for the $J = 3.5 - 2.5$ transition (Ashworth and Brown, 1992), and for other observed $\Delta F = \Delta J$ transitions, the splittings were estimated to be much smaller than the linewidth (Ashworth and Brown, 1992). Therefore, we neglected the hyperfine structure in the calculation of the energy levels.

When the author analyzed only the present data, the standard deviation of the fitting was 0.00016 cm^{-1} that was 1/46 of the resolution used in the present measurement. In the final fitting, we also included Λ-type doubling frequencies observed by the MBER experiment (Meerts and Dymanus, 1974, 1975) which were corrected for the hyperfine structure, with a weight 5 x 10^5 compared with the present data. The determined molecular constants are listed in Table 3 - 1 - 2. The standard deviation of the least squares fitting was 0.00015 cm^{-1}. The spin-orbit interaction constant *A* was fixed to the value determined by the re-analysis (Ashworth and Brown, 1992) of the $A^2\Sigma^+ - X^2\Pi$ 0 - 0 band (Ramsay, 1952).

For comparison, Table 3 - 1 - 2 lists also the constants determined by Ashworth and Brown (1992) through the analysis of FIR LMR and other data. Discrepancies more than three standard deviations were recognized between the present and Ashworth and Brown's results. Since the present measurement was extended to larger *J* transitions, higher-order centrifugal distortion constants were needed in the analysis. However, when we compared the observed with the calculated frequencies predicted by Ashworth and Brown (1992), the discrepancy is within the error limit of the present measurement; for example, they calculated the $J = 5.5 - 4.5$ transition frequencies in $^2\Pi_{3/2}$ to be 101.35548(7) [observed at 101.35570(16)] cm^{-1} and 101.30355(7) [observed at 101.30366(16)] cm^{-1} for the Λ-type doubling. Ashworth and Brown (1992) reported the value p_D+2q_D = -0.727(40) x 10^{-4} cm^{-1}, which is about two times larger than the present value. Winkel and Davis (1984) reported p_v+2q_v = 0.2838(12) cm^{-1} and p_D = -3.26(14)

x 10^{-5} cm^{-1} from the analysis of FT infrared emission spectroscopy, which are in good agreement with the present results. The set of molecular constants determined in the present study can be used to calculate accurate frequencies in the far-infrared spectrum. These frequencies may be useful for future astronomical searches of SH.

3 - 1 - 4. Discussion

The present observation is the first example of far-infrared FT spectroscopy of transient species, as far as the author knows. The absorption due to transient species can be detectable owing to large transition moment in far-infrared region. The pure rotational spectrum of the OH radical with 20 % absorption by the same method was also observed. This FT spectroscopy may be applicable to other transient species.

The strongest SH line showed about 15 % absorption, and rotational temperature was estimated to be 486 ± 14 K by a Boltzmann plot for the observed lines. Then the density of the produced SH radical was estimated to be 1.0 x 10^{11} molecules/cm^3, adopting the dipole moment of 0.7580 D (Meerts and Dymanus, 1974). This indicates that the present absorption method needs 5 x 10^9 molecules/cm^3 for definitive detection. This sensitivity is lower than that of FIR LMR by two orders of magnitude, where the minimum detectable number of molecules in the 100 cm^{-1} region is reported to be 5 x 10^7 molecules/cm^3 by Evenson *et al.* (1980). FIR LMR is known to be one of the most sensitive method for detection of paramagnetic species, but the frequency coverage is limited in the region lower than 100 cm^{-1}. For lack of suitable laser source in the 200 - 400 cm^{-1} region, FT spectroscopy has advantage in carrying out a systematic observation of important radical species.

References

Ashworth, S. H. and Brown, J. M.1992, J. Mol. Spectrosc. **153,** 41.

Benidar, A., Farrenq, R., Guelachvili, G., and Chackerian, Jr., C. 1991, J. Mol. Spectrosc. **147,** 383.

Bernath, P. F., Amano, T., and Wong, M. 1983, J. Mol. Spectrosc. **98,** 20.

Brown, J. M. and Thistlethwaite, P. J. 1972, Mol. Phys. **23,** 635.

Brown, J. M., Colbourn, E. A., Watson, J. K. G., and Wayne, F. D. 1979, J. Mol. Spectrosc. **74,** 294.

Davies, P. B., Handy, B. J., Lloyd, E. K. M., and Russell, D. K. 1978, Mol. Phys. **36,** 1005.

Evenson, K. M., Saykally, R. J., Jennings, D. A., Curl, Jr., R. F., and Brown, J. M. 1980, "*Chemical and Biochemical Applications of Lasers,*" Academic Press, New York, P.95.

Guelachvili, G. and Narahari Rao, K. 1986, "*Handbook of Infrared Standards,*" Academic Press, San Diego.

Heiles, C. E. and Turner, B. E. 1971, Astrophys. Lett. **8,** 89.

Johns, J. W. and Ramsay, D. A. 1961, Canad. J. Phys. **39,** 210.

McDonald, C. C. 1963, J. Chem. Phys. **39,** 2587.

Meeks, M. L., Gordon, M. A., and Litvak, M. M. 1969, Science, **163,** 173.

Meerts, W. L. and Dymanus, A.1974, Astrophys. J. **187,** L45.

_____. 1975, Canad. J. Phys. **53,** 2123.

Porter, G. 1950, Discuss. Faraday Soc. **9,** 60.

Radford, H. E. and Linzer, M. 1963, Phys. Rev. Lett. **10**,443.

Ramsay, D. A. 1952, J. Chem. Phys. **20,** 1920.

Tanimoto, M. and Uehara, H. 1973, Mol. Phys. **25,** 1193.

Uehara, H. and Morino, Y. 1970, J. Mol. Spectrosc. **36,** 158.

Winkel, Jr., R. J. and Davis, S. P. 1984, Canad. J. Phys. **62,** 1420.

Table 3 - 1 - 1

Observed rotational lines of the SH radical in the $X^2\Pi$ state[a]

		Ω = 3/2		Ω = 1/2	
J'	J''	$\nu_{obs.}$	δ[b]	$\nu_{obs.}$	δ
3.5^{-}[c]	2.5^{+}	64.55151	12		
3.5^{+}	2.5^{-}	64.57291	-22		
4.5^{+}	3.5^{-}	82.94556	-13	86.83677	14
4.5^{-}	3.5^{+}	82.98117	-2	87.08091	10
5.5^{-}	4.5^{+}	101.30366	-9	106.02694	-12
5.5^{+}	4.5^{-}	101.35570	3	106.25396	3
6.5^{+}	5.5^{-}	119.61690	-11		
6.5^{-}	5.5^{+}	119.68761	1		
7.5^{-}	6.5^{+}				
7.5^{+}	6.5^{-}				
8.5^{+}	7.5^{-}	156.07269	25	163.05010	-14
8.5^{-}	7.5^{+}	156.18569	40	163.21240	8
9.5^{-}	8.5^{+}	174.19504	-10	181.83142	11
9.5^{+}	8.5^{-}	174.33063	-6	181.96873	-21
10.5^{+}	9.5^{-}	192.23417	5	200.47920	62[d]
10.5^{-}	9.5^{+}	192.39271	-20	200.59100	2
11.5^{-}	10.5^{+}	210.17846	-24	218.98060	1
11.5^{+}	10.5^{-}	210.36097	9	219.06774	42[d]
12.5^{+}	11.5^{-}	228.01797	9	237.32637	0
12.5^{-}	11.5^{+}	228.22342	9	237.38732	5
13.5^{-}	12.5^{+}				
13.5^{+}	12.5^{-}	245.96877	-7		

[a] cm^{-1} unit.

[b] (obs. - calc.) x 10^5.

[c] The superscript denotes parity.

[d] Weight is set to zero due to poor signal-to-noise ratio.

Table 3 - 1 - 2

Molecular constants of SH in the $X^2\Pi$ state[a]

Constant	Present Study	Ashworth & Brown(1992)
B	9.460 4416(81)	9.460 2840(11)
D x 10^4	4.839 74(82)	4.829 87(40)
H x 10^8	1.462(26)	
A[b]	-376.832(14)[c]	-376.832(14)[c]
γ[b]	-0.152 54(22)	-0.1468(33)
γ_D[b] x 10^4	0.1522(82)	
p_V	0.300 4428(19)	0.300 1519(79)
p_D x 10^4	-0.356(12)	
p_H x 10^7	-0.147(57)	
q_V x 10^2	-0.949 053(31)	-0.948 44(10)
q_D x 10^5	0.1888(17)	
q_H x 10^9	-0.43(16)	

[a]cm^{-1} unit. The numbers in parentheses denote one standard deviation and apply to the last digits of the constants.

[b]Effective constants. A_D was constrained to zero.

[c]Fixed to the value (Ashworth & Brown, 1992) determined by the re-analysis of Ramsay's optical data (Ramsay, 1952).

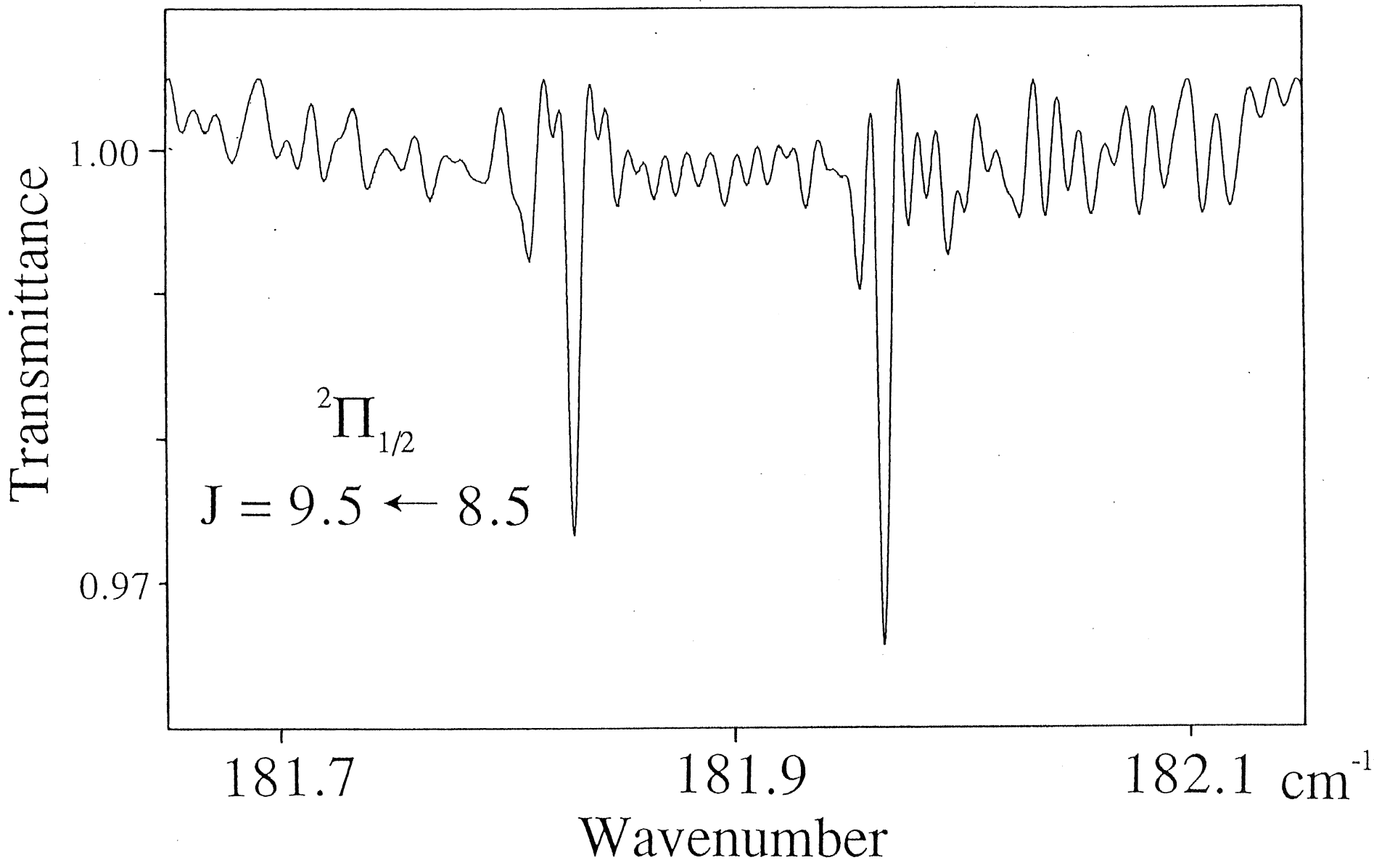

Figure 3 - 1 - 1. Observed spectrum of the $J = 9.5 - 8.5$ transition in the $^2\Pi_{1/2}$ state of the SH radical.

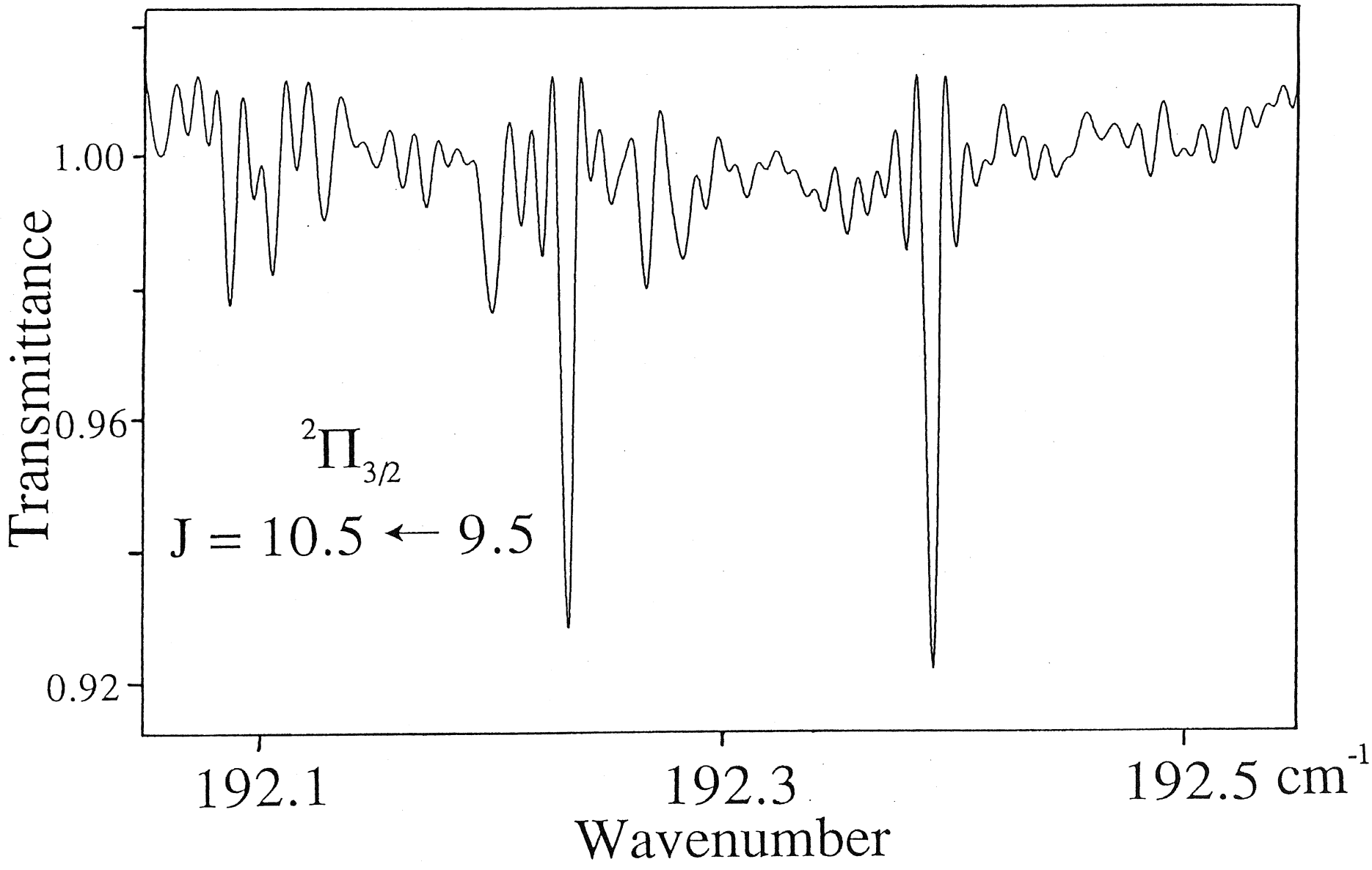

Figure 3 -1 - 2. Observed spectrum of the $J = 10.5 - 9.5$ transition in the $^2\Pi_{3/2}$ state of the SH radical.

3 - 2 Pure Rotational Spectra of the NH_2, NHD, and ND_2 Radicals

Abstract

The gas-phase far-infrared absorption spectra of the NH_2, NHD, and ND_2 radicals have been observed in the 51 - 366 cm^{-1} region with a high-resolution Fourier transform spectrometer. NH_2 was generated by a dc discharge in a NH_3 and Ar mixture, and NHD and ND_2 were generated by a dc discharge in a NH_3, D_2, and Ar mixture. The observed spectrum with a resolved fine structure was analyzed by a Watson's *A*-reduced Hamiltonian including a spin-rotation interaction term. The high-order rotational constants and spin-rotation parameters were determined. In the same experiment, the rotational spectrum of the NH radical was also observed.

From the determined rotational constants, inertia defect Δ and r_0 structure were determined, as follows with one standard deviation in parentheses,

	NH_2	ND_2
Δ_{obs} (amuÅ^2)	0.049571(8)	0.06775(5)
Δ_{calc} (amuÅ^2)	0.047653	0.066566
r(Å)	1.0242(29)	1.0240(18)
θ(degree)	103.39(42)	103.34(25)

The effective off-diagonal spin-rotation parameter ($\varepsilon_{ab} + \varepsilon_{ba}$) of NHD has been separated into two components by assuming a relation $\varepsilon_{ab}/\varepsilon_{ba} = A/B$.

3 - 2 - 1. Introduction

The NH_2 radical is an important intermediate species in considering NH_3 production mechanism in interstellar space. Cometary emission spectrum of the electronic transitions was observed by Swings, McKellar and Minkowski (1943). In interstellar space, the submillimeter wave transitions were first observed as absorption toward Sgr B2(N) and Sgr B2(M) by van Dishoeck *et al.* (1993). NH_2 was found to be located in a low-density envelope in front of the dense, hot cores of the molecular cloud.

In laboratory, there are a lot of studies for NH_2 in a wide wavelength region by many experimental techniques. The observations of the $\tilde{A}\,^2A_1$ - $\tilde{X}\,^2B_1$ electronic spectrum were carried out by emission, absorption, and laser-induced fluorescence techniques (Dressler and Ramsay, 1959; Johns, Ramsay, and Ross, 1976; Vervloet, Merienne-Lafore, and Ramsay, 1978; Vervloet and Merienne-Lafore, 1978; Birss *et al.* 1979; Birss *et al.* 1981; Vervloet and Merienne-Lafore, 1982; Vervloet, 1988; Chung-Hung, Shwu-Chyi, and Yit-Tsong, 1995). Infrared or Raman observations to study the vibration-rotation spectra were made by using a matrix isolation (Milligan and Jacox, 1965), laser magnetic resonance (Brown *et al.* 1977; Hills and McKellar, 1979a; Kawaguchi *et al.* 1980), tunable infrared laser (Amano. Bernath, and McKellar, 1982; Krivtsun *et al.* 1986), coherent anti-Stokes Raman (CARS) (Dreier and Wolfrum, 1984) and Fourier transform techniques (Burkholder, Howard, and McKellar 1988; McKellar *et al.* 1990). Far-infrared and submillimeter-wave observations to study rotational spectrum were carried out using a laser magnetic resonance (Hills *et al.* 1976; Davies *et al.* 1975; Davies *et al.* 1976; Davies *et al.* 1977), tunable laser (Cohen *at al.* 1989), and submillimeter wave spectrometer (Charo *et al.* 1981). The rotational and spin-rotation doublet spectra in ground and excited electronic states were observed by microwave optical double resonance (Cook, Hills, and Curl, 1976, 1977; Hills and Cook, 1976, 1977, 1982; Hills *et al.* 1976, 1978, 1982; Lowe *et al.* 1979) and microwave modulated saturation techniques (Kasper, Lowe, and Curl, 1979). The laser magnetic resonance spectrum of the excited electronic states and highly excited vibrationally states in the

ground electronic state were observed by using a infrared optical double resonance (Kawaguchi *et al.* 1987).

However, there are only a few studies for NHD. The electronic absorption spectrum was observed by Ramsay and Wayne (1979) with a grating spectrograph and with a tunable laser to determine the dipole moment by Brown, Chalkley, and Wayne (1979). The far-infrared laser magnetic spectrum was partly observed by Carrington *et al.* (1982). The spin-rotation doublet spectrum was measured using a microwave optical double resonance technique (Brown and Steimle, 1980; Steimle, and Brown, and Curl, 1980).

Dressler and Ramsay (1969) observed the electronic transition spectrum of ND_2 with a grating spectrograph. The laser magnetic resonance spectrum of the ν_2 band was measured by Hills and McKellar (1979b). Infrared optical double resonance spectrum was measured by Muenchausen and Hills (1983). The microwave optical double resonance technique was applied to observe spin-rotation doublet transitions in the ground electronic state by Cook and Hills (1983). Recently, Muenchausen *et al.* (1985) observed the electronic absorption spectrum and gave improved molecular parameters by simultaneous analysis with the data of microwave optical double resonance, laser magnetic, infrared optical double resonance. Kanada, Yamamoto, and Saito (1991) measured the pure rotational spectrum using a submillimeter microwave spectrometer, and determined the hyperfine coupling constants. However, there are no systematic observations of the rotational spectra of NHD and ND_2 in wide frequency range.

In the present study, the far-infrared absorption spectra of the rotational transitions of NH_2, NHD and ND_2 in the ground electronic state were observed with a high-resolution Fourier transform spectrometer combined with a dc discharge flow cell. The observed spectrum was analyzed by Watson's *A*-reduced Hamiltonian including a spin-rotation interaction term. The high-order rotational constants and spin-rotation interaction parameters were determined precisely.

3 - 2 - 2. Experimental

The experimental detail in this measurement was already described in Section 2 - 2. The NH_2 radical was produced by a dc discharge in a NH_3 and Ar mixture with partial pressures of 20 and 450 mTorr, respectively, and NHD and ND_2 were produced by a dc discharge in NH_3, D_2, and Ar mixture with 20, 30, 450 mTorr, respectively. The reaction products were pumped out continuously with a mechanical booster pump followed by a rotary pump. The dc discharge current was 150 mA for all radicals. The frequency region of 0 - 700 cm^{-1} was observed with a 0.0075 cm^{-1} resolution. The integration time was about 5.6 hr with 90 scans for NH_2, 4 hr with 67 scans for NHD and ND_2, and the noise level corresponded to 1 - 2 % absorption typically. The observed wavenumbers were calibrated against the rotational lines of H_2O in the 58 - 350 cm^{-1} region (Guelachvili and Narahari Rao, 1986).

3 - 2 - 3. Observed Spectrum and Analysis

The rotational spectrum of the NH_2 radical was observed with a resolved fine structure by a spin-rotation interaction in the 51 - 366 cm^{-1} region, where the lower frequency side was limited by the transmittance of the 23 μm Mylar beamsplitter, and the upper side was limited by the population of radical. No spectral lines were observed in the 128 - 152 and 261 - 294 cm^{-1} region because of low transmittance of the beamsplitter. The strongest lines showed about 55 % absorption. Figure 3 - 2 - 1 shows a typical spectrum of the rotational transitions of NH_2 with their assignments. Rotational transitions in the lowest vibrational state (010) were not observed, where the transition frequencies were calculated by molecular constants reported by Burkholder, Howard, and McKellar (1988). The assignments of the pure rotational transitions were carried out based on calculated frequencies with the molecular parameters by Burkholder, Howard, and McKellar (1988). The observed frequencies are listed in Table 3 - 2 - 1 with their

assignments. The maximum values of N' and K'_a in the assigned transitions were14 and 8, respectively.

The rotational spectrum of NHD was observed in the 103 - 363 cm^{-1} region, where the lower frequency side was limited by low transmittance of 6 μm Mylar beamsplitter, and the upper side was due to the population of the radical. The strongest line showed more than 50 % absorption. The typical spectrum of NHD is shown in Figure 3 - 2 - 2 with its assignment, together with the ND_2 spectrum. The observed lines were assigned using molecular parameters reported by Steimle, Brown, and Curl (1980) as listed in Table 3 - 2 - 2, but their parameters were only applicable to the energy levels with low N, K values up to 6. The assignments of higher N, K levels were done through step by step determination of the new parameters. The maximum values of N' and K'_a are 14 and 10, respectively. NHD has the dipole moment of 0.665(2) Debye along a-axis (Brown, Chalkley, and Wayne, 1979), because the principal axes of inertia a and b are rotated by 21.43° from those of NH_2. Therefore, NHD is expected to have a-type transitions in relatively lower frequency region, but a-type transitions of NHD were not detected because of large noise level of 5 % in the low frequency region by beamsplitter. The strongest line of the a-type transition is estimated to have 6 % absorption in the 100 cm^{-1} region, which is an order of magnitude weaker than b-type transitions.

The spectrum of ND_2 was observed in 102 - 265 cm^{-1}. The strongest absorption was more than 45 %. A typical spectrum of ND_2 is shown in Figure 3 - 2 - 2 with its assignment. The transitions of ND_2 were assigned based on calculated frequencies reported by Muenchausen *et al.* (1985), and listed Table 3 - 2 - 3. The maximum N' and K'_a values assigned in the present study are 13 and 10, respectively.

In the same experiment as NH_2, the rotational spectrum of the NH radical in the $X^3\Sigma^-$ state was also observed. The NH intensity observed in a condition of 300 mA discharge current was stronger than that in 150 mA discharge current by a factor of about 1.5. The strongest absorption was more than 10 %. The observed transitions of NH were assigned based on the frequencies calculated by term values reported by Brazier, Ram, and Bernath (1986). The observed frequencies of NH are listed in Table 3 - 2 - 4. Those

frequencies were calibrated against the rotational lines of H_2O in 117 - 350 cm^{-1} region (Guelachvili and Narahari Rao, 1986).

The observed spectral lines of the aminogen radical were analyzed by a least squares fitting procedure. The effective Hamiltonian for asymmetric-top molecule with an unpaired electron is expressed as follows,

$$\boldsymbol{H}_{\text{eff}} = \boldsymbol{H}_{\text{rot}} + \boldsymbol{H}_{\text{cd}} + \boldsymbol{H}_{\text{sr}} + \boldsymbol{H}_{\text{srcd}} \tag{1}$$

where $\boldsymbol{H}_{\text{rot}}$ is the rotational energy term, $\boldsymbol{H}_{\text{cd}}$ the centrifugal distortion term for rotational energy, $\boldsymbol{H}_{\text{sr}}$ the spin-rotation coupling term, and $\boldsymbol{H}_{\text{srcd}}$ the centrifugal distortion term for spin-rotation coupling. The terms including the hyperfine and other smaller interactions have been omitted, because splittings by these effects were smaller than the observed linewidth. The rotational term and centrifugal distortion term of the Hamiltonian are given by

$$\begin{aligned}
\boldsymbol{H}_{\text{rot}} + \boldsymbol{H}_{\text{cd}} = {} & \tilde{A}N_a^2 + \tilde{B}N_b^2 + \tilde{C}N_c^2 - \Delta_N(\mathbf{N}^2)^2 - \Delta_{KN}\mathbf{N}^2N_a^2 - \Delta_K N_a^4 \\
& -2\delta_N\mathbf{N}^2(N_b^2 - N_c^2) - \delta_K[N_a^2,(N_b^2 - N_c^2)]_+ \\
& +H_N(\mathbf{N}^2)^3 + H_{NK}(\mathbf{N}^2)^2N_a^2 + H_{KN}\mathbf{N}^2N_a^4 + H_K N_a^6 \\
& +2h_N(\mathbf{N}^2)^2(N_b^2 - N_c^2) + h_{NK}\mathbf{N}^2[N_a^2,(N_b^2 - N_c^2)]_+ + h_K[N_a^4,(N_b^2 - N_c^2)]_+ \\
& +L_N(\mathbf{N}^2)^4 + L_{NNK}(\mathbf{N}^2)^3N_a^2 + L_{NK}(\mathbf{N}^2)^2N_a^4 + L_{KKN}\mathbf{N}^2N_a^6 + L_K N_a^8 \\
& +2l_N(\mathbf{N}^2)^3(N_b^2 - N_c^2) + l_{NK}(\mathbf{N}^2)^2[N_a^2,(N_b^2 - N_c^2)]_+ \\
& +l_{KN}\mathbf{N}^2[N_a^4,(N_b^2 - N_c^2)]_+ + l_K[N_a^6,(N_b^2 - N_c^2)]_+ .
\end{aligned} \tag{2}$$

The centrifugal distortion corrections are expressed in the *A*-reduced from (Watson, 1977). The spin-rotation coupling and its centrifugal distortion terms are expressed as follows (Brown and Sears, 1979),

$$\begin{aligned}
\boldsymbol{H}_{\text{sr}} + \boldsymbol{H}_{\text{srcd}} = {} & \varepsilon_{aa}N_aS_a + \varepsilon_{bb}N_bS_b + \varepsilon_{cc}N_cS_c + (\varepsilon_{ab} + \varepsilon_{ba})(N_aS_b + N_bS_a)/2 \\
& +\Delta_N^S\mathbf{N}^2(\mathbf{N}\cdot\mathbf{S}) + (1/2)\Delta_{NK}^S[\mathbf{N}^2, N_aS_a]_+ + \Delta_{KN}^S N_a^2(\mathbf{N}\cdot\mathbf{S}) + \Delta_K^S N_a^3S_a \\
& +2\delta_N^S(N_b^2 - N_c^2)(\mathbf{N}\cdot\mathbf{S}) + \delta_K^S[N_aS_a,(N_b^2 - N_c^2)]_+ .
\end{aligned} \tag{3}$$

For NH_2 and ND_2, the off diagonal components of the spin-rotation coupling term $\varepsilon_{ab} + \varepsilon_{ba}$ do not exist, and for NHD these terms are included. Sextic spin-rotation term, H_K^S which was not considered by Brown and Sears (1979), was also added to the Hamiltonian in this analysis. As McKellar *et al.* (1990) assumed, the appropriate matrix

elements of H_K^S are obtained simply by replacing the quartic parameter Δ_K^S with $\Delta_K^S + N_a^2 H_K^S$.

For NH_2, when the observed 232 lines were analyzed, the standard deviation of the fitting was 0.00069 cm^{-1} that was 1/11 of the resolution in this measurement, and the accuracy of molecular parameters in this fitting was not better than those of the previous molecular parameters (Burkholder, Howard, and McKellar, 1988). Therefore, the spin-rotation doublet frequencies observed by the microwave optical double resonance experiment (Cook, Hills, and Curl, 1977) were included in the fitting with weight of 1710 compared with the present data, after the correction of hyperfine structure. The determined molecular parameters are listed in Table 3 - 2 - 5. The standard deviation of the least squares fitting was 0.00069 cm^{-1}, which was the same as the first fitting.

For NHD the observed 200 lines were analyzed. The spin-rotation doublet and a-type rotational frequencies by the microwave optical double resonance experiment (Steimle, Brown, and Curl, 1980) were also included with weight of 1958 compared with the present data. The molecular parameters were more accurately determined than the previous study (Steimle, Brown, and Curl, 1980). The standard deviation of the least squares fitting was 0.00082 cm^{-1} that was 1/9 of the resolution. The determined molecular parameters are listed in Table 3 - 2 - 6.

For ND_2, the observed 177 lines were analyzed, but the accuracy of molecular parameters in this fitting was not better than that of previous molecular parameters (Muenchausen *et al.* 1985). As in the case of NH_2 fitting, the spin-rotation doublet frequencies observed by the microwave optical double resonance experiment (Cook and Hills, 1983; Muenchausen *et al.* 1985) were analyzed simultaneously with a weight of 1716 compared with the present data. The determined molecular parameters are listed in Table 3 - 2 - 7. The standard deviation of this fitting was 0.00065 cm^{-1} that was 1/12 of the resolution in this observation.

3 - 2 - 4. Discussion

Fourier transform far-infrared spectroscopy was applied to the NH_2, NHD, and ND_2 radicals. In this study, the pure rotational transitions of NH_2, NHD, and ND_2 were systematically observed in a wide frequency range with high-resolution. The precise molecular parameters in the ground state were obtained, as listed in Tables 3 - 2 - 5, 3 - 2 - 6, and 3 - 2 - 7. The higher-order molecular parameters were also determined, but they were not consistent with previous parameters, because in this study the high N and K transitions were included. The major molecular parameters are consistent with those determined by previous studies. The directly observed frequencies in this experiment seem to be very useful for far-infrared and submillimeter wave astronomical observation.

The r_0 structure were determined form the molecular constants:

r (NH_2) = 1.0242(29) Å r (ND_2) = 1.0240(18) Å

θ(NH_2) = 103.39(42) Degree θ(ND_2) =103.34(25) Degree

where the numbers in parentheses denote one standard deviation and apply to the last digit of constants. These values were consistent with previous values reported by Dressler and Ramsay (1959).

In a planar molecule like NH_2, a relation among the principal moments of inertia $I_c = I_a + I_b$ should be hold for a rigid molecule. But, actually the relation is not hold because of the effect of vibration, centrifugal, and electronic effects. The inertia defect is defined as $\Delta^0_{obs} = I^0_C - I^0_A - I^0_B$, which has a small positive value in usual planar molecules. Thus, the value is useful for confirming the validity of the determined parameters. The inertia defects of NH_2 and ND_2 were determined from the observed rotational constants, and compared with the theoretical values estimated from a formula of $\Delta_{calc} = \Delta_{vib} + \Delta_{cent} + \Delta_{elec}$ (Oka and Morino, 1961). For the calculations of NH_2, the following values used; the Coriolis constant of $\zeta^{(c)}_{13} = 0.00071$ (Amano, Bernath, and McKellar, 1982), g-factors reported by Brown and Sears (1979), vibrational frequencies of the ν_1, ν_2, and ν_3 bands determined by McKellar *et al.* (1980) and Burkholder, Howard, and McKellar (1988), and the rotational constants determined in this study. For

ND_2, $\zeta_{13}^{(c)}$ is assumed to be equal to the value of D_2O because of the almost same mass ratio between H_2O and NH_2 or D_2O and ND_2, the g-factors reported by McKellar (1981) were used, and the rotational constants determined in this study were used. Since only the ν_2 vibrational frequency was reported by Muenchausen *et al.* (1986), the ν_1, and ν_3 frequencies were estimated from the NH_2 ν_1 and ν_3 frequencies, using a isotope effect (Herzberg, 1945). These results are listed in Table 3 - 2 - 8 together with those of H_2O and D_2O. The observed inertia defects of aminogen radical agree with the calculated values. Although the vibrational and centrifugal distortion contributions to the inertia defect in aminogen radical are almost equal to those in water due to the similar mass, the electronic contributions to the inertia defect in aminogen radical are much larger than those in water, because aminogen radical have the low electronic excited state in 10249 cm^{-1} (NH_2) and 10393 cm^{-1} (ND_2) (Dressler and Ramsay, 1959), and water has it in ultra-violet region. The inertia defect of the deuterated species are larger than those of normal species, since vibrational frequencies of deuterated species are smaller than those of normal species.

For NHD the spin-rotation interaction constants agree with those by the microwave optical double resonance experiment (Steimle, Brown, and Curl, Jr. 1980), but the value of ε_{cc} does not agree with that by the optical measurement (Ramsay and Wayne, 1979). However the value of ε_{cc} was not determined by the microwave optical double resonance experiment. In the present study, all major spin rotation interaction constants were determined for the first time.

The five independent parameters of the spin-rotation coupling were determined by assuming relationship $\varepsilon_{ab}/\varepsilon_{ba} = A/B$. This calculation was carried out for by Brown, Radford, and Sears (1991) for HCO. Using the values for the reduced spin-rotation parameter given in Table 3 - 2 - 6, the author obtains,

ε_{aa} = -0.234884 cm^{-1} ε_{bb} = -0.038355 cm^{-1}

ε_{ab} = 0.073431 cm^{-1} ε_{ba} = 0.029618 cm^{-1},

where the effective parameter ($\varepsilon_{ab} + \varepsilon_{ba}$) has been assumed to be positive. Brown, Sears, Watson (1980) calculated spin-rotation parameters by considering the isotope dependence

to be $\varepsilon_{ab} = 0.0655\ cm^{-1}$ and $\varepsilon_{ba} = 0.0266\ cm^{-1}$, which were consistent with the values in the present study.

References

Amano, T., Bernath, P. F., and McKellar, A. R. W. 1982, J. Mol. Spectrosc. **94,** 100.

Benedict, W. S., Gailar, N., and Plyler, E. K. 1956, J. Chem. Phys. **24,** 1139.

Briss, F. W., Ramsay, D. A., Ross, S. C., and Zauli. C. 1979, J. Mol. Spectrosc. **78,** 344.

Briss, F. W., Merienne-Lafore, M. -F., Ramsay, D. A., and Vervloet, M. 1981, J. Mol. Spectrosc. **85,** 493.

Brazier, C. R., Ram, R. S., and Bernath, P. F. 1986, J. Mol. Spectrosc. **120,** 381.

Brown, J. M., Buttenshaw, J., Carrington, A., and Parent, C. R. 1977, Mol. Phys. **33,** 589.

Brown, J. M., Chalkley, S. W., and Wayne, F. D. 1979, Mol. Phys. **38,** 1521.

Brown, J. M., Radford, H. E., and Sears, T. J., 1991, J. Mol. Spectrosc. **148,** 20.

Brown, J. M and Sears, T. J. 1979, J. Mol. Spectrosc. **75,** 111.

Brown, J. M., Sears, T. J., and Watson, J. K. G. 1980, Mol. Phys. **41,** 173.

Brown, J. M. and Steimle, T. C. 1980, Astrophys. J. **236,** L101.

Burkholder, J. B., Howard, C. J., and McKellar, A. R. W. 1988, J. Mol. Spectrosc. **127,** 415.

Carrington, A., Geiger, J. S., Smith, D. R., Bonnett, J. D., and Brown. C. 1982, Chem. Phys. Lett. **90,** 6.

Charo, A., Sastry, K. V. L., Herbst, E., and De Lucia, C. 1981, Astrophys. J. **244,** L111.

Chung-Hung C, Shwu-Chyi, L., and Yit-Tsong, C., 1995, J. Mol. Spectrosc. **169,** 427.

Cohen, R. C., Busarow, K. L, Schmuttenmaer, C. A., Lee, Y. T., and Saykally, R. J. 1989, Chem. Phys. Lett. **164,** 321.

Cook, J. M., Hills, G. W., and Curl, Jr., R. F. 1976, Astrophys. J. **207,** L139.

_____. 1977, J. Chem. Phys. **67,** 1450.

_____. 1983, J. Chem. Phys. **78,** 2144.

Davies, P. B., Russell, D. K., Thrush, B. A., and Wayne, F. D. 1975, J. Chem. Phys. **62,** 3739.

Davies, P. B., Russell, D. K., Thrush, B. A., and Radford, H. E. 1976, Chem. Phys. Lett. **42,** 35.

_____. 1977, Proc. R. Soc. Lond. A, **353,** 299.

Dreier, T. and Wolfrum, J. 1984, Appl. Phys. B. **33,** 213.

Dressler, K. and Ramsay, D. A. 1959, Philos. Trans. R. Soc. London Ser. A **251,** 553.

Guelachvili, G. and Narahari Rao, K. 1986, "*Handbook of Infrared Standards*", Academic Press, San Diego.

Herzberg, G. 1945, "*Molecular Spectra and Molecular Structure, II Infrared and Raman Spectra of Polyatomic Molecules*," Van Nostrand Reinhold Co. Inc.

Hills, G. W., Brazier, C. R. Brown, J. M., Cook, J. M. and Curl, Jr., R. F., 1982, J. Chem. Phys. **76,** 240.

Hills, G. W. and Cook, J. M. 1976, Astrophys. J. **209,** L157.

_____. 1977, J. Chem. Phys. **66,** 1507.

_____. 1982, J. Mol. Spectrosc. **94,** 456.

Hills, G. W., Cook, J. M., Curl, Jr., R. F., and Tittel, F. K. 1976, J. Chem. Phys. **65,** 823.

Hills, G. W., Lowe. R. S., Cook. J. M., and Curl, Jr., R. F. 1978, J. Chem. Phys. **68,** 4073.

Hills, G. W. and McKellar, A. R. W. 1979a, J. Mol. Spectrosc. **74,** 224.

_____. 1979b, J. Chem. Phys. **71,** 3330.

Johns, J. W. C., Ramsay, D. A., and Ross, S. C. 1976, Canad. J. Phys. **54,** 1804.

Kanada, M., Yamamoto, S., and Saito, S. 1991, J. Chem. Phys. **94,** 3423.

Kasper, J. V. V., Lowe, R. S. and, Curl, Jr. R. F. 1979, J. Chem. Phys. 70, 3350.

Kawaguchi, K., Yamada, C., Hirota, E., Brown, J. M., Buttenshaw, J. Parent, C. R., and Sears, T. J. 1980, J. Mol. Spectrosc. **81,** 60.

Kawaguchi, K., Suzuki, T., Saito, S., and Hirota, E. 1987, J. Opt. Soc. Am. B. **4,** 1203.

Krivtsun, V. M., Nadezhdin, B. B., Britov, A. D., Zasavitskii, I. I., and Shotov, A. P. 1986, Opt. Spectrosc.(USSR) **60,** 720.

Lowe, R. S., Kasper, J. V. V., Hills. G. W., Dillenschneider, M., and Curl, Jr., R. F. 1979, J. Chem. Phys. **70,** 3356.

McKellar, A. R. 1981, Frad. Discuss. Chem. Soc. **71,** 63.

McKellar, A. R. W., Vervloet, M., Burkholder, J. B., and Howard, C. J. 1990, J. Mol. Spectrosc. **142,** 319.

Milligan, D. E. and Jacox, M. E. 1965, J. Chem. Phys. **43,** 4487.

Muenchausen, R. E. and Hills, G. W. 1983, Chem. Phys. Lett. **99,** 335.

Muenchausen, R. E., Hills, G. W., Merienne-Lafore, M. F., Ramsay, D. A., Vervloet, M, and Birss. F. W. 1985, J. Mol. Spectrosc. **112,** 203.

Oka, T. and Morino, Y. 1961, J. Mol. Spectrosc. **8,** 9.

Ramsay, D. A. and Wayne, F. D. 1979, Canad. J. Phys. **57,** 761.

Steimle, T. C., Brown, J. M., and Curl, Jr., R. F. 1980, J. Chem. Phys. **73,** 2552.

Swings, P., McKellar, A., and Minkowski, R. 1943, Astrophys. J. **98,** 142.

van Dishoeck, E. F., Jansen, D. J., Schilke, P., and Phillips, T. G. 1993, Astrophys. J. **416,** L83.

Vervloet, M. 1988, Mol. Phys. **63,** 433.

Vervloet, M., Merienne-Lafore, M. -F., and Ramsay. D. A. 1978, Chem. Phys. Lett. **57,** 5.

Vervloet, M. and Merienne-Lafore, M. -F. 1978, J. Chem. Phys. **69,** 1257.

Vervloet, M. and Merienne-Lafore, M. -F. 1982, Canad. J. Phys. **60,** 49.

Watson, J. K. G. 1977, "*Vibrational Spectra and Structures, A Series of Advances,*" Dekker, New York, Vol. **6,** P. 1.

Table 3 - 2 - 1

Observed rotational transitions of the NH_2 radical in the $\tilde{X}\,^2B_1$ state[a]

N'	K'_a	K'_c	J'	N''	K''_a	K''_c	J''	$\nu_{obs.}$	δ[b]
3	0	3	2.5	2	1	2	1.5	51.41156	-99
3	0	3	3.5	2	1	2	2.5	51.47902	-170[c]
6	2	4	6.5	6	1	5	6.5	53.84246	65
6	2	4	5.5	6	1	5	5.5	53.93129	36
3	2	2	3.5	3	1	3	3.5	54.06621	46
3	2	2	2.5	3	1	3	2.5	54.35363	8
4	3	1	4.5	4	2	2	4.5	54.64342	-44
4	3	1	3.5	4	2	2	3.5	54.94365	-10
3	3	0	3.5	3	2	1	3.5	59.45147	60
3	1	3	3.5	2	0	2	2.5	62.68469	52
3	1	3	2.5	2	0	2	1.5	62.75049	51
4	1	3	3.5	3	2	2	2.5	64.46703	-108
4	2	3	4.5	4	1	4	4.5	64.60557	60
4	1	3	4.5	3	2	2	3.5	64.66659	-63
4	2	3	3.5	4	1	4	3.5	64.84821	-49
3	3	1	3.5	3	2	2	3.5	65.05627	-81
3	3	1	2.5	3	2	2	2.5	65.44562	-184[c]
5	1	4	5.5	5	0	5	5.5	66.32511	-105
5	1	4	4.5	5	0	5	4.5	66.46787	-65
4	3	2	4.5	4	2	3	4.5	68.23806	-66
4	3	2	3.5	4	2	3	3.5	68.54714	-114
4	0	4	3.5	3	1	3	2.5	70.93019	-12
4	0	4	4.5	3	1	3	3.5	70.95805	-12
5	3	3	5.5	5	2	4	5.5	73.70255	-1
5	3	3	4.5	5	2	4	4.5	73.95658	-38
4	1	4	4.5	3	0	3	3.5	76.81673	60
4	1	4	3.5	3	0	3	2.5	76.85196	78
6	4	2	6.5	6	3	3	6.5	77.16735	-35
5	2	4	5.5	5	1	5	5.5	77.40466	64
6	4	2	5.5	6	3	3	5.5	77.45922	-172[c]
5	2	4	4.5	5	1	5	4.5	77.62642	61
2	2	1	2.5	1	1	0	1.5	78.86347	-2
2	2	1	1.5	1	1	0	0.5	79.12751	72
6	3	4	6.5	6	2	5	6.5	81.70727	-16
6	3	4	5.5	6	2	5	5.5	81.92656	21
5	4	1	5.5	5	3	2	5.5	82.53264	38
5	4	1	4.5	5	3	2	4.5	82.87736	-92
2	2	0	2.5	1	1	1	1.5	84.89557	41
2	2	0	1.5	1	1	1	0.5	85.19113	2
2	2	0	1.5	1	1	1	1.5	85.42280	47
4	4	0	4.5	4	3	1	4.5	85.50543	-91
6	1	5	6.5	6	0	6	6.5	85.63920	-31
6	1	5	5.5	6	0	6	5.5	85.80376	-61
4	4	0	3.5	4	3	1	3.5	85.92274	-116
4	4	1	4.5	4	3	2	4.5	86.94363	-163[c]
4	4	1	3.5	4	3	2	3.5	87.35666	-173[c]
5	4	2	5.5	5	3	3	5.5	87.54253	-81
5	4	2	4.5	5	3	3	4.5	87.87905	-104

Table 3 - 2 - 1- *Continued*

N'	K'_a	K'_c	J'	N''	K''_a	K''_c	J''	$\nu_{obs.}$	δ^b
5	0	5	4.5	4	1	4	3.5	88.89380	19
5	0	5	5.5	4	1	4	4.5	88.90405	7
5	1	4	4.5	4	2	3	3.5	90.51244	-100
5	1	4	5.5	4	2	3	4.5	90.62429	-86
8	0	8	8.5	8	1	7	8.5	91.04712	-74
8	0	8	7.5	8	1	7	7.5	91.15400	-42
5	1	5	5.5	4	0	4	4.5	91.57853	6
5	1	5	4.5	4	0	4	3.5	91.59595	56
6	2	5	6.5	6	1	6	6.5	91.91121	126
6	2	5	5.5	6	1	6	5.5	92.12219	45
7	3	5	7.5	7	2	6	7.5	92.18008	-2
7	3	5	6.5	7	2	6	6.5	92.37658	-3
7	4	4	7.5	7	3	5	7.5	92.75540	-48
7	4	4	6.5	7	3	5	6.5	92.99568	-67
6	2	4	5.5	5	3	3	4.5	94.07035	-58
6	2	4	6.5	5	3	3	5.5	94.29654	20
3	2	2	3.5	2	1	1	2.5	95.25754	17
3	2	2	2.5	2	1	1	1.5	95.46403	25
8	5	3	7.5	8	4	4	7.5	100.21101	9
7	1	6	7.5	7	0	7	7.5	104.36407	-60
7	1	6	6.5	7	0	7	6.5	104.54849	-30
8	3	6	8.5	8	2	7	8.5	104.74990	-58
8	3	6	7.5	8	2	7	7.5	104.93243	-151[d]
7	5	2	7.5	7	4	3	7.5	104.93243	242[d]
7	5	2	6.5	7	4	3	6.5	105.24233	-106
6	0	6	5.5	5	1	5	4.5	105.91997	156[d]
6	0	6	6.5	5	1	5	5.5	105.91997	-166[d]
9	4	6	9.5	9	3	7	9.5	106.61916	2
9	4	6	8.5	9	3	7	8.5	106.80336	-158[c]
6	1	6	6.5	5	0	5	5.5	107.04528	-68
6	1	6	5.5	5	0	5	4.5	107.05429	62
7	2	6	7.5	7	1	7	7.5	107.52749	54
6	5	1	6.5	6	4	2	6.5	107.61763	11
7	2	6	6.5	7	1	7	6.5	107.73593	48
6	5	1	5.5	6	4	2	5.5	107.97176	31
6	5	2	6.5	6	4	3	6.5	108.86112	21
7	5	3	7.5	7	4	4	7.5	108.87737	7
5	5	1	5.5	5	4	2	5.5	109.03263	76
4	2	3	4.5	3	1	2	3.5	109.16487	76
7	5	3	6.5	7	4	4	6.5	109.18059	74
4	2	3	3.5	3	1	2	2.5	109.31985	67
5	5	1	4.5	5	4	2	4.5	109.44430	128
6	1	5	5.5	5	2	4	4.5	114.09575	-122
6	1	5	6.5	5	2	4	5.5	114.15618	-93
3	2	1	3.5	2	1	2	2.5	115.35108	70
3	2	1	2.5	2	1	2	1.5	115.61274	36
5	2	4	5.5	4	1	3	4.5	121.20876	106
5	2	4	4.5	4	1	3	3.5	121.33077	92
7	0	7	7.5	6	1	6	6.5	122.46639	-40[e]
7	0	7	6.5	6	1	6	5.5	122.46639	16[e]

Table 3 - 2 - 1- *Continued*

N'	K'_a	K'_c	J'	N''	K''_a	K''_c	J''	$\nu_{obs.}$	δ^b
7	1	7	7.5	6	0	6	6.5	122.92070	141[d]
7	1	7	6.5	6	0	6	5.5	122.92070	-218[d]
3	3	1	3.5	2	2	0	2.5	127.18073	-17
3	3	1	2.5	2	2	0	1.5	127.45393	-75
4	2	2	4.5	3	1	3	3.5	152.50499	100
4	2	2	3.5	3	1	3	2.5	152.74473	42
4	3	1	4.5	3	2	2	3.5	153.08165	-44
4	3	1	3.5	3	2	2	2.5	153.33325	-126
8	1	7	7.5	7	2	6	6.5	153.52329	-47
8	1	7	8.5	7	2	6	7.5	153.53384	-92
9	0	9	9.5	8	1	8	8.5	154.97943	-19[e]
9	0	9	8.5	8	1	8	7.5	154.97943	-25[e]
9	1	9	9.5	8	0	8	8.5	155.04971	-21[e]
9	1	9	8.5	8	0	8	7.	155.04971	-121[e]
8	2	7	8.5	7	1	6	7.5	158.35839	90
8	2	7	7.5	7	1	6	6.5	158.38578	182[c]
5	3	3	5.5	4	2	2	4.5	161.13946	21
5	3	3	4.5	4	2	2	3.5	161.36389	-27
9	3	6	8.5	8	2	7	7.5	170.82674	134[d]
9	3	6	9.5	8	2	7	8.5	170.82674	-152[d]
10	0	10	10.5	9	1	9	9.5	171.10014	97[e]
10	0	10	9.5	9	1	9	8.5	171.10014	56[e]
10	1	10	10.5	9	0	9	9.5	171.12762	-18[e]
10	1	10	9.5	9	0	9	8.5	171.12762	-80[e]
9	2	8	9.5	8	1	7	8.5	173.04648	17
9	2	8	8.5	8	1	7	7.5	173.06054	-22
4	4	1	4.5	3	3	0	3.5	173.28366	-88
6	3	4	6.5	5	2	3	5.5	173.32490	32
6	3	4	5.5	5	2	3	4.5	173.51425	-38
4	4	0	4.5	3	3	1	3.5	173.53070	-65
4	4	1	3.5	3	3	0	2.5	173.55574	-78
4	4	0	4.5	4	1	3	3.5	173.70892	-84
4	4	0	3.5	3	3	1	2.5	173.80997	-98
4	4	0	3.5	3	3	1	3.5	174.61133	-56
5	3	2	5.5	4	2	3	4.5	181.49600	-27
5	3	2	4.5	4	2	3	3.5	181.71484	-44
7	3	5	7.5	6	2	4	6.5	183.14579	77
7	3	5	6.5	6	2	4	5.5	183.30014	49
10	1	9	9.5	9	4	6	8.5	184.48406	35
10	1	9	10.5	9	4	6	9.5	184.63064	-2
11	0	11	11.5	10	1	10	10.5	187.15821	115[e]
11	0	11	10.5	10	1	10	9.5	187.15821	84[e]
11	1	11	11.5	10	0	10	10.5	187.16892	-52[e]
11	1	11	10.5	10	0	10	9.5	187.16892	-92[e]
6	3	3	6.5	6	0	6	6.5	187.32895	42
10	3	7	10.5	9	2	8	9.5	187.40810	-1[e]
10	3	7	9.5	9	2	8	8.5	187.40810	-51[e]
10	2	9	10.5	9	3	6	9.5	188.39442	-51
10	2	9	9.5	9	3	6	8.5	188.40356	46

Table 3 - 2 - 1- *Continued*

N'	K'_a	K'_c	J'	N''	K''_a	K''_c	J''	$\nu_{obs.}$	δ^b
8	3	6	8.5	7	2	5	7.5	191.82695	68
8	3	6	7.5	7	2	5	6.5	191.94600	11
5	4	2	5.5	4	3	1	4.5	194.03796	-77
5	4	2	4.5	4	3	1	3.5	194.29959	-91
5	4	1	5.5	4	3	2	4.5	195.78906	-76
5	4	1	4.5	4	3	2	3.5	196.04486	-42
5	2	3	5.5	4	1	4	4.5	196.24268	-5
5	2	3	4.5	4	1	4	3.5	196.48140	67
10	4	6	9.5	9	3	7	8.5	198.25673	-98
10	4	6	10.5	9	3	7	9.5	198.28664	45
9	3	7	9.5	8	0	8	8.5	200.87554	60
9	3	7	8.5	8	0	8	7.5	200.96030	40
12	2	10	12.5	11	1	11	11.5	203.15777	223[d]
12	2	10	11.5	11	1	11	10.5	203.15777	202[d]
12	1	12	12.5	11	0	11	11.5	203.15777	-393[d]
12	1	12	11.5	11	0	11	10.5	203.15777	-418[d]
11	3	8	11.5	10	2	9	10.5	203.61838	23[d]
11	3	8	10.5	10	2	9	9.5	203.61838	-141[d]
11	2	10	11.5	10	3	7	10.5	204.05178	150[d]
11	2	10	10.5	10	3	7	9.5	204.05178	-347[d]
4	3	2	4.5	3	0	3	3.5	209.66039	57
4	3	2	3.5	3	0	3	2.5	210.24837	21
10	3	8	10.5	9	4	5	9.5	211.48970	93
10	3	8	9.5	9	4	5	8.5	211.54362	6
6	4	3	6.5	5	3	2	5.5	212.73067	-79
6	4	3	5.5	5	3	2	4.5	212.97751	-100
6	3	3	6.5	5	2	4	5.5	215.84596	-18
6	3	3	5.5	5	2	4	4.5	216.03810	-27
11	4	7	10.5	10	3	8	9.5	217.12571	-252[c]
11	4	7	11.5	10	3	8	10.5	217.14112	147
5	5	1	5.5	4	4	0	4.5	217.56549	123
5	5	0	5.5	4	4	1	4.5	217.60247	112
5	5	1	4.5	4	4	0	3.5	217.82119	157
5	5	0	4.5	4	4	1	3.5	217.85754	102
5	5	1	4.5	4	4	0	4.5	218.90170	154
5	5	0	4.5	4	4	1	4.5	218.93897	175
13	2	11	13.5	12	1	12	12.5	219.09522	255[d]
13	2	11	12.5	12	1	12	11.5	219.09522	242[d]
13	1	13	13.5	12	2	10	12.5	219.09522	-131[d]
13	1	13	12.5	12	2	10	11.5	219.09522	-147[d]
6	4	2	6.5	5	3	3	5.5	219.31064	-64
6	4	2	5.5	5	3	3	4.5	219.54140	-95
12	3	9	12.5	11	2	10	11.5	219.62862	11[d]
12	3	9	11.5	11	2	10	10.5	219.62862	-175[d]
12	2	11	12.5	11	3	8	11.5	219.81722	23[d]
12	2	11	11.5	11	3	8	10.5	219.81722	-306[d]
11	3	9	11.5	10	4	6	10.5	223.95051	15
11	3	9	10.5	10	4	6	9.5	223.98272	-70
7	4	4	7.5	6	3	3	6.5	228.05305	-62

Table 3 - 2 - 1- *Continued*

N'	K'_a	K'_c	J'	N''	K''_a	K''_c	J''	$\nu_{obs.}$	δ^b
7	4	4	6.5	6	3	3	5.5	228.28455	-98
12	4	8	12.5	11	3	9	11.5	234.45553	-286[d]
12	4	8	11.5	11	3	9	10.5	234.45553	-11[d]
14	2	12	13.5	13	1	13	12.5	234.96615	121[d]
14	1	14	14.5	13	2	11	13.5	234.96615	-182[d]
14	1	14	13.5	13	2	11	12.5	234.96615	-190[d]
13	3	10	13.5	12	2	11	12.5	235.51411	-158[d]
13	3	10	12.5	12	2	11	11.5	235.51411	-331[d]
13	2	12	13.5	12	3	9	12.5	235.59681	-154[d]
13	2	12	12.5	12	3	9	11.5	235.59681	-388[d]
12	3	10	12.5	11	4	7	11.5	237.82008	-35
12	3	10	11.5	11	4	7	10.5	237.83959	-54
6	5	2	6.5	5	4	1	5.5	239.06061	50
6	5	2	5.5	5	4	1	4.5	239.31102	74
6	5	1	6.5	5	4	2	5.5	239.38597	51
8	4	5	8.5	7	3	4	7.5	239.57004	-15
6	5	1	5.5	5	4	2	4.5	239.63438	68
8	4	5	7.5	7	3	4	6.5	239.78178	-99
5	3	3	5.5	4	0	4	4.5	242.68571	65
5	3	3	4.5	4	0	4	3.5	243.17862	46
6	2	4	6.5	5	1	5	5.5	245.40250	-44
7	4	3	7.5	6	3	4	6.5	245.64256	-60
6	2	4	5.5	5	1	5	4.5	245.65329	-42
7	4	3	6.5	6	3	4	5.5	245.84535	-68
9	4	6	9.5	8	1	7	8.5	247.91653	356[c]
9	4	6	8.5	8	1	7	7.5	248.09955	-78
10	4	7	10.5	9	1	8	9.5	254.31147	45
10	4	7	9.5	9	1	8	8.5	254.46825	-87
7	3	4	7.5	6	2	5	6.5	256.94228	13
7	3	4	6.5	6	2	5	5.5	257.12030	-3
7	5	3	7.5	6	4	2	6.5	259.76327	1
7	5	3	6.5	6	4	2	5.5	260.00441	-3
6	6	1	6.5	5	5	0	5.5	260.21036	595[d]
6	6	0	6.5	5	5	1	5.5	260.21036	95[d]
11	4	8	11.5	10	1	9	10.5	260.29412	89
7	5	2	7.5	6	4	3	6.5	261.30774	-2
7	5	2	6.5	6	4	3	5.5	261.54214	-15
9	5	5	9.5	8	4	4	8.5	294.64514	-29
9	5	5	8.5	8	4	4	7.5	294.87306	-58
7	7	1	7.5	6	6	0	6.5	301.14499	-229[e]
7	7	0	7.5	6	6	1	6.5	301.14499	-294[e]
7	7	1	6.5	6	6	0	5.5	301.36236	-80[e]
7	7	0	6.5	6	6	1	5.5	301.36236	-145[e]
8	6	3	8.5	7	5	2	7.5	303.28155	70
8	6	3	7.5	7	5	2	6.5	303.51073	90
8	6	2	8.5	7	5	3	7.5	303.58156	50
8	6	2	7.5	7	5	3	6.5	303.80920	97
8	1	7	8.5	7	2	6	7.5	304.16463	89
8	1	7	7.5	7	2	6	6.5	304.34342	73

Table 3 - 2 - 1- *Continued*

N'	K'_a	K'_c	J'	N''	K''_a	K''_c	J''	$\nu_{obs.}$	δ^b
10	5	6	9.5	9	4	5	8.5	306.78144	-64
9	5	4	9.5	8	4	5	8.5	308.34800	13
9	5	4	8.5	8	4	5	7.5	308.54252	38
9	4	5	9.5	8	3	6	8.5	314.17564	48
9	4	5	8.5	8	3	6	7.5	314.32547	66
7	3	5	7.5	6	0	6	6.5	322.62678	45
8	7	2	8.5	7	6	1	7.5	322.98089	-180[c]
8	7	1	8.5	7	6	2	7.5	322.99014	-58
7	3	5	6.5	6	0	6	5.5	323.03520	26
8	7	2	7.5	7	6	1	6.5	323.19967	-114
8	7	1	7.5	7	6	2	6.5	323.20902	22
9	6	4	9.5	8	5	3	8.5	323.89880	40
9	6	4	8.5	8	5	3	7.5	324.12164	21
9	6	3	9.5	8	5	4	8.5	325.10183	60
9	6	3	8.5	8	5	4	7.5	325.31862	21
7	4	4	7.5	6	1	5	6.5	329.74295	26
7	4	4	6.5	6	1	5	5.5	330.22682	-10
10	5	5	10.5	9	4	6	9.5	336.24075	-18
10	5	5	9.5	9	4	6	8.5	336.40836	-34
8	8	1	8.5	7	7	0	7.5	340.31684	77[e]
8	8	0	8.5	7	7	1	7.5	340.31684	68[e]
8	8	1	7.5	7	7	0	6.5	340.51434	66[e]
8	8	0	7.5	7	7	1	6.5	340.51434	58[e]
10	6	5	10.5	9	5	4	9.5	343.09717	88
10	6	5	9.5	9	5	4	8.5	343.31470	-18
9	7	3	9.5	8	6	2	8.5	344.54119	-8
9	7	2	9.5	8	6	3	8.5	344.59391	25
9	7	3	8.5	8	6	2	7.5	344.75688	14
9	7	2	8.5	8	6	3	7.5	344.80884	-7
10	6	4	10.5	9	5	5	9.5	346.88573	59
10	6	4	9.5	9	5	5	8.5	347.08928	-7
8	0	8	8.5	7	1	7	7.5	352.10943	-14
8	0	8	7.5	7	1	7	6.5	352.41323	-40
9	1	8	9.5	8	2	7	8.5	355.93597	219[c]
9	1	8	8.5	8	2	7	7.5	356.12563	-14
10	2	8	10.5	9	3	7	9.5	358.14944	-83
10	2	8	9.5	9	3	7	8.5	358.28725	1
11	6	6	11.5	10	5	5	10.5	359.80558	146
11	6	6	10.5	10	5	5	9.5	360.02076	-135
8	4	5	8.5	7	1	6	7.5	361.59137	54
8	4	5	7.5	7	1	6	6.5	362.00904	-78
10	7	4	9.5	9	6	3	8.5	365.88621	-1
10	7	3	10.5	9	6	4	9.5	365.91631	-11
10	7	4	10.5	9	6	3	9.5	365.93603	32
10	7	3	9.5	9	6	4	8.5	366.12558	-18

[a] cm^{-1} unit.

[b] (obs. - calc.) x 10^5.

[c] Weight is set to 0.0 in this analysis.

[d] Weight is set to 0.0 due to blended lines.

[e] Weight is set to 0.5 due to blended lines.

Table 3 -2 - 2

Observed rotational transitions of the NHD radical in the $\tilde{X}\,^2A''$ state[a]

N'	K'_a	K'_c	J'	N''	K''_a	K''_c	J''	$\nu_{obs.}$	δ[b]
6	2	5	6.5	5	1	4	5.5	103.90236	140
6	2	5	5.5	5	1	4	4.5	103.96325	53
10	1	9	10.5	10	0	10	10.5	105.92201	-161
10	1	9	9.5	10	0	10	9.5	106.08706	54
4	2	2	4.5	3	1	3	3.5	106.27487	-13
4	2	2	3.5	3	1	3	2.5	106.47492	135
3	3	1	3.5	2	2	0	2.5	106.54354	82
3	3	1	2.5	2	2	0	1.5	106.75920	54
3	3	0	3.5	2	2	1	2.5	106.90491	85
3	3	0	2.5	2	2	1	1.5	107.12320	77
9	1	9	9.5	8	0	8	8.5	107.27125	44[e]
9	1	9	8.5	8	0	8	7.5	107.27125	32[e]
9	5	4	9.5	9	4	5	9.5	110.66102	-223[c]
9	5	4	8.5	9	4	5	8.5	110.84233	-12
7	2	6	7.5	6	1	5	6.5	111.24825	4
7	2	6	6.5	6	1	5	5.5	111.29200	54
9	2	8	9.5	8	1	7	8.5	112.61724	-147
9	2	8	8.5	8	1	7	7.5	112.60611	-314[c]
9	5	5	9.5	9	4	6	9.5	112.82029	-101
8	5	4	8.5	8	4	5	8.5	113.47755	42
8	5	4	7.5	8	4	5	7.5	113.68540	98
7	5	3	7.5	7	4	4	7.5	114.11558	-4
7	5	3	6.5	7	4	4	6.5	114.34643	-89
6	5	1	6.5	6	4	2	6.5	114.55954	28
6	5	2	6.5	6	4	3	6.5	114.64722	-26
6	5	1	5.5	6	4	2	5.5	114.82816	-148
6	5	2	5.5	6	4	3	5.5	114.91562	-222[c]
5	5	0	5.5	5	4	1	5.5	115.02949	299[c]
5	5	1	5.5	5	4	2	5.5	115.04616	139[c]
5	5	0	4.5	5	4	1	4.5	115.34583	-222[c]
5	5	1	4.5	5	4	2	4.5	115.36290	-324[c]
8	2	7	8.5	7	1	6	7.5	118.54932	92
8	2	7	7.5	7	1	6	6.5	118.57738	58
10	1	10	10.5	9	0	9	9.5	118.65079	52[e]
10	1	10	9.5	9	0	9	8.5	118.65079	-19[e]
10	0	10	10.5	9	1	9	9.5	119.01107	-115[e]
10	0	10	9.5	9	1	9	8.5	119.01107	-114[e]
4	3	2	4.5	3	2	1	3.5	119.52394	26
4	3	2	3.5	3	2	1	2.5	119.71719	-68
4	3	1	4.5	3	2	2	3.5	121.34706	104
4	3	1	3.5	3	2	2	2.5	121.54770	50
9	1	8	9.5	8	2	7	8.5	126.31786	-7
9	1	8	8.5	8	2	7	7.5	126.33675	63
10	2	9	9.5	9	1	8	8.5	126.50430	43[d]
10	2	9	10.5	9	1	8	9.5	126.50430	-381[d]
11	1	11	11.5	10	0	10	10.5	129.92082	155[d]
11	1	11	10.5	10	0	10	9.5	129.92082	7[d]

Table 3 - 2 - 2-*Continued*

N'	K'_a	K'_c	J'	N''	K''_a	K''_c	J''	$\nu_{obs.}$	δ^b
5	2	3	5.5	4	1	4	4.5	129.94884	-229[c]
11	0	11	11.5	10	1	10	10.5	130.09932	-158[e]
11	0	11	10.5	10	1	10	9.5	130.09932	-67[e]
5	2	3	4.5	4	1	4	3.5	130.15006	70
5	3	3	5.5	4	2	2	4.5	131.30407	44
5	3	3	4.5	4	2	2	3.5	131.46896	29
10	1	9	10.5	9	2	8	9.5	134.86708	-6
10	1	9	9.5	9	2	8	8.5	134.87861	20
5	3	2	5.5	4	2	3	4.5	136.69810	70
5	3	2	4.5	4	2	3	3.5	136.87986	-17
12	1	12	12.5	11	0	11	11.5	141.11847	318[d]
12	1	12	11.5	11	0	11	10.5	141.11847	42[d]
12	0	12	12.5	11	1	11	11.5	141.20565	-263[d]
12	0	12	11.5	11	1	11	10.5	141.20565	-55[d]
6	3	4	6.5	5	2	3	5.5	141.48224	32
6	3	4	5.5	5	2	3	4.5	141.61967	-15
11	2	10	11.5	10	1	9	10.5	144.21845	-90
11	2	10	10.5	10	1	9	9.5	144.22754	134
4	4	1	4.5	3	3	0	3.5	145.89175	33
4	4	0	4.5	3	3	1	3.5	145.92208	-15
4	4	1	3.5	3	3	0	2.5	146.10397	-15
4	4	0	3.5	3	3	1	2.5	146.13449	-52
7	3	5	7.5	6	2	4	6.5	149.98389	57
7	3	5	6.5	6	2	4	5.5	150.09685	-41
12	3	9	12.5	11	2	10	11.5	152.45572	148[d]
12	3	9	11.5	11	2	10	10.5	152.45572	15[d]
13	1	13	13.5	12	0	12	12.5	152.26310	595[d]
13	1	13	12.5	12	0	12	11.5	152.26310	139[d]
13	0	13	13.5	12	1	12	12.5	152.30310	-573[d]
13	0	13	12.5	12	1	12	11.5	152.30310	-195[d]
6	3	3	6.5	5	2	4	5.5	153.61189	-128
6	3	3	5.5	5	2	4	4.5	153.78211	8
12	2	11	12.5	11	1	10	11.5	154.21130	298[d]
12	2	11	11.5	11	1	10	10.5	154.21130	-112[d]
8	3	6	7.5	7	2	5	6.5	157.08723	45
6	2	4	6.5	5	1	5	5.5	157.17489	93
6	2	4	5.5	5	1	5	4.5	157.38290	252[c]
5	4	2	5.5	4	3	1	4.5	159.47317	-23
5	4	2	4.5	4	3	1	3.5	159.67131	-183
5	4	1	5.5	4	3	2	4.5	159.69163	45
5	4	1	4.5	4	3	2	3.5	159.88962	-82
9	7	2	8.5	9	6	3	8.5	161.36398	147[e]
9	7	3	8.5	9	6	2	8.5	161.36398	152[e]
8	7	1	8.5	8	6	2	8.5	161.75648	573[d]
8	7	2	8.5	8	6	3	8.5	161.75648	503[d]
8	7	1	7.5	8	6	2	7.5	162.02724	414[d]
8	7	2	7.5	8	6	3	7.5	162.02724	345[d]
9	3	7	9.5	8	2	6	8.5	162.86027	96

Table 3 - 2 - 2-*Continued*

N'	K'_a	K'_c	J'	N''	K''_a	K''_c	J''	$\nu_{obs.}$	δ^b
9	3	7	8.5	8	2	6	7.5	162.93038	3
13	3	10	13.5	12	2	11	12.5	163.14535	60[e]
13	3	10	12.5	12	2	11	11.5	163.14535	-28[e]
14	0	14	13.5	13	1	13	12.5	163.38149	14
13	2	12	13.5	12	3	9	12.5	164.62343	135[d]
13	2	12	12.5	12	3	9	11.5	164.62343	-92[d]
10	3	8	10.5	9	2	7	9.5	168.02188	59
10	3	8	9.5	9	2	7	8.5	168.07427	41
6	4	3	6.5	5	3	2	5.5	172.68048	-18
6	4	3	5.5	5	3	2	4.5	172.86348	-91
7	3	4	7.5	6	2	5	6.5	172.88759	-19
7	3	4	6.5	6	2	5	5.5	173.05326	16
6	4	2	6.5	5	3	3	5.5	173.54356	-91
6	4	2	5.5	5	3	3	4.5	173.72940	-103
14	3	11	13.5	13	2	12	12.5	174.50172	360[c]
14	2	13	13.5	13	3	10	12.5	175.28517	-6
5	5	1	5.5	4	4	0	4.5	184.36774	101[d]
5	5	0	5.5	4	4	1	4.5	184.36774	-116[d]
5	5	1	4.5	4	4	0	3.5	184.57131	56[d]
5	5	0	4.5	4	4	1	3.5	184.57131	-162[d]
7	4	4	7.5	6	3	3	6.5	185.14549	-78
7	4	4	6.5	6	3	3	5.5	185.31179	-74
5	5	1	4.5	4	4	0	4.5	185.40624	21[d]
5	5	0	4.5	4	4	1	4.5	185.40624	-197[d]
7	4	3	7.5	6	3	4	6.5	187.69158	-56
7	4	3	6.5	6	3	4	5.5	187.86248	-100
7	2	5	7.5	6	1	6	6.5	189.43303	-88
7	2	5	6.5	6	1	6	5.5	189.65919	151
5	3	3	4.5	4	0	4	3.5	191.13791	-164
5	3	3	5.5	4	0	4	4.5	192.87481	64
8	3	5	8.5	7	2	6	7.5	195.26724	64
8	3	5	7.5	7	2	6	6.5	195.43232	-27
8	4	5	7.5	7	3	4	6.5	196.52062	-96
6	5	2	6.5	5	4	1	5.5	197.94467	-60
6	5	1	6.5	5	4	2	5.5	197.96497	-12
6	5	2	5.5	5	4	1	4.5	198.14170	-91
6	5	1	5.5	5	4	2	4.5	198.16202	-25
8	4	4	8.5	7	3	5	7.5	202.49519	-102
8	4	4	7.5	7	3	5	6.5	202.65245	122
9	4	6	9.5	8	3	5	8.5	205.90068	-47
9	4	6	8.5	8	3	5	7.5	206.03165	-46
7	5	3	7.5	6	4	2	6.5	211.39101	-99
7	5	2	7.5	6	4	3	6.5	211.49129	-53
7	5	3	6.5	6	4	2	5.5	211.57381	-96
7	5	2	6.5	6	4	3	5.5	211.67211	-72
10	4	7	10.5	9	3	6	9.5	213.48659	91
9	4	5	9.5	8	3	6	8.5	218.51252	-8
9	4	5	8.5	8	3	6	7.5	218.66392	-38
11	4	8	11.5	10	3	7	10.5	219.22305	19

Table 3 - 2 - 2-*Continued*

N'	K'_a	K'_c	J'	N''	K''_a	K''_c	J''	$\nu_{obs.}$	δ^b
11	4	8	10.5	10	3	7	9.5	219.31893	123
8	2	6	8.5	7	1	7	7.5	221.19705	-5[e]
9	3	6	9.5	8	2	7	8.5	221.19705	-5[e]
8	2	6	7.5	7	1	7	6.5	221.43196	73
6	6	1	6.5	5	5	0	5.5	221.97738	111[e]
6	6	0	6.5	5	5	1	5.5	221.97738	97[e]
6	6	1	5.5	5	5	0	4.5	222.16992	73[e]
6	6	0	5.5	5	5	1	4.5	222.16992	59[e]
12	4	9	12.5	11	1	10	11.5	223.46179	-196
12	4	9	11.5	11	1	10	10.5	223.54192	40
8	5	4	8.5	7	4	3	7.5	224.58996	-64
8	5	4	7.5	7	4	3	6.5	224.76321	-97
8	5	3	8.5	7	4	4	7.5	224.94577	-47
8	5	3	7.5	7	4	4	6.5	225.11972	-65
7	6	2	7.5	6	5	1	6.5	235.44335	147[d]
7	6	1	7.5	6	5	2	6.5	235.44335	-5[d]
7	6	2	6.5	6	5	1	5.5	235.63238	145[d]
7	6	1	6.5	6	5	2	5.5	235.63238	-7[d]
10	4	6	10.5	9	3	7	9.5	236.46917	87
10	4	6	9.5	9	3	7	8.5	236.61614	75
9	5	5	8.5	8	4	4	7.5	237.52658	-119
9	5	4	9.5	8	4	5	8.5	238.41026	-23
9	5	4	8.5	8	4	5	7.5	238.57330	-87
8	6	3	8.5	7	5	2	7.5	248.80626	118
8	6	2	8.5	7	5	3	7.5	248.81673	79
8	6	3	7.5	7	5	2	6.5	248.99001	12
8	6	2	7.5	7	5	3	6.5	249.00004	102
10	5	6	10.5	9	4	5	9.5	249.40016	-42
10	5	6	9.5	9	4	5	8.5	249.55067	-184
10	3	7	10.5	9	2	8	9.5	250.69709	-135
10	3	7	9.5	9	2	8	8.5	250.87982	-45
10	5	5	10.5	9	4	6	9.5	252.03292	-39
10	5	5	9.5	9	4	6	8.5	252.18703	-130
11	4	7	11.5	10	3	8	10.5	257.15499	41
11	4	7	10.5	10	3	8	9.5	257.30189	84
7	7	1	7.5	6	6	0	6.5	258.64138	127[e]
7	7	0	7.5	6	6	1	6.5	258.64138	126[e]
7	7	1	6.5	6	6	0	5.5	258.82238	181[e]
7	7	0	6.5	6	6	1	5.5	258.82238	180[e]
11	5	7	11.5	10	4	6	10.5	260.27011	-71
11	5	7	10.5	10	4	6	9.5	260.40733	-104
8	3	6	8.5	7	0	7	7.5	260.88283	124
8	3	6	7.5	7	0	7	6.5	261.19456	55
9	6	4	9.5	8	5	3	8.5	262.03899	163
9	6	3	9.5	8	5	4	8.5	262.07822	115
9	6	4	8.5	8	5	3	7.5	262.21309	64
9	6	3	8.5	8	5	4	7.5	262.25205	38
11	5	6	11.5	10	4	7	10.5	266.10381	-46
11	5	6	10.5	10	4	7	9.5	266.24837	-36

Table 3 - 2 - 2-*Continued*

N'	K'_a	K'_c	J'	N''	K''_a	K''_c	J''	$\nu_{obs.}$	δ^b
12	5	8	12.5	11	4	7	11.5	269.48559	-39
12	5	8	11.5	11	4	7	10.5	269.60990	-39
8	7	2	8.5	7	6	1	7.5	271.95692	-53[e]
8	7	1	8.5	7	6	2	7.5	271.95692	-64[e]
8	7	2	7.5	7	6	1	6.5	272.13764	144[e]
8	7	1	7.5	7	6	2	6.5	272.13764	133[e]
10	6	5	10.5	9	5	4	9.5	275.08130	46
10	6	4	10.5	9	5	5	9.5	275.21670	61
10	6	5	9.5	9	5	4	8.5	275.24406	-4
10	6	4	9.5	9	5	5	8.5	275.38049	102
13	5	9	13.5	12	4	8	12.5	276.66643	38
13	5	9	12.5	12	4	8	11.5	276.77771	100
12	5	7	12.5	11	4	8	11.5	281.07358	-22
12	5	7	11.5	11	4	8	10.5	281.21116	-44
11	1	10	11.5	10	2	9	10.5	283.41627	35
11	1	10	10.5	10	2	9	9.5	283.60990	-21
9	7	3	9.5	8	6	2	8.5	285.17800	-70[e]
9	7	2	9.5	8	6	3	8.5	285.17800	-145[e]
9	7	3	8.5	8	6	2	7.5	285.35394	157[e]
9	7	2	8.5	8	6	3	7.5	285.35394	83[e]
11	6	6	11.5	10	5	5	10.5	287.83968	44
11	6	6	10.5	10	5	5	9.5	287.99040	154
11	6	5	11.5	10	5	6	10.5	288.23644	29
11	6	5	10.5	10	5	6	9.5	288.38733	147
10	2	8	10.5	9	1	9	9.5	293.96039	39
10	2	8	9.5	9	1	9	8.5	294.22491	-30
8	8	1	8.5	7	7	0	7.5	294.29903	-157[e]
8	8	0	8.5	7	7	1	7.5	294.29903	-157[e]
8	8	1	7.5	7	7	0	6.5	294.46793	-37[e]
8	8	0	7.5	7	7	1	6.5	294.46793	-37[e]
13	5	8	13.5	12	4	9	12.5	297.56550	-74
13	5	8	12.5	12	4	9	11.5	297.70127	159
10	7	4	10.5	9	6	3	9.5	298.28987	149[d]
10	7	3	10.5	9	6	4	9.5	298.28987	-269[d]
10	7	4	9.5	9	6	3	8.5	298.45327	228[d]
10	7	3	9.5	9	6	4	8.5	298.45327	-143[d]
12	6	7	12.5	11	5	6	11.5	300.16275	103
12	6	7	11.5	11	5	6	10.5	300.30680	-80
12	6	6	12.5	11	5	7	11.5	301.18821	-13
12	6	6	11.5	11	5	7	10.5	301.33380	-102
9	4	6	9.5	8	1	7	8.5	303.73700	111
9	4	6	8.5	8	1	7	7.5	304.05116	-11
9	8	2	9.5	8	7	1	8.5	307.44189	-139[e]
9	8	1	9.5	8	7	2	8.5	307.44189	-140[e]
9	8	2	8.5	8	7	1	7.5	307.61001	-75[e]
9	8	1	8.5	8	7	2	7.5	307.61001	-75[e]
11	7	5	11.5	10	6	4	10.5	311.24842	90
11	7	4	11.5	10	6	5	10.5	311.26311	90
11	7	5	10.5	10	6	4	9.5	311.40900	82

Table 3 - 2 - 2-*Continued*

N'	K'_a	K'_c	J'	N''	K''_a	K''_c	J''	$\nu_{obs.}$	δ^b
11	7	4	10.5	10	6	5	9.5	311.42342	59
13	6	8	13.5	12	5	7	12.5	311.80256	67
13	6	8	12.5	12	5	7	11.5	311.93781	-18
13	6	7	13.5	12	5	8	12.5	314.18619	-120
13	6	7	12.5	12	5	8	11.5	314.32526	-59
10	8	3	10.5	9	7	2	9.5	320.48545	-139[e]
10	8	2	10.5	9	7	3	9.5	320.48545	-144[e]
10	8	3	9.5	9	7	2	8.5	320.65031	-72[e]
10	8	2	9.5	9	7	3	8.5	320.65031	-78[e]
12	7	6	12.5	11	6	5	11.5	324.03865	39
12	7	5	12.5	11	6	6	11.5	324.08691	-25
12	7	6	11.5	11	6	5	10.5	324.19143	2
12	7	5	11.5	11	6	6	10.5	324.24034	2
9	9	1	9.5	8	8	0	8.5	328.91896	-50[e]
9	9	0	9.5	8	8	1	8.5	328.91896	-50[e]
9	9	1	8.5	8	8	0	7.5	329.07555	40[e]
9	9	0	8.5	8	8	1	7.5	329.07555	40e
11	8	4	11.5	10	7	3	10.5	333.41531	-125[e]
11	8	3	11.5	10	7	4	10.5	333.41531	-157[e]
11	8	4	10.5	10	7	3	9.5	333.57599	-45[e]
11	8	3	10.5	10	7	4	9.5	333.57599	-77[e]
13	7	7	13.5	12	6	6	12.5	336.60515	4
13	7	6	13.5	12	6	7	12.5	336.74725	-96[d]
13	7	7	12.5	12	6	6	11.5	336.74725	436[d]
10	9	2	10.5	9	8	1	9.5	341.86245	1[e]
10	9	1	10.5	9	8	2	9.5	341.86245	1[e]
10	9	2	9.5	9	8	1	8.5	342.01911	21[e]
10	9	1	9.5	9	8	2	8.5	342.01911	21[e]
12	8	5	12.5	11	7	4	11.5	346.22116	-413[d]
12	8	4	12.5	11	7	5	11.5	346.22116	-560[d]
12	8	5	11.5	11	7	4	10.5	346.37148	-7[e]
12	8	4	11.5	11	7	5	10.5	346.37148	-147[e]
11	9	3	11.5	10	8	2	10.5	354.70197	61[e]
11	9	2	11.5	10	8	3	10.5	354.70197	60[e]
11	9	3	10.5	10	8	2	9.5	354.85675	87[e]
11	9	2	10.5	10	8	3	9.5	354.85675	87[e]
10	10	1	10.5	9	9	0	9.5	362.45568	128[e]
10	10	0	10.5	9	9	1	9.5	362.45568	128[e]
10	10	1	9.5	9	9	0	8.5	362.59900	-107[e]
10	10	0	9.5	9	9	1	8.5	362.59900	-107[e]

a, b, c, d, [e]See the footnotes of Table 3 - 2 - 1.

Table 3 - 2 - 3

Observed rotational transitions of the ND_2 radical in the $\tilde{X}^2B_1$ state[a]

N'	K'_a	K'_c	J'	N''	K''_a	K''_c	J''	$\nu_{obs.}$	δ[b]
7	3	5	7.5	6	2	4	6.5	102.50143	83
7	3	5	6.5	6	2	4	5.5	102.59300	140
11	3	8	11.5	10	2	9	10.5	106.94737	49[e]
11	3	8	10.5	10	2	9	9.5	106.94737	46[e]
12	0	12	12.5	11	1	11	11.5	106.97588	-64[e]
12	0	12	11.5	11	1	11	10.5	106.97588	-79[e]
12	1	12	12.5	11	0	11	11.5	106.98582	-4[e]
12	1	12	11.5	10	0	11	10.5	106.98582	-23[e]
6	4	2	6.5	6	1	5	6.5	107.15060	70
8	3	6	8.5	7	2	5	7.5	107.22262	66
8	3	6	7.5	7	2	5	6.5	107.29578	48
11	2	10	11.5	10	3	7	10.5	107.71352	121
11	2	10	10.5	10	3	7	9.5	107.71718	53
5	4	2	5.5	4	3	1	4.5	108.49758	39
5	4	1	5.5	4	3	2	4.5	108.95273	-114
5	4	1	4.5	4	3	2	3.5	109.10063	-137
11	4	7	10.5	10	3	8	9.5	111.44865	-102
11	4	7	11.5	10	3	8	10.5	111.46591	-25
9	3	7	9.5	8	2	6	8.5	111.52838	55
9	3	7	8.5	8	2	6	7.5	111.58691	108
6	3	3	6.5	5	2	4	4.5	112.42658	124
6	3	3	5.5	5	2	4	4.5	112.71715	8
13	2	11	12.5	12	1	12	11.5	115.44596	197[d]
13	1	13	12.5	12	0	12	11.5	115.44596	-222[d]
12	3	9	12.5	11	2	10	11.5	115.58263	-22[e]
12	3	9	11.5	11	2	10	10.5	115.58263	-93[e]
12	1	11	11.5	11	4	8	10.5	115.75799	-30
12	1	11	12.5	11	4	8	11.5	115.81229	-113
12	2	11	12.5	11	3	8	11.5	115.94747	136
12	2	11	11.5	11	3	8	10.5	115.94747	-136[d]
10	3	8	10.5	9	0	9	9.5	116.04407	27
10	3	8	9.5	9	0	9	8.5	116.08643	-3
6	4	3	6.5	5	3	2	5.5	118.60320	-9
6	4	3	5.5	5	3	2	4.5	118.74270	-19
6	4	2	6.5	5	3	3	5.5	120.38220	41
6	4	2	5.5	5	3	3	4.5	120.51725	27
11	3	9	10.5	10	0	10	9.5	121.33065	143[c]
5	5	1	5.5	4	4	0	4.5	123.45966	-121
5	5	0	5.5	4	4	1	4.5	123.46838	-43
5	5	1	4.5	4	4	0	3.5	123.61274	-135
5	5	0	4.5	4	4	1	3.5	123.62048	-67
13	3	10	13.5	12	2	11	12.5	124.10496	92[e]
13	3	10	12.5	12	2	11	11.5	124.10496	2[e]
13	2	12	12.5	12	3	9	11.5	124.27563	-22
12	3	10	12.5	11	4	7	11.5	127.50201	84
12	3	10	11.5	11	4	7	10.5	127.51935	-55
7	4	4	7.5	6	3	3	6.5	127.55042	-18
7	4	4	6.5	6	3	3	5.5	127.67925	-29

Table 3 - 2 - 3-*Continued*

N'	K'_a	K'_c	J'	N''	K''_a	K''_c	J''	$\nu_{obs.}$	δ^b
7	3	4	7.5	6	2	5	6.5	131.06264	-33
7	3	4	6.5	6	2	5	5.5	131.16626	-28
13	4	9	12.5	12	3	10	11.5	131.55030	104
7	4	3	7.5	6	3	4	6.5	132.57236	-46
7	4	3	6.5	6	3	4	5.5	132.69567	26
6	5	2	6.5	5	4	1	5.5	134.39118	67
6	5	1	6.5	5	4	2	5.5	134.45273	-105
6	5	2	5.5	5	4	1	4.5	134.53913	48
6	5	1	5.5	5	4	2	4.5	134.60067	-107
8	4	5	8.5	7	3	4	7.5	134.86708	123[e]
8	4	5	7.5	7	3	4	6.5	134.98444	-41
9	4	6	9.5	8	3	5	8.5	140.44582	-1
9	4	6	8.5	8	3	5	7.5	140.55445	66
10	4	7	10.5	9	1	8	9.5	144.57086	178
10	4	7	9.5	9	1	8	8.5	144.66469	-20
7	5	3	7.5	6	4	2	6.5	145.13369	-35
7	5	3	6.5	6	4	2	5.5	145.27393	-40
7	5	2	7.5	6	4	3	6.5	145.44456	-36
7	5	2	6.5	6	4	3	5.5	145.58293	-44
8	4	4	8.5	7	3	5	7.5	146.21704	-84
8	4	4	7.5	7	3	5	6.5	146.32704	-46
11	4	8	11.5	10	1	9	10.5	147.73413	0
11	4	8	10.5	10	1	9	9.5	147.81508	-27
6	6	1	6.5	5	5	0	5.5	148.58098	40[e]
6	6	0	6.5	5	5	1	5.5	148.58098	-30[e]
6	6	1	5.5	5	5	0	4.5	148.72785	41[e]
6	6	0	5.5	5	5	1	4.5	148.72785	-29[e]
7	2	5	7.5	6	1	6	6.5	149.78366	63
7	2	5	6.5	6	1	6	5.5	149.92103	-4
6	3	4	6.5	5	0	5	5.5	150.69642	178
8	3	5	8.5	7	2	6	7.5	152.76220	86
8	3	5	7.5	7	2	6	6.5	152.85876	-192[c]
8	5	4	8.5	7	4	3	7.5	155.44897	-45
8	5	4	7.5	7	4	3	6.5	155.58094	-67
8	5	3	8.5	7	4	4	7.5	156.54142	-70
8	5	3	7.5	7	4	4	6.5	156.67291	95
7	6	2	7.5	6	5	1	6.5	159.57080	59
7	6	1	7.5	6	5	2	6.5	159.57767	-18
7	6	2	6.5	6	5	1	5.5	159.71371	60
7	6	1	6.5	6	5	2	5.5	159.72171	-20
9	4	5	9.5	8	3	6	8.5	162.15916	-142
9	4	5	8.5	8	3	6	7.5	162.25728	-72
9	5	5	9.5	8	4	4	8.5	164.92373	-39
9	5	5	8.5	8	4	4	7.5	165.05010	-58
9	5	4	9.5	8	4	5	8.5	167.99872	-41
9	5	4	8.5	8	4	5	7.5	168.11859	-57
8	6	3	8.5	7	5	2	7.5	170.47662	-35
8	6	2	8.5	7	5	3	7.5	170.52195	32
8	6	3	7.5	7	5	2	6.5	170.61533	-22
8	6	2	7.5	7	5	3	6.5	170.65996	-11

Table 3 - 2 - 3-*Continued*

N'	K'_a	K'_c	J'	N''	K''_a	K''_c	J''	$\nu_{obs.}$	δ^b
7	3	5	6.5	6	0	6	5.5	171.08923	221[c]
6	4	3	6.5	5	1	4	5.5	172.95812	371[c]
10	5	6	10.5	9	4	5	9.5	173.02607	7
7	7	1	7.5	6	6	0	6.5	173.08927	51[e]
7	7	0	7.5	6	6	1	6.5	173.08927	44[e]
10	5	6	9.5	9	4	5	8.5	173.14645	93
7	7	1	6.5	6	6	0	5.5	173.22880	66[e]
7	7	0	6.5	6	6	1	5.5	173.22880	60[e]
7	7	1	6.5	6	6	0	6.5	174.13945	64[e]
7	7	0	6.5	6	6	1	6.5	174.13945	57[e]
9	1	8	9.5	8	2	7	8.5	177.44034	-508[c]
11	5	7	10.5	10	4	6	9.5	179.43180	-3
10	5	5	10.5	9	4	6	9.5	180.27226	30
10	5	5	9.5	9	4	6	8.5	180.38166	13
10	4	6	10.5	9	3	7	9.5	181.11408	61
10	4	6	9.5	9	3	7	8.5	181.20037	-64
9	6	4	9.5	8	5	3	8.5	181.22106	-47
9	6	4	8.5	8	5	3	7.5	181.35386	-8
9	6	3	9.5	8	5	4	8.5	181.40777	3
9	6	3	8.5	8	5	4	7.5	181.53982	-22
12	5	8	12.5	11	4	7	11.5	183.71066	-61
12	5	8	11.5	11	4	7	10.5	183.81951	-115
8	7	2	8.5	7	6	1	7.5	184.11568	135[e]
8	7	1	8.5	7	6	2	7.5	184.11568	50[e]
8	7	2	7.5	7	6	1	6.5	184.25404	139[e]
8	7	1	7.5	7	6	2	6.5	184.25404	54[e]
10	6	5	10.5	9	5	4	9.5	191.65710	-1
10	6	5	9.5	9	5	4	8.5	191.78388	23
10	6	4	10.5	9	5	5	9.5	192.27788	-17
10	6	4	9.5	9	5	5	8.5	192.40236	-34
11	5	6	11.5	10	4	7	10.5	194.03805	-69
11	5	6	10.5	10	4	7	9.5	194.13647	-57
9	7	3	9.5	8	6	2	8.5	195.08384	579[d]
9	7	2	9.5	8	6	3	8.5	195.08384	4[d]
9	7	3	8.5	8	6	2	7.5	195.21902	625[d]
9	7	2	8.5	8	6	3	7.5	195.21902	52[d]
8	8	1	8.5	7	7	0	7.5	196.93145	22[e]
8	8	0	8.5	7	7	1	7.5	196.93145	21[e]
8	8	1	7.5	7	7	0	6.5	197.06386	136[e]
8	8	0	7.5	7	7	1	6.5	197.06386	136[e]
8	4	5	8.5	7	1	6	7.5	197.80574	4
8	4	5	7.5	7	1	6	6.5	198.05330	10
11	6	6	11.5	10	5	5	10.5	201.52056	-18
11	6	6	10.5	10	5	5	9.5	201.64244	-70
11	6	5	11.5	10	5	6	10.5	203.25705	-30
11	6	5	10.5	10	5	6	9.5	203.37453	-24
10	1	9	10.5	9	2	8	9.5	204.50233	114
10	7	4	10.5	9	6	3	9.5	205.94512	56

Table 3 - 2 - 3-*Continued*

N'	K'_a	K'_c	J'	N''	K''_a	K''_c	J''	$\nu_{obs.}$	δ^b
10	7	3	10.5	9	6	4	9.5	205.97253	39
10	7	4	9.5	9	6	3	8.5	206.07516	46
10	7	3	9.5	9	6	4	8.5	206.10250	30
9	0	9	8.5	8	1	8	7.5	206.20618	-28
9	8	2	9.5	8	7	1	8.5	207.99018	69[e]
9	8	1	9.5	8	7	2	8.5	207.99018	60[e]
9	8	2	8.5	8	7	1	7.5	208.12188	93[e]
9	8	1	8.5	8	7	2	7.5	208.12188	84[e]
12	5	7	12.5	11	4	8	11.5	210.10662	-6
12	5	7	11.5	11	4	8	10.5	210.19376	44
12	6	7	12.5	11	5	6	11.5	210.40224	-5
12	6	7	11.5	11	5	6	10.5	210.52114	-9
9	4	6	9.5	8	1	7	8.5	214.21353	-155[c]
9	4	6	8.5	8	1	7	7.5	214.43422	-72
12	6	6	12.5	11	5	7	11.5	214.61039	-71
12	6	6	11.5	11	5	7	10.5	214.72065	4
11	7	5	11.5	10	6	4	10.5	216.66131	54
11	7	4	11.5	10	6	5	10.5	216.76614	67
11	7	5	10.5	10	6	4	9.5	216.78600	-15
11	7	4	10.5	10	6	5	9.5	216.89016	-47
10	8	3	10.5	9	7	2	9.5	218.99022	90[e]
10	8	2	10.5	9	7	3	9.5	218.99022	21[e]
10	8	3	9.5	9	7	2	8.5	219.11977	106[e]
10	8	2	9.5	9	7	3	8.5	219.11977	37[e]
9	9	1	9.5	8	8	0	8.5	220.06637	-149[e]
9	9	0	9.5	8	8	1	8.5	220.06637	-49[e]
9	9	1	8.5	8	8	0	7.5	220.18991	-93[e]
9	9	0	8.5	8	8	1	7.5	220.18991	-93[e]
13	6	7	12.5	12	5	8	11.5	226.88893	34
12	7	6	12.5	11	6	5	11.5	227.13804	68
12	7	6	11.5	11	6	5	10.5	227.25879	56
12	7	5	12.5	11	6	6	11.5	227.47163	31
12	7	5	11.5	11	6	6	10.5	227.59206	69
13	5	8	13.5	12	4	9	12.5	229.16436	15
13	5	8	12.5	12	4	9	11.5	229.24054	-2
11	8	4	11.5	10	7	3	10.5	229.91048	297[d]
11	8	3	11.5	10	7	4	10.5	229.91048	-75[d]
11	8	4	10.5	10	7	3	9.5	230.03666	290[d]
11	8	3	10.5	10	7	4	9.5	230.03666	-80[d]
10	9	2	10.5	9	8	1	9.5	231.15690	-115[e]
10	9	1	10.5	9	8	2	9.5	231.15690	-116[e]
10	9	2	9.5	9	8	1	8.5	231.28164	-53[e]
10	9	1	9.5	9	8	2	8.5	231.28164	-54[e]
11	1	10	11.5	10	2	9	10.5	233.08414	49
11	1	10	10.5	10	2	9	9.5	233.20245	127
13	7	7	13.5	12	6	6	12.5	237.22239	107
13	7	7	12.5	12	6	6	11.5	237.33436	-59
13	7	6	13.5	12	6	7	12.5	238.14438	32

Table 3 - 2 - 3-*Continued*

N'	K'_a	K'_c	J'	N''	K''_a	K''_c	J''	$\nu_{obs.}$	δ^b
13	7	6	12.5	12	6	7	11.5	238.25816	-14
10	3	8	10.5	9	0	9	9.5	240.65303	-4
10	3	8	9.5	9	0	9	8.5	240.85561	-205[c]
12	8	5	12.5	11	7	4	11.5	240.71614	-6
12	8	4	12.5	11	7	5	11.5	240.73237	39
12	8	5	11.5	11	7	4	10.5	240.83868	-16
12	8	4	11.5	11	7	5	10.5	240.85561	104[e]
11	9	3	11.5	10	8	2	10.5	242.18792	-48[e]
11	9	2	11.5	10	8	3	10.5	242.18792	-56[e]
11	9	3	10.5	10	8	2	9.5	242.31128	-36[e]
11	9	2	10.5	10	8	3	9.5	242.31128	-44[e]
10	10	1	10.5	9	9	0	9.5	242.46881	-19[e]
10	10	0	10.5	9	9	1	9.5	242.46881	-19[e]
10	10	1	9.5	9	9	0	8.5	242.58391	-10[e]
10	10	0	9.5	9	9	1	8.5	242.58391	-10[e]
10	5	6	10.5	9	0	9	9.5	248.89902	73
10	5	6	9.5	9	0	9	8.5	249.16572	-21
13	8	6	13.5	12	7	5	12.5	251.37915	101
13	8	5	13.5	12	7	6	12.5	251.43394	-23
13	8	6	12.5	12	7	5	11.5	251.49445	-267[c]
13	8	5	12.5	12	7	6	11.5	251.55251	-48
12	9	4	12.5	11	8	3	11.5	253.13946	-106[e]
12	9	3	12.5	11	8	4	11.5	253.13946	-153[e]
12	9	4	11.5	11	8	3	10.5	253.26037	-144[e]
12	9	3	11.5	11	8	4	10.5	253.26037	-191[e]
11	10	2	11.5	10	9	1	10.5	253.59146	108[e]
11	10	1	11.5	10	9	2	10.5	253.59146	108[e]
11	10	2	10.5	10	9	1	9.5	253.70804	81[e]
11	10	1	10.5	10	9	2	9.5	253.70804	81[e]
11	4	7	11.5	10	1	10	10.5	262.08952	-157
11	4	7	10.5	10	1	10	9.5	262.27939	70
13	9	5	13.5	12	8	4	12.5	263.99386	-71[d]
13	9	4	13.5	12	8	5	12.5	263.99386	-291[d]
13	9	5	12.5	12	8	4	11.5	264.11250	-82[d]
13	9	4	12.5	12	8	5	11.5	264.11250	-302[d]
12	10	3	12.5	11	9	2	11.5	264.64901	54e
12	10	2	12.5	11	9	3	11.5	264.64901	53[e]
12	10	3	11.5	11	9	2	10.5	264.76545	8[e]
12	10	2	11.5	11	9	3	10.5	264.76545	7[e]

a, b, c, d, eSee the footnotes of Table 3 - 2 - 1.

Table 3 - 2 - 4

Observed frequencies of the rotational transitions of the NH radical in the $X^3\Sigma^-$ state[a]

N'	J'	N''	J''	$\nu_{obs.}$	δ[b]
3	2	2	1	98.05044	14
3	3	2	2	97.87443	-137
4	5	3	4	130.23878	-2
4	4	3	3	130.31137	47
4	3	3	2	130.41821	181
5	6	4	5	162.51782	32
5	5	4	4	162.58379	19
5	4	4	3	162.66640	50
6	7	5	6	194.59255	115
6	6	5	5	194.65430	70
6	5	5	4	194.72584	74
7	8	6	7	226.42296	56
7	7	6	6	226.48222	42
7	6	6	5	226.54781	51
8	9	7	8	257.97255	85
8	8	7	7	258.02989	89
8	7	7	6	258.09132	102
9	8	8	7	289.20068	-63
9	9	8	8	289.25752	82
10	9	9	8	320.07484	144
10	10	9	9	320.12894	174

[a]Unit is cm^{-1}.

[b]δ = (obs. - calc.) x 10^5. The calculated frequencies were obtained from term values reported by Brazier, Ram, and Bernath (1986).

Table 3 - 2 - 5

Molecular parameters of NH_2[a]

Parameters	This work	FTIR & MODR[b]
A	23.692 859(54)	23.692 993(46)
B	12.951 866(28)	12.952 008(29)
C	8.172 911(27)	8.172 737(18)
Δ_K x 10^2	2.189 63(33)	2.195 29(48)
Δ_{NK} x 10^2	-0.414 70(23)	-0.416 03(26)
Δ_N x 10^2	0.105 502(44)	0.105 821(63)
δ_K x 10^3	0.9278(16)	0.9943(32)
δ_N x 10^3	0.423 14(23)	0.425 16(36)
H_K x 10^5	6.000(11)	6.243(18)
H_{KN} x 10^5	-0.8877(92)	-0.941(18)
H_{NK} x 10^5	-0.1175(38)	-0.1169(53)
H_N x 10^5	0.038 67(26)	0.043 34(70)
h_K x 10^5	0.8140(78)	1.511(17)
h_{NK}x 10^5	-0.0424(26)	-0.0071(23)
h_N x 10^5	0.019 34(13)	0.021 62(36)
L_K x 10^7	-2.137(61)	1.40
$LKKN$ x 10^7	1.267(98)	
L_{NK} x 10^7	0.408(37)	
l_K x 10^7	-0.314(17)	
ε_{aa}	-0.309 089(17)	-0.308 897(39)
ε_{bb}	-0.045 1972(74)	-0.045 214(18)
ε_{cc}	0.000 4061(43)	0.000 404(34)
Δ^S_K x 103	1.0801(57)	1.0067(60)
$(\Delta^S_{KN} + \Delta^S_{NK})$ x 10^3	-0.1056(12)	-0.1029(24)
Δ^S_N x 10^3	0.010 890(92)	0.011 08(24)
δ^S_K x 10^5	2.05(10)	2.13(25)
δ^S_N x 10^5	0.5447(49)	0.552(13)
H^S_K x 10^6	-3.221(80)	

[a]cm^{-1} unit. The numbers in parentheses denote one standard deviation and apply to the last digits of the constants.
[b]Burkholder, Howard, and McKellar (1988).

Table 3 - 2 - 6

Molecular parameters of NHD

Parameters	This work	MODR & Optical[b]	Optical[c]
A	20.109 022(57)	20.1150(17)	20.1162(32)
B	8.110 865(50)	8.1114(6)	8.1114(16)
C	5.666 620(52)	5.6674(3)	5.6681(16)
Δ_K x 10^3	8.2909(25)	8.81(19)	8.94(39)
Δ_{NK} x 10^3	1.0321(14)	0.97(5)	0.97(18)
Δ_N x 10^3	0.313 09(83)	0.32(1)	0.32(3)
δ_K x 10^3	1.5890(18)	1.52(4)	1.52(49)
δ_N x 10^3	0.102 46(18)	0.102(2)	0.10(1)
H_K x 10^6	24.013(51)		
H_{KN} x 10^6	-5.464(71)		
H_{NK} x 10^6	1.474(21)		
H_N x 10^6	0.0568(54)		
h_K x 10^6	4.188(58)		
h_{NK} x 10^6	0.719(14)		
h_N x 10^6	0.0189(20)		
L_K x 10^9	-41.46(20)		
L_{KKN} x 10^9	2.68(25)		
L_N x 10^9	-0.069(12)		
l_N x 10^9	-0.0155(63)		
ε_{aa}	-0.234 784(22)	-0.2348(2)	-0.2324(51)
ε_{bb}	-0.038 395(19)	-0.0384(1)	-0.0373(55)
ε_{cc}	0.000 276(31)	0.000 26(13)	-0.0019(63)
$\lvert\varepsilon_{ab} + \varepsilon_{ba}\rvert$	0.070 69(59)	0.0714(56)	
Δ^S_K x 10^3	0.5110(89)	0.48(12)	
Δ^S_N x 10^3	0.005 21(52)		
δ^S_K x 10^3	0.0441(71)		
δ^S_N x 10^3	0.001 98(30)	0.006(2)	
H^S_K x 10^6	-1.210(55)		

[a]cm^{-1} unit. The numbers in parentheses denote one standard deviation and apply to the last digits of the constants.
[b]Steimle, Brown, and Curl (1980).
[c]Ramsay and Wayne (1979).

Table 3 - 2 - 7

Molecular parameters of ND_2

Parameters	This work	Optical, MODR, IODR, & MIR-LMR[b]
A	13.341 933(65)	13.342 600(17)
B	6.487 735(40)	6.487 831(7)
C	4.289 883(48)	4.290 280(7)
Δ_K x 10^3	6.6039(15)	6.5709(13)
Δ_{NK} x 10^3	-1.1159(17)	-1.072 46(33)
Δ_N x 10^3	0.261 17(41)	0.259 658(67)
δ_K x 10^3	0.2779(11)	0.271 83(67)
δ_N x 10^3	0.103 13(14)	0.101 066(33)
H_K x 10^6	9.971(31)	7.8218(200)
H_{KN} x 10^6	-1.500(38)	
H_{NK} x 10^6	-0.190(14)	
H_N x 10^6	0.0455(14)	
h_K x 10^6	1.144(26)	
h_{NK} x 10^6	-0.0276(82)	
h_N x 10^6	0.025 42(58)	
L_K x 10^8	-1.450(18)	
L_{KKN} x 10^8	0.266(19)	
l_K x 10^8	-0.1192(76)	
ε_{aa}	-0.171 040(16)	-0.171 039(3)
ε_{bb}	-0.022 308(63)	-0.022 302(1)
ε_{cc}	0.000 1078(48)	0.000 108(1)
Δ^S_K x 10^4	3.138(38)	3.216(13)
$(\Delta^S_{KN} + \Delta^S_{NK})$ x 10^5	-2.88(11)	-3.154(23)
Δ^S_N x 10^6	2.61(12)	2.490(20)
δ^S_K x 10^6	5.3(1.4)	2.79(23)
δ^S_N x 10^6	1.177(62)	1.205(10)
H^S_K x 10^6	-4.99(27)	

[a]cm^{-1} unit. The numbers in parentheses denote one standard deviation and apply to the last digits of the constants.
[b]Muenchausen *et al.* (1985).

Table 3 - 2 - 8

Inertia defect for NH_2, H_2O, ND_2, and D_2O in the ground state[a]

	NH_2	H_2O[b]	ND_2	D_2O[b]
Δ_{obs}	0.049571(8)	0.0486	0.06775(5)	0.0648
Δ_{calc}	0.0476	0.0467	0.0666	0.0635
Δ_{calc}^{vib}	0.0514	0.0460	0.0694	0.0627
Δ_{calc}^{cent}	0.0009	0.0008	0.0009	0.0008
Δ_{calc}^{elec}	-0.0047	0.0000	-0.0038	0.0000

[a]amu Å^2 unit.

[b]Observed and calculated values were reported by Benedict, Gailar, and Plyler (1956) and Oka and Morino (1961), respectively.

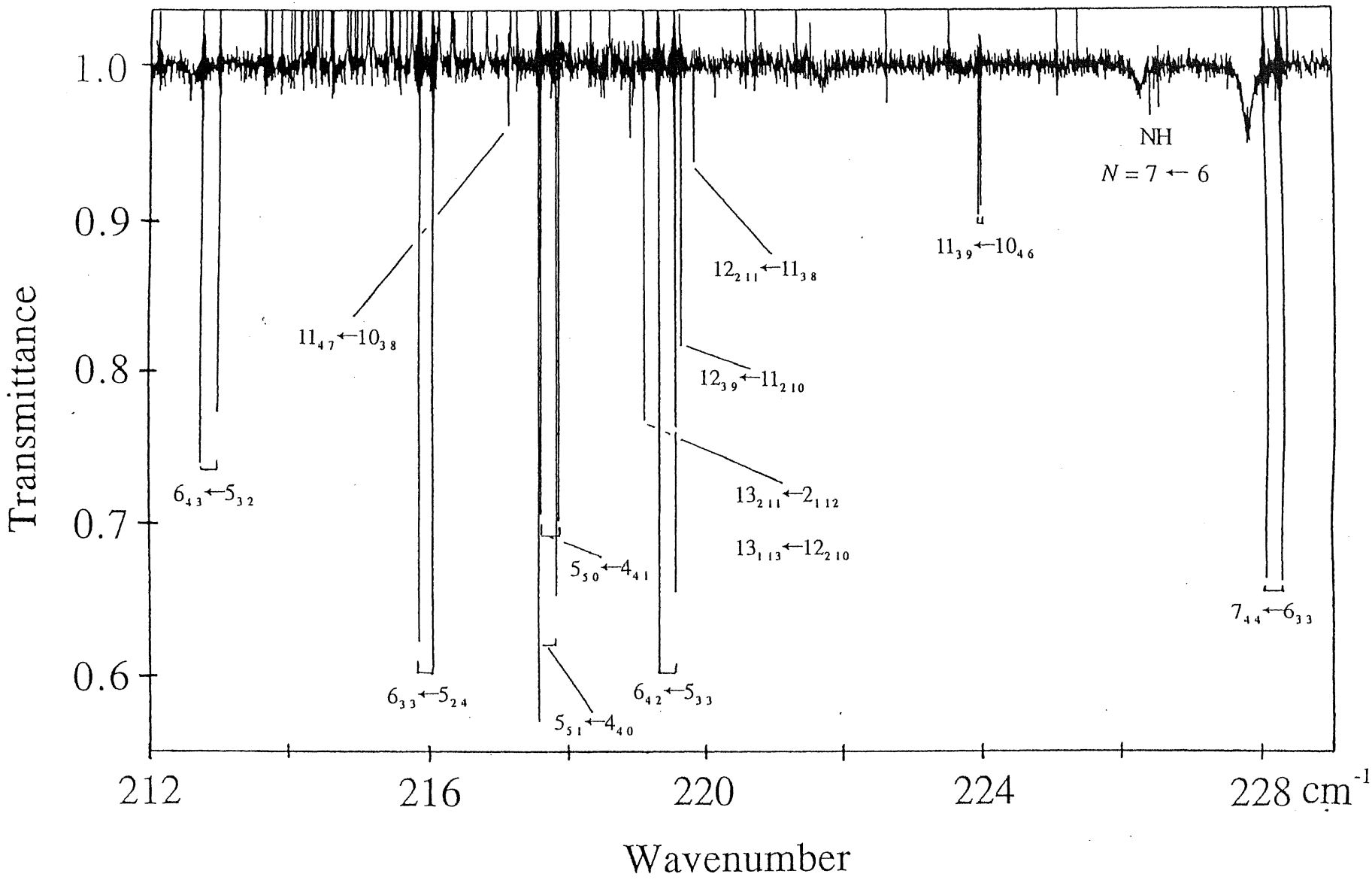

Figure 3 - 2 - 1. Observed spectrum of the rotational transitions of the NH_2 radical between 212 and 229 cm^{-1}. NH_2 has a doublet structure due to a spin-rotation interaction. The upward lines are due to the rotational transitions of NH_3, where the observed spectrum with discharge was divided by that without discharge, to obtain the transmittance spectrum. Weak absorption lines in 226 cm^{-1} region are assigned to the rotational transitions of the NH radical.

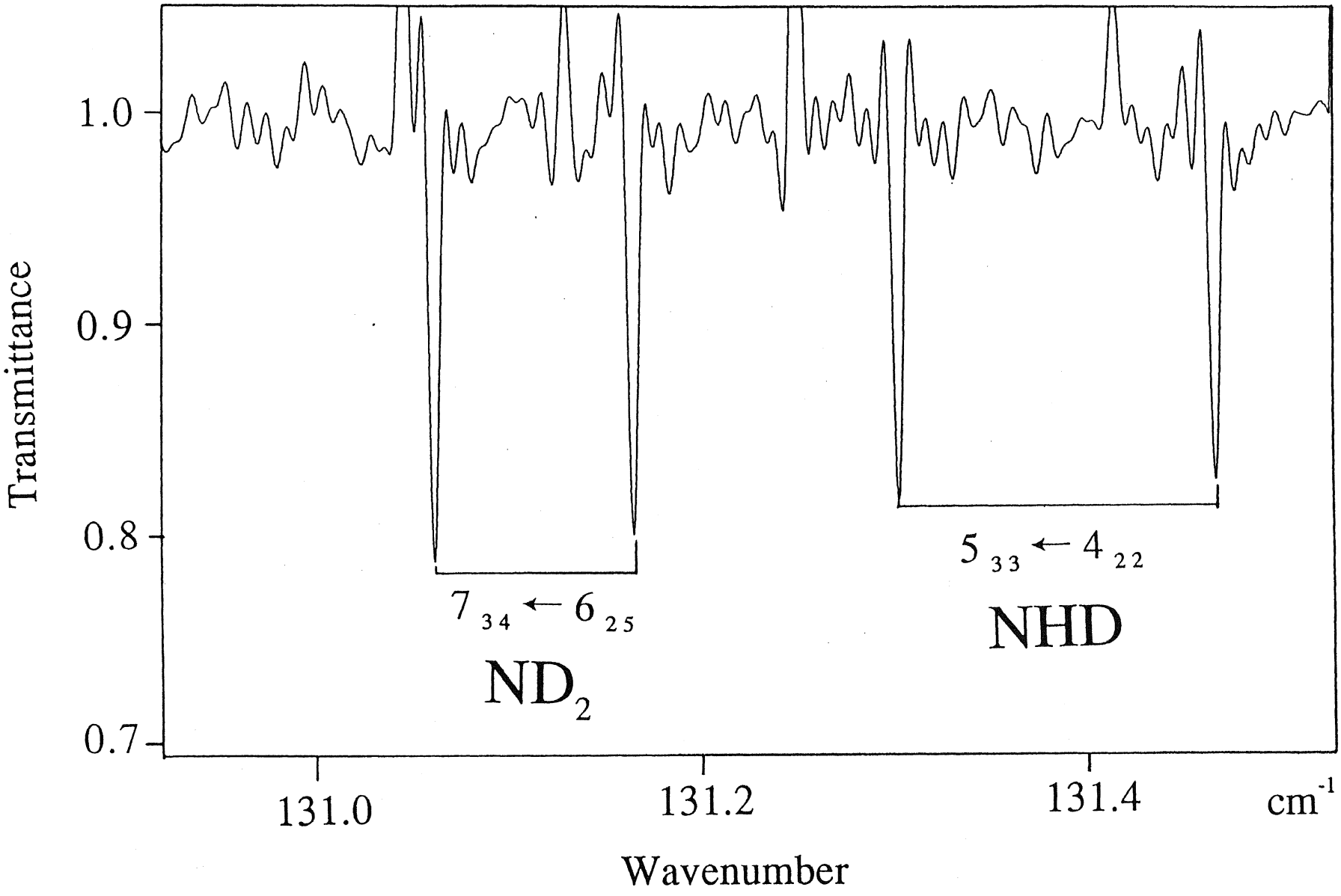

Figure 3 -2 - 2. Observed spectrum of the NHD and ND_2 radicals.

3 - 3. Vibration-Rotation Spectrum of NH_2OH

Abstract

The OH torsional bands of hydroxylamine NH_2OH have been observed for the first time with high-resolution in the 385 cm^{-1} region using a high-resolution Fourier transform infrared spectrometer. About 5000 lines belonging to ν_9 and the two hot bands $2\nu_9 - \nu_9$ and $3\nu_9 - 2\nu_9$ have been measured with an accuracy of about 0.001 cm^{-1}. Molecular parameters have been derived with a Watson S-reduced asymmetric-top Hamiltonian. The band origin frequencies have been determined to be ν_{1-0} = 385.963 31(8) cm^{-1}, ν_{2-1} = 365.112 20(14) cm^{-1}, and ν_{3-2} = 345.841 24(22) cm^{-1}. The splittings due to the inversion of the NH_2 group are not resolved in the observed spectrum.

3 - 3 - 1. Introduction

High resolution spectroscopic studies on hydroxylamine NH_2OH are still fairly limited, in spite of its potential, astronomical interest. The microwave spectrum of hydroxylamine and all its deuterated species was reported by Tsunekawa (1972), who determined its molecular structure. The OH-stretching fundamental mode ν_1 around 3650 cm^{-1} was studied by Coles *et al.* (1984) with a color center laser spectrometer. Taubmann and Jones (1987) observed the diode laser spectrum of hydroxylamine in the region of the NH_2 wagging ν_5 (1115 cm^{-1}) and NO stretching ν_6 (895 cm^{-1}) fundamentals, as well as several bands in the 700 cm^{-1} region. The OH bending mode ν_4 (1354 cm^{-1}) was reported in a subsequent paper by Birk and Jones (1988).

In this Section, the high resolution infrared spectroscopy of hydroxylamine to the lowest vibrational mode ν_9 is reported. The ν_9 band corresponds to the torsional motion of the OH-group around the NO-axis, near 380 cm^{-1}. So far, there has been no direct high resolution observation of this mode. The only previous study in this region is the low resolution work by Tamagake *et al.* (1974), who observed the *Q*-branches and discussed the internal-rotation potential function. The $\nu_1 + \nu_9 - \nu_9$ band was observed by Coles *et al* . (1984), and the $2\nu_9$, $3\nu_9 - \nu_9$ and $\nu_5 - \nu_9$ bands by Taubmann and Jones (1987), who have shown that the $3\nu_9$ level is perturbed through a Coriolis interaction with the nearby ν_5 level. One pure rotational transition in the ν_9 level, one in the $2\nu_9$ level, and one in the $3\nu_9$ level have been also reported by Tsunekawa (1972).

3 - 3 - 2. Experimental

Hydroxylamine NH_2OH was produced by thermal decomposition of the tertiary hydroxylammonium phosphate salt $(H_3NOH)_3PO_4$ (Aldrich Chemicals, 98% purity, used without further purification) in an oil bath at a temperature of about 120 °C. The decomposition products were continuously pumped out by a high speed mechanical

booster followed by a rotary pump. The pressure inside the absorption cell was maintained at 10 mTorr, as measured by a Baratron gauge.

Detail of the absorption cell in this study was already described in Chapter 2. The far-infrared beam (Hg lamp) from a FT spectrometer was focused on the window of the absorption cell and detected by a Si composite bolometer cooled at liquid helium temperature, equipped with a low-pass filter cutting at 600 cm^{-1}. The beamsplitter used is a 6 μm Mylar sheet.

The signal was integrated during about 1 hr, between 0 and 720 cm^{-1}, with a resolution of 0.010 cm^{-1}. The noise level corresponded typically to about 1% absorption.

The observed frequencies were calibrated against the residual water lines between 230 and 344 cm^{-1} (Guelachvili and Narahari Rao, 1986). The accuracy of the frequency measurements is estimated to be about 0.001 cm^{-1}.

3 - 3 - 3. Observed Spectrum and Analysis

The absorption spectrum of NH_2OH was observed in the 220 - 450 cm^{-1} region. The NH_2OH transitions show a classical b-type spectrum, with *Q*-branches clearly discernible, as seen in Figure 3 - 3 - 1. The lines show a maximum of about 20 % absorption. Between 378 and 384 cm^{-1}, the transmittance of the beamsplitter is low, and only the strongest lines of NH_2OH could be measured accurately. The transmittance of the beamsplitter decreases again above 457 cm^{-1}, and the transitions at higher frequencies could not be observed.

The lines of the ν_9 fundamental band and of the two lowest hot bands, $2\nu_9 - \nu_9$ and $3\nu_9 - 2\nu_9$, were easily assigned using the parameters determined by Taubmann and Jones(1987). The observed intensities of the lines lead to a rotational and kinetic temperature of 354 ± 9 K for the ν_9 band, 344 ± 11 K for the $2\nu_9 - \nu_9$ band, and 330 ± 30 K for the $3\nu_9 - 2\nu_9$ band. The temperature in this last band has a larger uncertainty owing to the weakness of the lines. The parameters of the $4\nu_9$ level were extrapolated from the first four levels, but the next hot band, $4\nu_9 - 3\nu_9$ was not observed in the

spectrum, as expected since the Boltzmann factor at this temperature of about 350 K is not favorable. Altogether, around 5000 lines belonging to the three bands were assigned. Table 3 - 3 - 1 gives the repatriation of the lines between these three bands along with the maximal J and K values.

NH_2OH is a very nearly prorate symmetric-top molecule, with an asymmetry parameter $\kappa = 0.99923$, as calculated from the ground state rotational constants (Tsunekawa, 1972). The observed lines were thus analyzed with a standard Watson-type asymmetric-top Hamiltonian written in the S-reduction (Watson, 1977). Due to the high rotational quantum numbers, it was necessary to introduce for the first three levels one of the sixth-order distortion constants, H_K. The other distortion constants could not be accurately determined and were fixed to 0.0 cm^{-1} in the further analysis.

In a first step, each band was analyzed separately by a least squares fitting procedure, and combination differences in the lower state were formed to check every line. In the $3\nu_9$ level, the transitions with $K = 2$ and $K = 3$ show a systematic deviation. As shown by Taubmann and Jones (1987), the $3\nu_9$ level is perturbed by a Coriolis-type interaction with the closeby ν_5 level, which shifts only these two series. Since the b and c axis in the ν_5 state are exchanged, as shown by Birk and Jones (1988), the interaction cannot be described by the classical expressions for Coriolis perturbation. Therefore, these lines were given a weight 0 in the fit. As a consequence, the d_2 parameter in the $3\nu_9$ level could not be determined precisely, because its effect appears mainly in the $K = 2$ rotational levels (Watson, 1977). For this reason, this parameter was fixed to the approximate expected value of 0.50 x 10^{-7} cm^{-1}.

In a second step, the three bands were fitted simultaneously, together with the combination differences in the $2\nu_9$ state obtained from the transitions of the $3\nu_9 - 2\nu_9$ band with $K = 2$ and $K = 3$ in the upper level. The microwave transitions measured by Tsunekawa (1972) were also included. Isolated infrared lines were given a weight 1, and both components of non-resolved doublets a weight 0.5. The microwave transitions were given a weight 300 000, according to the accuracy of their frequency measurements. The standard deviation of the fit is about 0.0009 cm^{-1}.

The resulting molecular parameters are given in Table 3 - 3 - 2. They show no significant deviation compared to the parameters obtained in the separate fits or the ones reported by Taubmann and Jones (1987). The set of parameters determined in the this study is both more accurate and more complete than that in the previous study.

3 - 3 - 4. Discussion

The behavior of the rotational constants B and C, of the distortion constants, and of the splitting constants, is almost regular. The slight irregularities these constants show can be ascribed to the composition of the data sets of the various bands.

On the contrary, the rotational constant A shows a large variation with the vibrational quantum number : $A_0 - A_1 = 0.04282$ cm^{-1}, $A_1 - A_2 = 0.03495$ cm^{-1}, and $A_2 - A_3 = 0.02974$ cm^{-1}, whereas these quantities are generally of the same value, α_e^A. Similarly, using the customary expression, we obtain for the equilibrium vibrational constants $\omega_9 = 405.76(98)$ cm^{-1} and $x_{99} = 10.03(23)$ cm^{-1}, that have uncertainties far below the experimental precision. These results reflect the expected strong anharmonicity of the torsion motion, and higher order terms are required to describe the apparently anomalous behavior of the A constants and of the band centers.

Further work will have to be carried out to enable a complete determination of the potential function of hydroxylamine, which has already been discussed in previous studies (Tsunekawa, 1972; Tamagake, 1974).

References

Birk, H. and Jones, H. 1988, J. Mol. Spectrosc. **129**, 333.

Coles, M. E., Merer, A. J., and Curl, R. F. 1984, J. Mol. Spectrosc. **103**, 300.

Guelachvili, G., and Narahari. Rao, K. 1986, "*Handbook of Infrared Standards,*" Academic Press, San Diego.

Tamagake, K., Hamada, Y., Yamaguchi, J., Hirakawa, A. Y., and Tsuboi, M. 1974, J. Mol. Spectrosc. **49**, 232.

Taubmann, G. and Jones, H. 1987, J. Mol. Spectrosc. **123**, 366.

Tsunekawa, S. 1972, J. Phys. Soc. Jpn. **33**, 167.

Watson, J. K. G. 1977, "*Vibrational Spectra and Structures, A Series of Advances,*" Dekker, New York, Vol. **6,** P. 1.

Table 3 -2 - 1

Distribution of the observed lines in the different bands

Band	Number of lines[a]	J_{max}	K_{max}
ν_9	2358	40	11
$2\nu_9 - \nu_9$	1683	36	10
$3\nu_9 - 2\nu_9$	783	28	8

[a]Both components of unresolved doublets are counted.

Table 3 - 2 - 2

Molecular constants of NH_2OH[a]

	ground	ν_9	$2\nu_9$	$3\nu_9$
A	6.370 2814(15)	6.327 4660(59)	6.292 5160(97)	6.262 772(12)
B	0.841 206 26(21)	0.840 938 01(72)	0.840 5464(12)	0.840 1808(26)
C	0.839 132 38(20)	0.834 664 91(70)	0.830 4191(12)	0.826 2626(24)
$D_J \times 10^5$	0.251 429(44)	0.248 145(52)	0.245 773(71)	0.242 68(20)
$D_{JK} \times 10^4$	0.219 381(71)	0.207 497(91)	0.199 63(13)	0.188 94(26)
$D_K \times 10^3$	0.117 83(18)	0.111 41(20)	0.107 94(35)	0.105 54(18)
$d_1 \times 10^7$	-0.3674(12)	-0.4322(35)	-0.5275(69)	-0.671(26)
$d_2 \times 10^7$	0.5283(13)	0.5283(12)	0.5138(26)	0.50[b]
$H_K \times 10^7$	0.106(11)	0.135(18)	0.216(36)	0[b]
ν_0	0[b]	385.963 31(8)	751.075 51(12)	1096.916 75(18)

[a]In units of cm^{-1}. Figures in parentheses denote one standard deviation.
[b]Fixed.

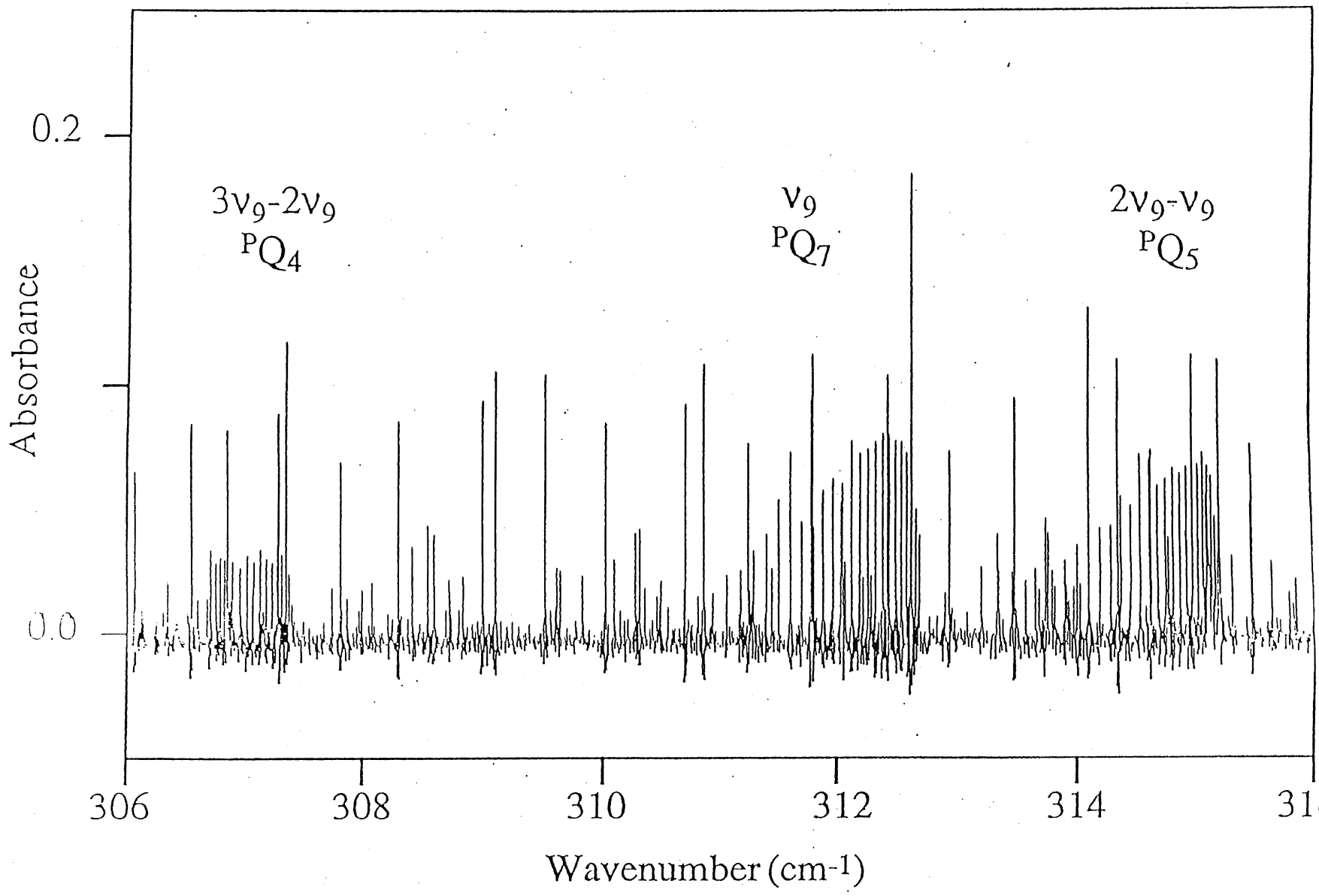

Figure 3 - 3 - 1. Observed spectrum of NH_2OH between 306 and 316 cm^{-1}.

4. Fourier Transform Emission Infrared Spectroscopy of Transient Molecules

4 - 1. Vibration-Rotation Spectrum of the CD Radical

Abstract

The gas-phase vibration-rotation emission spectrum of the CD radical in the $X^2\Pi$ state was observed in the 1832 - 2150 cm^{-1} region with a high-resolution Fourier transform spectrometer. The radical was generated by a dc discharge in a CD_4 and He mixture. The spectra of the v = 1 - 0 and 2 - 1 bands were analyzed by an effective Hamiltonian in Hund's case (a) parity-conserving basis set written in the N^2-formalism. Molecular constants of the vibrationally excited states were determined for the first time with a high precision, and the equilibrium molecular constants were determined: ω_e = 2100.3457(10) cm^{-1}, $\omega_e x_e$ = 34.155 82(39) cm^{-1}, B_e = 7.807 826(33) cm^{-1}, and α_e = 0.212 255(80) cm^{-1}, with one standard deviation in parentheses. The internuclear distance, r_e was also determined to be 1.117 915(10) Å from the corrected equilibrium rotational constant for the second-order electronic contribution to the rotational constant. Quantitative discussions on the Herman-Wallis effect were presented for the CH and CD radicals. The analysis of this effect on the CH radical led to the transition moment of -0.190(11) D for the v = 1 - 0 band.

4 - 1 - 1. Introduction

The methylidyne radical has attracted much interest of many scientists because it is involved in a wide variety of chemical and physical systems. It is one of the most abundant interstellar molecules (Dunham, 1937; Swings and Rosefeld, 1937; Rydbeck, Elldér, and Irvine, 1973; Stacey, Lugten, and Genzel, 1987) and thought to be a significant intermediate in the evolution of interstellar molecules (Zuckerman and Turner, 1975).

Although many spectroscopic studies have been carried out on the normal species (CH), there is only a few studies on deuterated species (CD). The electronic spectrum of the CD radical was studied by Shindei (1936), Gerö (1941), and Herzberg and Johns (1969). Recently, Brown and Evenson (1989) observed the pure rotational spectrum of CD using a far-infrared laser magnetic resonance (FIR LMR) technique. This last work provided precise values for the spin-orbit constant, rotational constant, centrifugal distortion constants, spin-rotation constants, Λ-doubling constants, hyperfine parameters, and two *g*-factors in the $X^2\Pi$ v = 0 state. The high-resolution infrared spectrum of CH was first reported by Lubic and Amano (1984) using a tunable difference frequency laser. Further rovibrational studies of CH were carried out with a Fourier transform spectrometer by Bernath (1987) and Bernath *et al.* (1991, 1994), who observed the highly excited vibration-rotation emission spectrum up to the v = 4 - 3 band, and determined the equilibrium molecular constants. So far no infrared spectrum of CD has been observed.

For many molecules, anomalous intensity distribution in vibration-rotation spectra has been reported. In these cases, the intensity differences between *P*- and *R*-branch lines are explained by the Herman-Wallis effect (1955), which is caused by the mixing of the permanent dipole moment and the vibrational transition moment through centrifugal distortion effect due to molecular rotation and is already described for simple diatomic molecule in Chapter 1. This effect is important for the determination of the transition

moment of transient species, the concentration of which is difficult to estimate by usual experimental techniques.

In the present study, the v = 1 - 0 and 2 - 1 vibration-rotation emission spectra of CD in the $X^2\Pi$ state were observed for the first time by using a high-resolution Fourier transform infrared spectrometer. Molecular constants in the vibrationally excited states and equilibrium molecular constants of CD were precisely determined. Quantitative comments on the Herman-Wallis effect on CH and CD were also presented in the discussion.

4 - 1 - 2. Experimental

The vibration-rotation emission spectrum of the CD radical was recorded with a high-resolution Fourier transform spectrometer. The radical was produced in the positive column discharge emission cell shown in Figure 4 - 1 - 1. Detail of the emission cell in this study was already described in Chapter 2. In short, the cell is made of Pyrex tube with a water-cooled jacket. The anode and cathode are mounted inside the water-cooled glass tube. He gas was introduced from the end of both electrodes. CD_4 gas was introduced from both ends of the cell. The reaction products were continuously pumped out by a rotary pump from the central part of the cell. The CaF_2 was used as window.

The infrared emission from the cell was focused by a CaF_2 lens with 75 mm focal length onto the iris of the Fourier transform spectrometer. The incident beam from the iris was let into the Michelson interferometer, and detected by an InSb detector through a low-pass filter (< 4000 cm^{-1}).

The CD radical was produced by a dc discharge (250 mA) in a CD_4 (99 % purity) and He mixture with partial pressures of 50 mTorr and 10 Torr, respectively. These conditions were optimized by observing the infrared emission signal of the CH radical.

The 1800 - 4000 cm^{-1} region was observed with a 0.0181 cm^{-1} resolution, where the lower wavenumber side was limited by the sensitivity of the InSb detector. The integration time was 108 minutes with 200 scans. The observed wavenumbers were

calibrated using two v = 1 - 0 transitions ($P(19)$ and $P(9)$) of $^{12}C^{16}O$ (Guelachvili and Narahari Rao, 1986).

4 - 1 - 3. Observed Spectrum and Analysis

As discussed by Brown and Evenson (1989), the rotational energy levels of the molecule with the spin-orbit interaction parameter in magnitude about $A = 4B$ in the $X^2\Pi$ state follow accidentally Hund's case (b) behavior. Therefore, vibration-rotation spectral line of CD is observed with quartet fine structure. Unfortunately, the signal of CD is not so strong ($S/N < 5$), and the region around the band origin (2000 cm^{-1}) was interrupted by many strong vibration-rotation emission lines of CO that was produced by a small air leak in the discharge cell. The author calculated each transition frequency using the molecular constants in the ground state (Brown and Evenson, 1989) and those predicted from the isotope scaling factor for the equilibrium constants of CH (Bernath, 1987), and determined the rotational numbering N of the observed lines. The assignments of the parity and total angular momentum quantum number J for the v = 1 - 0 band were carried out by taking the combination differences from P- and R-branch transition frequencies. Total of 48 lines were observed for the v = 1 - 0 band, as listed in Table 4 - 1 - 1. The assignments of the v = 2 - 1 transitions were carried out using the results of the least squares fitting of the v = 1 - 0 band. The author assigned 43 lines for the v = 2 - 1 band, which are also summarized in Table 4 - 1 - 1. The v = 3 - 2 band was not identified in the spectrum.

It is easier and more familiar to write the energy matrix in the Hund's case (a) basis set. The observed 91 spectral lines in Table 4 - 1 - 1 were analyzed by an effective Hamiltonian in Hund's case (a) parity-conserving basis set written in the N^2-formalism (Brown *et al.* 1979). Giving zero weights for the transitions with low signal-to-noise ratio, the observed spectra in Table 4 - 1 - 1 were submitted to a least squares fitting to determine the spectroscopic constants, where the molecular constants in the ground state were fixed to the values obtained by Brown and Evenson (1989). The derived

spectroscopic constants are summarized in Table 4 - 1 - 2. The standard deviation was 0.0012 cm^{-1} that was 1/15 of the resolution in the present measurement. The equilibrium vibrational and rotational constants were precisely determined from the values in Table 4 - 1 - 2, and are listed in Table 4 - 1 - 3.

4 - 1 - 4. Discussion

Fourier transform emission spectroscopy was applied to the CD radical generated by a dc discharge in a CD_4 and He mixture. In the present study, the author analyzed the spectra of the v = 1 - 0 and 2 - 1 bands and obtained precise molecular constants in the excited vibrational states as listed in Table 4 - 1 - 2. The equilibrium constants determined from these constants are consistent with those given by Herzberg and Johns (1969), as shown in Table 4 - 1 - 3, and the precision was improved by three orders of magnitude.

The r_e values of CH and CD were determined to be 1.119 789(7) Å and 1.118 883(5) Å from B_e by Bernath *et al.* (1991, 1994) and the present study, respectively. The difference in r_e between CH and CD was 0.000 906(9) Å. Since the value was large compared with these in other molecules, the author considered the second-order electronic contribution from other states.

First, the author converted B values in the $\mathbf{N}^2$-formalism to the values in the $\mathbf{R}^2$-formalism by using the following formula (Brown *et al.* 1979),

$$B_v(\mathbf{R}^2) = B_v(\mathbf{N}^2) - 2\Lambda^2 D_v(\mathbf{N}^2) + 3\Lambda^4 H_v(\mathbf{N}^2) + \cdots, \quad (1)$$

where $B_v(\mathbf{R}^2)$ and $B_v(\mathbf{N}^2)$ are rotational constants in the $\mathbf{R}^2$- and $\mathbf{N}^2$-formalism, respectively. The $B_v(\mathbf{R}^2)$ value is an effective one containing the second-order electronic contribution form Σ and Δ states, and expressed as (Amano, 1984),

$$B_v(\mathbf{R}^2) = B_v^{cor} + q_v^*, \quad (2)$$

where B_v^{cor} is the corrected constant and $q_v^* = 2\sum_{n'=\Sigma,\Delta} \frac{\left|\langle n\Lambda | B_v L_+ | n'\Lambda' \rangle\right|^2}{\Delta E_{nn'}}$. The q_v^* value is also related to the g-factors as follows (Brown *et al.* 1978; Amano, 1984; Lubic and Amano, 1984),

$$q_v^* = -\frac{g_r^N - g_r}{g_L + g_r^N} B_v, \tag{3}$$

where g_r^N is the nuclear rotational g-factor, g_L the electron orbital g-factor, g_r the rotational g-factor, and the vibrational dependence of the g-factor is neglected. Brown and Evenson (1989) reported the following g-factors by FIR LMR of the CD ground state,

$g_L' = g_L + \Delta g_L = 1.000\ 661(76)$, $g_l = 0.001010$, $g_r = -0.001\ 560(16)$,

$g_L^{e'} = -0.00147$,

where Δg_L is ascribed to a slight quenching of the orbital angular momentum by the rotation of the molecule. When the relativistic correction for Δg_L is neglected and isotopic relation for $\Delta g_L = 0.011\ 6(13)$ of CH (Brown and Evenson, 1983) is assumed, g_L(CD) is obtained to be 0.993 93(75). g_r^N was calculated to be 0.0002727 for CD by using the following formula (Carrington, Levy, and Miller, 1970),

$$g_r^N = m\sum_\alpha \left\langle \eta \left| \frac{Z_\alpha r_\alpha^2}{I} \right| \eta' \right\rangle \tag{4}$$

where m is the electron mass, η the vibronic state, Z_α the charge of α-th nuclei, r_α the distance of α-th nuclei from the center of mass, and I the nuclear moment of inertia.

Using Eq. (3), q_0^* for CD was obtained to be -431.4(3.8) MHz for CD. Similar calculation for CH gave q_0^* = -1433(22) MHz by Lubic and Amano(1984). These give B_e^{cor} = 14.456 86(15) cm^{-1} for CH and 7.821 35(13) cm^{-1} for CD, respectively. Then, the corrected r_e values for CH and CD are determined to be 1.118 056(29) Å and 1.117 915(10) Å, respectively. The difference in the corrected r_e between CH and CD was 0.000 141(31) Å , which was about 1/6 of the difference in non-corrected r_e. This difference is still relatively large compared with that in other molecule. In the case of the hydroxyl radical (Amano, 1984), for example, r_e(OD) was determined to be 0.969 680(10) Å, which is only 0.000 052(13) Å longer than the corresponding value 0.969 628(9) Å of OH. The reason why the breakdown of the Born-Oppenheimer approximation is so large in the methylidyne radical is not clear.

Unfortunately the observed signal for CD was not strong enough to discuss the Herman-Wallis effect. On the other hand, the vibration-rotation emission spectrum of CH

was observed in the preliminary measurement with good signal to noise ratio. Therefore, in the present paper we would like to discuss the Herman-Wallis effect of CH and predict its effect on CD by using the isotopic relation.

The electric dipole moment of a diatomic molecule is written as a function of the bond length :

$$M(\xi) = M_0 + M_1\xi + M_2\xi^2 + \cdots, \tag{5}$$

where ξ is equal to $(r - r_e)/r_e$. For the v = 1 - 0 band, the centrifugally perturbed vibrational transition moment μ_{10} is expressed by the product of the unperturbed transition moment μ_{10}^0 and of the rotation dependent factor as follows (Herman and Wallis, 1955; Tipping and Herman, 1970),

$$\mu_{10} = \mu_{10}^0(1 + \frac{1}{2}m\alpha_{10} + \cdots), \tag{6}$$

where

$$\mu_{10}^0 = (B_e/\omega_e)^{1/2}M_1 \tag{7}$$

and

$$\alpha_{10} = -(8B_e/\omega_e)(M_0/M_1). \tag{8}$$

In Eq. (6), m is an running number which takes the values 1, 2, ··· for the $R(0)$, $R(1)$, ··· and the values -1, -2, ··· for $P(1)$, $P(2)$, ···. The Herman-Wallis factor for the intensity is defined by

$$F_{10} = (\mu_{10}/\mu_{10}^0)^2. \tag{9}$$

In the case of CH, the intensities of the R-branch lines were observed much stronger than those of the P-branch lines. For example, the emission line strength of $R(8)$ was observed with about 2.9 times stronger in intensity than that of $P(10)$, and the first order Herman-Wallis effect parameter α_{10} was determined to be 0.022 2(10) using Eq. (9). The positive value of α_{10} means that the sign of M_1 is different from that of M_0 in the methylidyne radical. Using Eq. (8), the Herman-Wallis effect of CD is predicted to be 74% of CH, and α_{10} is calculated to be 0.016. Due to the poor signal-to-noise ratio, the effect was not recognized in the CD spectrum. The magnitude of the α_{10} value obtained for the methylidyne radical is seemed to be reasonable compared with those for other radicals. As shown in Eq. (8), α_{10} is inversely proportional to the square-root of the

reduced mass. For relatively heavy radicals such as ClO (Burkholder *et al.* 1987) and BrO (Orlando *et al.* 1991), the values of α_{10} were reported to be 0.00563, and 0.00732, respectively. On the other hand, the α_{10} values of relatively light molecules such as SH (Benidar *et al.* 1991) and OH were, respectively, determined to be 0.0987 and -0.1280, where the value of OH was calculated from the dipole moment functions (Nelson *et al.* 1990).

Using Eqs. (7) and (8), and α_{10} above, the unperturbed transition moment μ_{10}^0, that is, the transition moment for the v = 1 - 0 band of CH was determined to be -0.190(11) Debye, where the equilibrium molecular constants reported by Bernath (1987) and the permanent dipole moment of 1.46(6) Debye reported by Phelps and Dalby (1966) were used. An ab initio calculation by Meyer and Rosmus (1975) estimated μ_{10}^0 to be -0.117 Debye that was 62 % of that determined in the present work.

References

Amano, T. 1984, J. Mol. Spectrosc. **103,** 436.

Benidar, A., Farrenq, R., Guelachvili, G., and Chackerian, Jr. 1991, C., J. Mol. Spectrosc. **147,** 383.

Bernath, P. F. 1987, J. Chem. Phys. **86,** 4838.

Bernath, P. F., Brazier, C. R., Olsen, T., Hailey, R., Fernando, W. T. M. L., Woods, C., and Hardwick, J. L. 1991, J. Mol. Spectrosc. **147,** 16; 1994, **165,** 310.

Brown, J. M., Kaise, M., Kerr, C. M. L., and Milton, D. J. 1978, Mol. Phys. **36,** 553.

Brown, J. M., Colbourn, E. A., Watson, J. K. G., and Wayne, F. D. 1979, J. Mol. Spectrosc. **74,** 294.

Brown, J. M. and Evenson, K. M. 1983, J. Mol. Spectrosc. **98,** 392.

Brown, J. M., Cheung, A. S-C., and A. Merer, J. 1987, J. Mol. Spectrosc. **124,** 464.

Brown, J. M. and Evenson, K. M. 1989, J. Mol. Spectrosc. **136,** 68.

Burkholder, J. B., Hammer, P. D., Howard, C. J., Maki, A. G., Thompson, G., and Chackerian, Jr., C. 1987, J. Mol. Spectrosc. **124,** 139.

Carrington, A., Levy, D. H., and Miller, T. A. 1970, Adv. Chem. Phys. **18,** 149.

Dunham, Jr., T. 1937, Publ. Astron. Soc. Pacific, **49,** 26.

Gerö, L. 1941, Z. Phys. **118,** 709.

Guelachvili, G. and Narahari Rao, K. 1986, "*Handbook of Infrared Standards,*" Academic Press, San Diego.

Herman, R. and Wallis, R. F. 1955, J. Chem. Phys. **23,** 637.

Herzberg, G. and Johns, J. W. C. 1969, Astrophys. J. **158,** 399.

Lubic, K. G. and Amano, T. 1984, J. Chem. Phys. **81,** 1655.

Meyer, W. and Rosmus, P. 1975, J. Chem. Phys. **63,** 2356.

Nelson, Jr., D. D., Schiffman, A., Nesbitt, D. J., Orlando, J. J., and Burkholder, J. B. 1990, J. Chem. Phys. **93,** 7003.

Orlando, J. J., Burkholder, J. B., Bopegedera, A. M. R. P., and Howard, C. J. 1991, J. Mol. Spectrosc. **145,** 278.

Phelps, D. H. and Dalby, F. W. 1966, Phys. Rev. Lett. **16,** 3.

Rydbeck, O. E. H., Elldér, J., and Irvine, W. M. 1973, Nature, **246,** 466.

Shindei, T. 1936, Jpn. J. Phys. **11,** 23.

Stacey, G. J., Lugten, J. B., and Genzel, R. 1987, Astrophys. J. **313,** 859.

Swings, P. and Rosefeld, L. 1937, Astrophys. J. **86,** 483.

Tipping, R. H., and Herman, R. M. 1970, J. Mol. Spectrosc. **36,** 404.

Zuckerman, B. and Turner, B. E. 1975, Astrophys. J. **197,** 123.

Table 4 - 1 - 1

Observed line positions of the vibration-rotation emission spectrum of the CD radical in the $X^2\Pi$ state[a]

N'	N''	J'	J''	v = 1 - 0		v = 2 - 1	
				$\nu_{obs.}$	δ [b]	$\nu_{obs.}$	δ [b]
1	2	1.5^{+c}	2.5^-	2000.8454	6	1933.2937	8
		1.5^-	2.5^+	2000.8065	-13	1933.2560	-2
2	3	1.5^+	2.5^-			1917.6042	4
		1.5^-	2.5^+	1984.6368	10		
		2.5^-	3.5^+	1984.6066	5	1917.5238	12
		2.5^+	3.5^-	1984.5476	12	1917.4623	-10
3	4	2.5^+	3.5^-	1968.0784	4	1901.5103	-12
		3.5^+	4.5^-	1968.0065	4	1901.3671	-10
		2.5^-	3.5^+	1967.9742	5	1901.4103	6
		3.5^-	4.5^+	1967.9214	-16	1901.2843	-15
4	5	3.5^-	4.5^+	1951.1126	10	1884.9614	17
		4.5^-	5.5^+	1951.0329	-5	1884.8358	8[e]
		3.5^+	4.5^-	1950.9846	18	1884.8358	18[e]
		4.5^+	5.5^-	1950.9262	-3	1884.7278	-16
5	6	4.5^+	5.5^-	1933.7670	-22	1868.0408	-15
		5.5^+	6.5^-	1933.6967	33[d]	1867.9328	-6
		4.5^-	5.5^+	1933.6157	4	1867.8926	0
		5.5^-	6.5^+	1933.5617	-6	1867.8016	-28[d]
6	7	5.5^-	6.5^+	1916.0668	2	1850.7680	-29[d]
		6.5^-	7.5^+	1915.9965	7	1850.6745	-2
		5.5^+	6.5^-	1915.8898	26	1850.5954	-17
		6.5^+	7.5^-	1915.8389	-7	1850.5234	12
7	8	6.5^+	7.5^-	1898.0156	-3	1833.1568	6
		7.5^+	8.5^-	1897.9509	6	1833.0696	-7
		6.5^-	7.5^+	1897.8096	-5		
		7.5^-	8.5^+	1897.7670	-13	1832.8913	-29[d]
8	9	7.5^+	8.5^-	1879.3937	-13		
		8.5^+	9.5^-	1879.3585	-2		
1	1	1.5^-	1.5^+	2031.3718	5		
2	2	1.5^+	1.5^-	2031.0419	-17	1962.7468	-6
		1.5^-	1.5^+	2030.9297	4		
		2.5^-	2.5^+			1962.3030	-1

Table 4 - 1 - 1 -*Continued*

N'	N''	J'	J''	v = 1 - 0		v = 2 - 1	
				$\nu_{obs.}$	δ [b]	$\nu_{obs.}$	δ [b]
2	1	2.5^{-}[c]	1.5^{+}	2061.1787	20	1992.1002	19
		2.5^{+}	1.5^{-}	2061.2119	-6	1992.1297	-30[d]
		1.5^{-}	0.5^{+}			1993.0839	-2
		1.5^{+}	0.5^{-}			1993.1328	40[d]
3	2	3.5^{+}	2.5^{-}	2075.4193	-12	2005.8913	-8
		3.5^{-}	2.5^{+}	2075.4777	5	2005.9453	-13
		2.5^{+}	1.5^{-}	2076.0000	-7	2006.3747	6
		2.5^{-}	1.5^{+}	2076.0760	31[d]		
4	3	4.5^{-}	3.5^{+}			2019.1785	-1
		4.5^{+}	3.5^{-}			2019.2539	13
		3.5^{-}	2.5^{+}	2089.5012	28[d]	2019.4999	2
		3.5^{+}	2.5^{-}	2089.5879	-19		
5	4	5.5^{+}	4.5^{-}	2102.3514	17	2031.9873	13
		5.5^{-}	4.5^{+}	2102.4456	-7	2032.0789	4
		4.5^{+}	3.5^{-}	2102.6182	2	2032.2283	11
		4.5^{-}	3.5^{+}			2032.3319	-16
6	5	6.5^{-}	5.5^{+}	2115.0848	-11	2044.3158	-8
		6.5^{+}	5.5^{-}	2115.2016	11	2044.4269	4
		5.5^{-}	4.5^{+}	2115.2964	1	2044.5097	-4
		5.5^{+}	4.5^{-}	2115.4225	-11	2044.6348	17
7	6	7.5^{+}	6.5^{-}	2127.3362	8		
		7.5^{-}	6.5^{+}	2127.4674	8		
		6.5^{+}	5.5^{-}	2127.5119	35[d]		
		6.5^{-}	5.5^{+}			2056.4686	19
8	7	8.5^{-}	7.5^{+}	2139.0890	-25	2067.5284	5
		7.5^{-}	6.5^{+}	2139.2378	-6	2067.6671	-4[e]
		8.5^{+}	7.5^{-}	2139.2388	13	2067.6671	-16[e]
		7.5^{+}	6.5^{-}			2067.8184	-18
9	8	8.5^{+}	7.5^{-}	2150.4753	12		
		9.5^{-}	8.5^{+}	2150.5079	28[d]	2078.5493	7

[a] cm^{-1} unit.
[b] (obs. - calc.) x 10^4.
[c] The superscript denotes parity.
[d] Weight is set to zero due to poor signal to noise ratio.
[e] Blended lines. Weight is set to 0.5.

Table 4 - 1 - 2

Molecular constants of CD in the $X^2\Pi$ state[a]

Constants	v = 0[b]	v = 1	v = 2
T_v	0.0	2032.034 09(39)	3995.756 53(56)
B_v	7.701 868 2(15)	7.490 970(24)	7.281 429(34)
D_v x 10^4	4.276 89(47)	4.209 6(31)	4.137 0(42)
H_v x 10^8	1.585		
A_v[c]	28.096 392(11)	28.236 1(16)	28.375 0(24)
γ_v[c] x 10^2	-1.413 65(29)	-1.355 1(75)	-1.289(12)
γ_{Dv}[c] x 10^6	2.44		
p_v x 10^2	1.816 06(73)	1.725(12)	1.662(18)
p_{Dv} x 10^6	-1.93(50)		
p_{Hv} x 10^{10}	1.7		
q_v x 10^2	1.132 18(23)	1.109 4(30)	1.080 8(40)
q_{Dv} x 10^6	-2.552(90)	-3.97(48)	-4.19(64)
q_{Hv} x 10^{10}	2.79		

[a]cm^{-1} unit. The numbers in parentheses denote one standard deviation and apply to the last digits of the constants.

[b]Fixed to the values determined by Brown and Evenson(1989). The constants without standard errors were obtained by scaling from the corresponding values of CH[see Brown and Evenson(1989)].

[c]Effective constants. A_D was constrained to zero.

Table 4 - 1 - 3

Equilibrium values of CD in the $X^2\Pi$ state[a]

Constants	This work	Herzberg and Johns(1969)
B_e	7.807 826(33)	7.806
B_e^{cor}	7.821 35(13)	
α_e	0.212 255(80)	0.208
γ_e	0.000 678(30)	
D_e	0.000 431 83(42)	
β_e	0.000 007 3(10)	
r_e	1.118 883(5) Å	1.119 Å
r_e(corrected)	1.117 915(10) Å	
ω_e	2100.345 7(10)	2099.7_5
$\omega_e x_e$	34.155 82(39)	34.02

[a]cm^{-1} unit. The numbers in parentheses denote one standard deviation and apply to the last digits of the constants.

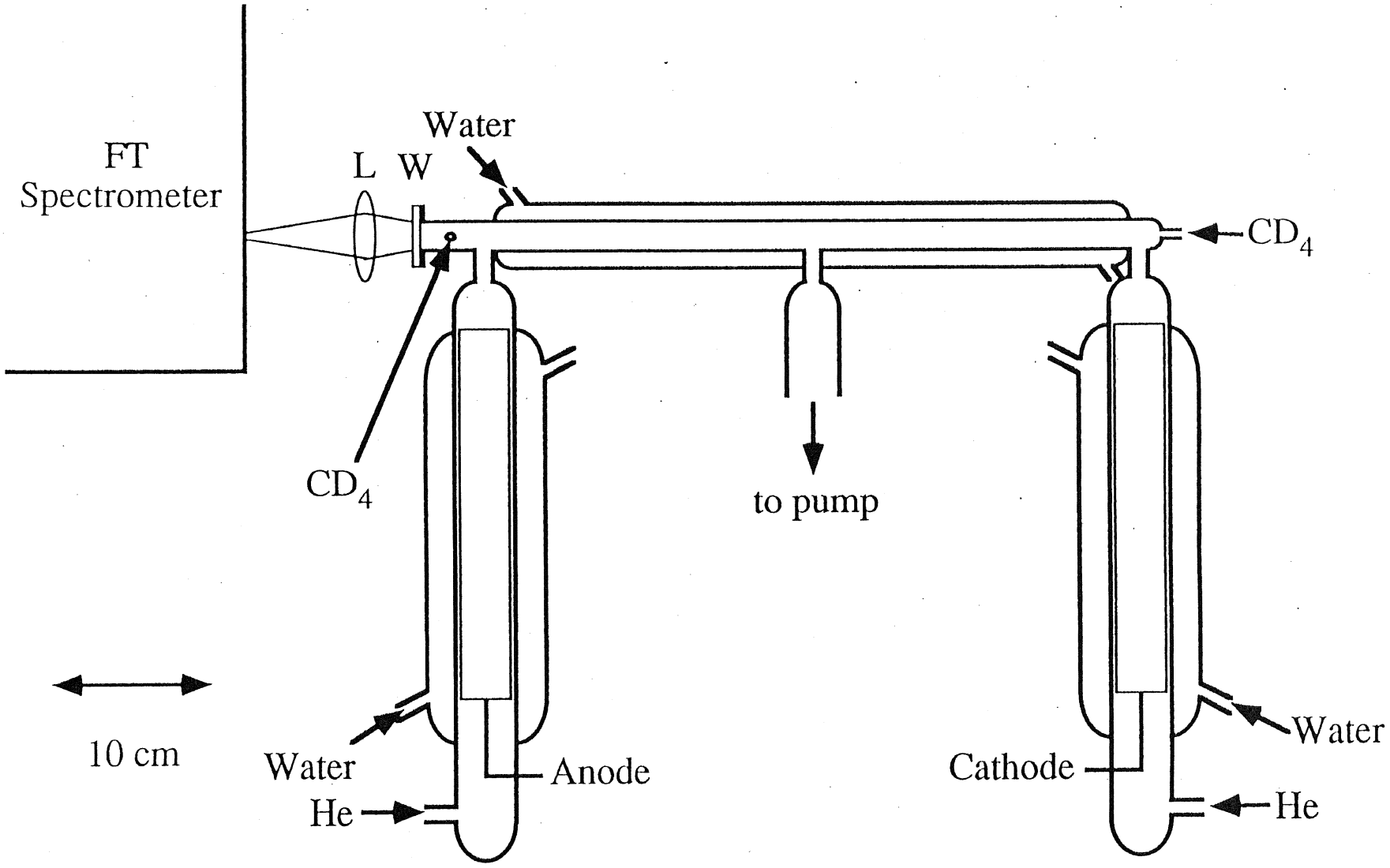

Figure 4 - 1 - 1. Schematic diagram of the positive column dc discharge cell designed to observe infrared emission spectra. W is a CaF_2 window, and L is a CaF_2 lens.

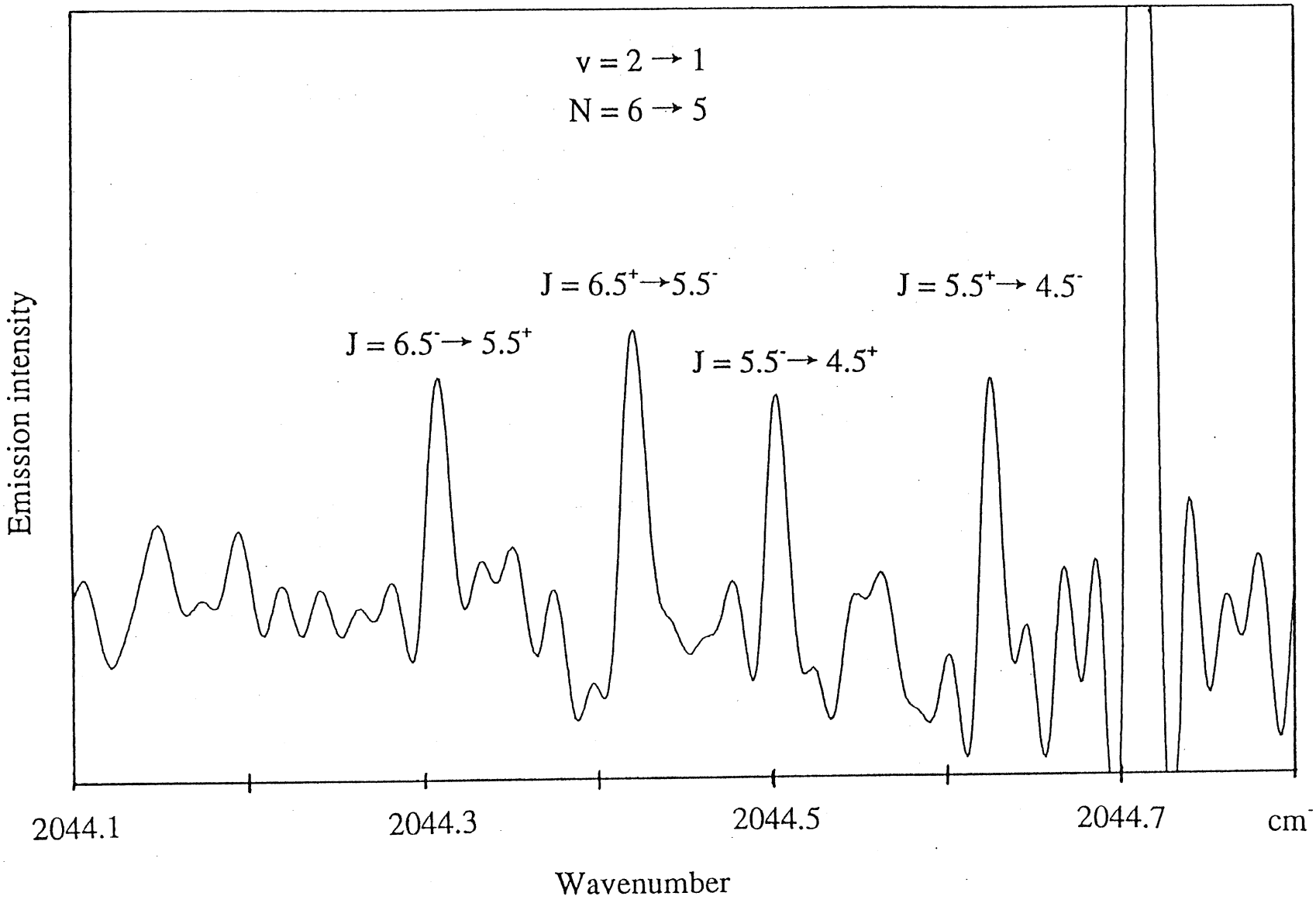

Figure 4 - 1 - 2. Observed emission spectrum of the v = 2 - 1, N = 6 - 5 transition of the CD radical. The strong line at 2044.72 cm^{-1} is a highly excited rovibrational transition of CO.

4 - 2. Vibration-Rotation Spectrum of the ^{18}OH Radical

Abstract

The gas-phase emission spectra of the v = 1 - 0, 2 - 1, 3 - 2 bands of the ^{18}OH radical in the $X^2\Pi$ state have been observed with a high-resolution Fourier transform spectrometer. The radical was produced by a dc discharge in a $H_2{}^{18}O$ and He mixture. The spectrum observed between 2921 and 3773 cm^{-1} region was analyzed by an effective Hamiltonian in Hund's case (a) parity-conserving basis set written by $\mathbf{R}^2$-formalism. Molecular constants in the vibrationally excited states and equilibrium molecular constants of ^{18}OH were determined for the first time. The anomalous intensity is discussed in comparison with that of ^{16}OH.

4 - 2 - 1. Introduction

The OH radical is one of the most extensively studied molecules in various frequencies regions because of the importance as an intermediate matter for chemical reaction in interstellar medium and upper atmosphere. The ultra-violet electronic transitions of the $A^2\Sigma^+$ - $X^2\Pi$ system of OH were detected in the spectrum of comet Conninham, by Swings, Elvey, and Babcock (1941) for the first time. The infrared vibration-rotation transitions were identified in the air glow of the upper atmosphere by Meinel (1950a, 1950b). The centimeter-wave Λ-doublet transitions were detected against a number of continuum sources in interstellar medium by Weinreb *et al.* (1963). The far-infrared rotational transitions were detected in interstellar medium by Storey, Watson, and Twones (1981). The Λ-doublet transitions of the isotopic species ^{18}OH were observed for the first time in interstellar medium by Gardner, McGee, and Sinclair (1970), and Wilson and Barrett (1970). Recently, the rotational transition was observed in interstellar medium by Melnick *et al.* (1990) toward Orion-KL, and from these observation, it was thought the isotopic abundance in Orion-KL was the same as that on the earth.

In laboratory, many studies on OH were carried out, but studies for the isotopic species ^{18}OH are not so many. Dousmanis, Sanders, and Townes (1955) observed the two Λ-doublet transitions of ^{18}OH by a conventional microwave spectrometer. Gottlieb, Radford, and Smith (1974) observed the same Λ-doublet transitions using a molecular beam microwave spectrometer. Kolbe, Zollner, and Leslovar (1981) reported an extended measurements of high-J transition. Comben *et al.* (1986) measured the far-infrared laser magnetic resonance spectrum of the pure rotational transitions, to determine the spin-orbit interaction, rotational, centrifugal distortion, spin-rotation coupling. Recently, Morino *et al.* (1995) measured directly the far-infrared transition frequencies by using a tunable far-infrared spectrometer, and provided the more accurate molecular constants, including the hyperfine coupling constants. The $A^2\Sigma^+$ - $X^2\Pi$ band in ultra-

violet region was measured with a grating spectrograph by Cheung, Chan and Sze (1995).

The high-resolution infrared emission spectrum of ^{16}OH was observed with a Fourier transform spectrometer by Maillard, Chauville, and Mantz (1976), and Abrams *et al.* (1994a). Amano (1984) observed the infrared absorption spectra of ^{16}OH and OD by using a tunable difference frequency laser, and determined the internuclear distances for both radicals by considering the correction of the second-order electronic contribution to the rotational constants. The rovibrational emission spectrum of OD was measured with a Fourier transform spectrometer by Abrams *et al.* (1994b). There is no measurement for the vibration-rotation spectrum of ^{18}OH in infrared region so far.

In vibration-rotation spectra, intensity differences between *P*- and *R*-branch have been reported and lines are explained by the Herman-Wallis effect (1955), which is caused by the mixing of the permanent dipole moment to the vibrational transition moment through centrifugal distortion effect due to molecular rotation, and is already described for the simple diatomic molecules in Chapter 1. The intensity analysis considering this effect is important in order to determine the vibrational transition moment and concentration of transient species. Usually the transition moment is determined by a measurement of absorbance, if the concentration of molecule is known. Since in the case of transient species, it is not easy to determine the concentration, the usage of Herman-Wallis effect has advantage. The intensity analysis for ^{16}OH was already reported by Nelson *et al.* (1989a) and Nelson, Schiffman and Nesbitt (1989b, 1990).

In the present study, the author observed of the v = 3 - 2, 2 - 1, 1 - 0 band spectra of ^{18}OH by using a high-resolution Fourier transform spectrometer combined with a dc discharge flow emission cell. The observed spectrum was analyzed by an effective Hamiltonian in Hund's case (a) parity-conserving basis set written by $\mathbf{R}^2$-formalism together with the microwave and far-infrared frequencies. Molecular constants in the vibrationally excited states and equilibrium molecular constants of ^{18}OH were determined for the first time.

4 - 2 - 2. Experimental

The radical was produced in the discharge emission cell shown in Figure 4 - 2 - 1. The cell is made of a 10 cm long (1.2 cm inner diameter) Pyrex tube. The cathode is made of 27 cm long stainless steel sheets with 0.1 mm thickness and mounted inside the water-cooled glass tube with 4.0 cm inner diameter. The anode is made of 2.0 cm long stainless steel sheet with 0.1 mm thickness and mounted inside the cell with 1.2 cm inner diameter. He and $H_2{}^{18}O$ were introduced from the cathode side. The reaction products were continuously pumped out by a rotary pump from the anode side of the cell. The cell without water cooling parts was air-cooled.

The infrared emission from a CaF_2 window of the cell was focused onto the iris of the Fourier transform spectrometer by an off-axial parabolic mirror with a 120 mm focal length. In the case of weak emission, a blackbody radiation produced by heating Nichrome wire was used to attain an interferogram with a high signal-to-noise ratio. The incident beam from the iris was let into the Michelson interferometer, and detected by an InSb detector through a low-pass filter (< 4000 cm^{-1}).

The ^{18}OH radical was produced by a dc discharge (125 mA) in a $H_2{}^{18}O$ and He mixture with partial pressures of 140 mTorr and 340 mTorr measured by Pirani gauge, respectively. These conditions were optimized by observing the infrared emission signal of ^{16}OH.

The 1800 - 4000 cm^{-1} region was observed with a 0.0181 cm^{-1} resolution, where the lower wavenumber side was limited by the sensitivity of the InSb detector. The integration time was 108 minutes with 200 scans. The observed wavenumbers were calibrated using the vibration-rotation transitions of $^{12}C^{18}O$ in the 2033 - 2070 cm^{-1} region (Guelachvili and Narahari Rao, 1986). $^{12}C^{18}O$ emission was strongly observed in the same reaction system due to carbon containing residue inside the cell.

4 - 2 - 3. Observed Spectrum and Analysis

Since the spin-orbit interaction parameter A is larger than (about 7.6 times) the rotational constant B in the $X^2\Pi$ state, the rotational energy levels follow Hund's case (a) behavior for low J, and each vibration-rotation spectral line of OH is observed with doublet fine structure. Figure 4 - 2 - 2 shows a typical spectrum of P-branch transitions with their assignments. Not only v = 1 - 0 but also v = 2 - 1 bands were observed strongly. On the other hand, R-branch transitions were observed more weakly than P-branch transition with about one tenth intensity. Figure 4 - 2 - 3 shows a typical spectrum of R-branch transitions with their assignments. In the R-branch transitions, it was hard to recognize the characteristic spectral patterns of ^{18}OH because of the $H_2{}^{18}O$ rovibrational emission lines. These differences in intensities are caused by the Herman-Wallis effect. Total 138 emission lines(58 lines for v = 1 - 0, 53 v = 2 - 1, 23 v = 3 - 2)were observed and assigned, as listed in Table 4 - 2 - 1.

The observed lines were analyzed by an effective Hamiltonian in Hund's case (a) parity-conserving basis set written by $\mathbf{R}^2$-formalism (Brown *et al.* 1978). Giving zero weights for the transitions with low signal-to-noise ratios, the observed transitions in Table 4 - 2 - 1 were submitted to a least squares fitting to determine the spectroscopic constants. This fitting included also the microwave frequencies of Λ-doublet transitions (Table 4 - 2 - 2) reported by Gottlieb *et al.* (1974) and Kolbe, Zollner, and Leslovar (1986), and far-infrared transition frequencies (Table 4 - 2 - 3) measured by Morino *et al.* (1995). These transition frequencies were corrected for hyper-fine structure and were weighted according to frequency precision. The determined molecular constants are listed in Table 4 - 2 - 4. The standard deviation of this least squares fitting was 0.00078 cm^{-1}, which was 1/23 of the resolution in this experiment.

From molecular constants B, D, and H of the v = 0, 1, 2, and 3 states, the author derived the vibrational, rotational constants at equilibrium configuration, where the vibrational dependence of molecular constants are assumed as follows (Maillard, Chauvilli, and Mantz, 1976),

$$A(v) = A_0 + A_1(v + 1/2) + \cdots, \quad (1)$$

$$q_V(v) = q_0 + q_1(v + 1/2) + \cdots, \quad (2)$$

$$q_D(v) = q_0' + q_1'(v + 1/2) + \cdots, \quad (3)$$

$$p_V(v) = p_0 + p_1(v + 1/2) + \cdots, \quad (4)$$

$$p_D(v) = p_0' + p_1'(v + 1/2) + \cdots, \quad (5)$$

$$\gamma(v) = \gamma_0 + \gamma_1(v + 1/2) + \cdots, \quad (6)$$

These coefficients of ^{18}OH were determined by a least square fitting as listed Table 4 - 2 - 5, which contains also the constants of ^{16}OH determined by in the same method from Maillard's constants. Both constants of ^{18}OH and ^{16}OH are almost consistent.

4 - 2 - 4. Discussion

Fourier transform emission spectroscopy was applied to the ^{18}OH radical generated by a dc discharge in $H_2{}^{18}O$ and He mixture. In this experiment, the rovibrational transitions of the v = 1 - 0, 2 - 1, and 3 - 2 bands were assigned, and determined molecular constants are listed Table 4 - 2 - 4. The observed spectrum was analyzed by a least-squares fitting using an effective Hamiltonian in Hund's case (a) parity-conserving basis set written by N^2-formalism (Brown *et al.* 1979). Molecular constants obtained in this fitting were agreed with those determined in far-infrared measurement by Morino *et al.* (1995) within three standard deviations.

The effective equilibrium internuclear distance r_e of ^{18}OH was first experimentally determined to be 0.969 810(29) Å from the effective equilibrium rotational constant. The r_e values of ^{16}OH and OD were determined to be 0.969 628(9) Å and 0.969 680(10) Å, respectively, including the correction of the second order electronic contribution to the rotational constant, q^*, by Amano (1984). The same correction was applied to the case of ^{18}OH, where the q^* value was determined to be -560.8 MHz by the same method as Amano (1984). Then the r_e values of ^{18}OH was determined to be 0.969 360(29) Å. The difference in r_e between ^{18}OH and ^{16}OH is 0.000 268(30) Å, and is rather large compared with the difference of 0.000 052(13) Å between ^{16}OH and OD. Since the q^*

values of ^{16}OH and OD are determined to be -644(11) MHz and -190(6) MHz by Amano (1984), respectively, the value of q^* of ^{18}OH is reasonable if the isotope dependence is the same as that of the rotational constant. The effective equilibrium rotational constant of ^{16}OH was determined to be 18.910 829 cm^{-1} of a FT spectroscopic study by Maillard, Chauville, and Mantz (1976). On the other hands, Amano (1984) reported B_e = 18.890 041 cm^{-1} using a tunable difference laser spectrometer. Because those constants do not agree each other, it seems that the further discussion about the difference in r_e between ^{18}OH and ^{16}OH is not suitable. It is necessary to analyze transition frequencies of ^{16}O and ^{18}OH by the same method.

The rotational temperature was estimated to be 404.7 ± 9.3 K for the v = 1 - 0 band and 435 ± 25 K for the v = 2 - 1 band by Boltzmann plots of the observed lines. The accuracy of the temperature of the v = 2 - 1 band is worse than that of the v = 1 - 0 band, because of the low signal-to-noise ratio in the v = 2 -1 band. The vibrational temperature was also estimated to be 3340 ± 290 K by intensity ratio between the same rotational transition in the v = 2 - 1 and the v = 1 - 0 bands. The rotational temperature is very lower than the vibrational temperature, and this reason is thought that the rotational relaxation with He gas is much faster than the vibrational relaxation. The intensity ratios of *P*- and *R*-branch transitions with the same initial level in ^{18}OH state for the v = 1 - 0 band were compared with those of ^{16}OH reported by Nelson *et al.* (1990). Since the ratios of ^{18}OH are almost agreed with those of ^{16}OH within error limit, the vibrational transition moment of ^{18}OH in the v = 1 - 0 bands seems to be equal to that of ^{16}OH.

References

Abrams, M. C., Davis, S. P., Rao, M. L. P., Engleman, Jr. R., and Brault, J. W. 1994a, Astrophys. J. Suppl. **93,** 351.

Abrams, M. C., Davis, S. P., Rao, M. L. P., and Engleman, Jr. R. 1994b, J. Mol. Spectrosc. **165,** 57.

Amano, T. 1984, J. Mol. Spectrosc. **103,** 436.

Brown, J. M., Kaise, M., Ker, C. M. L., and Milton, D. J. 1978, Mol. Phys. **36,** 553.

Brown, J. M., Colbourn, E. A., Watson, J. K. G., and Wayne, F. D. 1979, J. Mol. Spectrosc. **74,** 294.

Cheung, A. S-C., Chan, C. M-T. and Sze, N. S-K. 1995, J. Mol. Spectrosc. **174,** 205.

Comben, E. R., Brown, J. M., Steimle, T. C., Leopold, K. R., and Evenson, K. M. 1986, Astrophys. J. **305,** 513.

Dousmanis, G. C., Sanders, T. M., and Townes, C. H. 1955, Phys. Rev. **100,** 1735.

Gardner, F .F., Mcgee, R. X., and Sinclair, M. W. 1970, Astrophys. Lett. **5,** 67.

Gottieb, C. A., Radford, H. E., and Smith, B. P. 1974, Unpublished Data given in R. Deaudet, A. and Poynter, R. L. 1978, J. Phys. Chem. Ref. Data **7,** 311.

Guelachvili, G. and Narahari Rao, K. 1986, "*Handbook of Infrared Standards*," Academic Press, San Diego.

Herman, R., and Wallis, R. F. 1955, J. Chem. Phys. **23,** 637.

Kolbe, W. F., Zollner, W. -D., and Leskovar, B. 1981, Rev. Sci. Instrum. **52,** 523.

Maillard, J. P., Chauville, J., and Mantz, A. W. 1976, J. Mol. Spectrosc. **63,** 120.

Meinel, A. B. 1950a, Astrophys. J. **111,** 555.

_____. 1950b, Astrophys. J. **112,** 120.

Melnick, G. J., Stacey, G. Genzel, J., R., Lugten, J. B., and Poglitsch, A. 1990, Astrophys. J. **348,** 161.

Morino, I., Odashima, H., Matsushima, F., Tsunekawa, S., and Takagi, K. 1995, Astrophys. J. **442,** 907.

Nelson, Jr. D. D., Schiffman, A., Nesbitt, D. J., and Yarcon, D. J. 1989a, J. Chem. Phys. **90,** 5443.

Nelson, Jr. D. D., Schiffman, A., and Nesbitt, D. J. 1989b, J. Chem. Phys. **90,** 5455.

_____. 1990, J. Chem. Phys. **93,** 7003.

Swings, P., Elvey, C. T., and Babcock, H. W. 1941, Astrophys. J. **94,** 320.

Storey, J. W. V., Watson, D. M., and Townes, C. H. 1981, Astrophys. J. **244,** L27.

Weinreb, S., Barrett, A. H., Meeks, M. L., and Henry, J. C. 1963, Nature, **200,** 829.

Wilson, W. J. and Barrett, A. H. 1970, Astrophys. Lett. **6,** 231.

Table 4 - 2 - 1

Observed lines of vibration-rotation emission spectrum of the ^{18}OH radical in the $X^2\Pi$ state[a]

J''	*P*-branch		*Q*-branch		*R*-branch	
	$\nu_{obs.}$	δ[b]	$\nu_{obs.}$	δ	$\nu_{obs.}$	δ
v = 1 - 0 F_1						
1.5 *e*			3557.2788	5	3637.4797	3
1.5 *f*			3557.1725	-6		
2.5 *e*	3474.0137	0	3554.4462	-31[c]	3667.4787	-8
2.5 *f*	3473.8664	2	3554.0677	4	3667.6928	-7
3.5 *e*	3436.7884	-3	3550.4151	3	3696.6221	-2
3.5 *f*	3436.5319	7	3549.5624	10	3696.9145	-1
4.5 *e*	3397.7740	-1	3545.1231	-42[c]	3724.6957	-1
4.5 *f*	3397.4022	-8	3543.6108	3	3725.0551	-10
5.5 *e*	3357.1096	-2	3538.5487	-67[c]	3751.5124	11
5.5 *f*	3356.6261	-9	3536.2033	78[c]	3751.9219	-72[c]
6.5 *e*	3314.9482	1				
6.5 *f*	3314.3565	-3				
7.5 *e*	3271.4251	3				
7.5 f	3270.7283	9				
8.5 *e*	3226.6536	1				
8.5 *f*	3225.8513	-4				
9.5 *e*	3180.7299	-2				
9.5 *f*	3179.8249	2				
v = 1 - 0 F_2						
0.5 *e*			3557.9676	-1	3616.1046	12
0.5 *f*			3557.6602	-5	3616.1940	-11
1.5 *e*	3497.0445	-2	3555.5772	-20	3651.8464	24
1.5 *f*	3496.9350	6	3555.0704	3		
2.5 *e*	3454.7483	-1	3551.5229	-49[c]	3685.2388	-9
2.5 *f*	3454.7235	1	3550.9856	-25[c]	3685.1550	12
3.5 *e*	3411.7080	-8			3716.3759	-5
3.5 *f*	3411.7870	7			3716.2088	33[c]
4.5 *e*	3367.9655	-6			3745.3842	-11
4.5 *f*	3368.1512	12				
5.5 *e*	3323.4748	-6			3772.3855	82[c]
5.5 *f*	3323.7650	10				
6.5 *e*	3278.1799	-1				
6.5 *f*	3278.5713	5				
7.5 *e*	3232.0424	8				
7.5 *f*	3232.5312	-14				
8.5 *e*	3185.0435	-4				
8.5 *f*	3185.6345	5				

Table 4 - 2 - 1 -*Continued*

J''	*P*-branch		*Q*-branch		*R*-branch	
	$\nu_{obs.}$	δ	$\nu_{obs.}$	δ	$\nu_{obs.}$	δ
v = 2 - 1	F_1					
1.5 *e*			3392.7595	-4	3470.0317	6
1.5 *f*			3392.6628	-2	3470.1513	6
2.5 *e*	3312.4614	-4	3389.9491	-5	3498.7776	-17
2.5 *f*	3312.3237	-6	3389.5965	9	3498.9778	-2
3.5 *e*	3276.5650	-3	3385.9485	7	3526.6410	-32[c]
3.5 *f*	3276.3235	1	3385.1506	-25[c]	3526.9167	1
4.5 *e*	3238.9458	2	3380.7107	17		
4.5 *f*	3238.5950	4	3379.2902	-7		
5.5 *e*	3199.7225	0				
5.5 *f*	3199.2634	-1				
6.5 *e*	3159.0332	2				
6.5 *f*	3158.4686	0				
7.5 *e*	3117.0031	0				
7.5 *f*	3116.3353	-5				
8.5 *e*	3073.7408	0				
8.5 *f*	3072.9719	-7				
9.5 *e*	3029.3383	2				
9.5 *f*	3028.4709	5				
v = 2 - 1	F_2					
0.5 *e*			3393.4484	-2	3449.1474	6
0.5 *f*			3393.1564	-4	3449.2349	-2
1.5 *e*	3335.0220	10	3391.0989	-6		
1.5 *f*	3334.9126	-15	3390.6144	19		
2.5 *e*	3294.3477	0	3387.1210	61[c]	3515.3417	5
2.5 *f*	3294.3196	-3	3386.5930	9	3515.2624	-8
3.5 *e*	3252.8795	-7				
3.5 *f*	3252.9494	3				
4.5 *e*	3210.6730	-7				
4.5 *f*	3210.8435	-4				
5.5 *e*	3167.6997	-13				
5.5 *f*	3167.9727	12				
6.5 *e*	3123.9184	-2				
6.5 *f*	3124.2875	6				
7.5 *e*	3079.2953	1				
7.5 *f*	3079.7596	7				
8.5 *e*	3033.8182	2				
8.5 *f*	3034.3745	-9				
9.5 *e*						
9.5 *f*	2988.1352	-63[c]				

Table 4 - 2 - 1 -*Continued*

J'	*P*-branch		*Q*-branch		*R*-branch	
	$\nu_{obs.}$	δ	$\nu_{obs.}$	δ	$\nu_{obs.}$	δ
v = 3 - 2 F_1						
1.5 *e*			3230.1458	-21		
1.5 *f*			3230.0589	0		
2.5 *e*	3152.7893	16				
2.5 *f*	3152.6606	4				
3.5 *e*	3118.1895	5				
3.5 *f*	3117.9628	0				
4.5 *e*	3081.9270	-5				
4.5 *f*	3081.5968	-1				
5.5 *e*	3044.1044	4				
5.5 *f*	3043.6687	-6				
6.5 *e*	3004.8413	1				
6.5 *f*	3004.3048	5				
7.5 *e*	2964.2546	-5				
7.5 *f*	2963.6180	2				
8.5 *e*	2922.4473	3				
8.5 *f*	2921.7105	-1				
v = 3 - 2 F_1						
2.5 *e*	3135.7750	0				
2.5 *f*	3135.7440	-4				
3.5 *e*	3095.8482	2				
3.5 *f*	3095.9088	6				
4.5 *e*	3055.1420	-3				
4.5 *f*	3055.2988	-2				
5.5 *e*	3013.6474	2				
5.5 *f*	3013.9041	35[c]				
6.5 *e*	2971.3308	0				
6.5 *f*	2971.6793	0				
7.5 *e*	2928.1685	0				
7.5 *f*	2928.6106	0				

[a] cm^{-1} unit.

[b] $\delta = (\nu_{obs.} - \nu_{calc.}) \times 10^4$.

[c] Weight = 0.0.

Table 4 - 2 - 2

Microwave Λ-doubling transitions of ^{18}OH for the v = 0 level in the $X^2\Pi$ state corrected for the hyperfine structure[a]

F_{ie}	J	$\nu_{obs.}$	δ[b]	ref.
F_1	1.5	1638.7754	0.0	c
F_1	2.5	5937.1684	0.0	c
F_1	7.5	69904.0654	0.0	d
F_2	0.5	4716.1903	-0.1	c

[a]MHz unit.

[b]$\delta = (\nu_{obs.} - \nu_{calc.}) \times 10^3$.

[c]Measured by Gottieb, Radford, and Smith (1974).

[d]Measured by Kolbe, Zollner, and Leskovar (1981).

Table 4 - 2 - 3

Observed rotational transitions of ^{18}OH in the $X^2\Pi$ v = 0 state by Morino *et al.* (1995) corrected for the hyperfine structure[a]

F_i'	F_i''		$\nu_{obs.}$	δ[b]
F_1	F_1	R(1.5)*e*[c]	2494696.4232	0.4
		R(1.5)*f*	2498994.8162	0.4
		R(2.5)*e*	3521860.9787	0.5
		R(2.5)*f*	3529158.1178	-2.4
		R(3.5)*e*	4563705.3668	20.6
		R(3.5)*f*	4573946.5521	9.6
F_2	F_2	R(0.5)*e*	1821937.1491	-16.1
		R(0.5)*f*	1825015.7436	3.6
		R(1.5)*e*	3015366.7157	-15.2
		R(1.5)*f*	3015788.0133	14.4
		R(2.5)*f*	4181129.7134	-23.6
		R(2.5)*e*	4183703.7770	4.3
F_2	F_1	P(1.5)*e*	3787812.9186	15.5
		P(2.5)*e*	3115053.6445	-1.1
		P(2.5)*f*	3116911.2610	18.6
		P(3.5)*f*	2603541.1564	35.3

[a]MHz unit.

[b]$\delta = (\nu_{obs.} - \nu_{calc.}) \times 10^3$.

[c]The first letters indicate type of transition for ΔJ, number in parentheses denotes the J value of the lower state, and the last letter *e* or *f* denotes the parity of the level.

Table 4 - 2 - 4

Molecular constants of ^{18}OH in the $X^2\Pi$ state[a]

Constants	v = 0	v = 1	v = 2	v = 3
T_v	0.0	3558.38843(23)	6952.25712(33)	10183.51341(58)
A_v	-139.0717464(25)	-139.33990(39)	-139.60514(54)	-139.86132(87)
B_v	18.42917785(54)	17.724499(36)	17.029125(55)	16.34050(11)
D_v x10^4	18.90701(64)	18.553(13)	18.233(23)	17.941(47)
H_v x10^6	0.1399(22)	0.155(13)	0.188(26)	0.212(61)
γ_v[b]x10	-0.206137(28)	-0.19326(94)	-0.1852(15)	-0.1752(24)
γ_{Dv}[b]x10^5	0.455(15)			
p_v	0.19557419(18)	0.18631(13)	0.17703(19)	0.16758(35)
p_{Dv}x10^5	-0.7996(66)	-0.61(30)	1.35(51)	2.91(98)
q_v x10	-0.38263850(81)	-0.36624(23)	-0.34930(38)	-0.33229(76)
q_{Dv}x10^4	0.14454(12)	0.1571(39)	0.1673(70)	0.193(16)
q_{Hv}x10^8	0.236(18)			

[a]cm^{-1} unit. The numbers in parentheses denote one standard deviation and apply to the last digits of the constants.

[b]Effective constants. The fit was performed with the constant A_D constrained to zero.

Table 4 - 2 - 5

Equilibrium values of OH in the $X^2\Pi$ state[a]

Constants	^{18}OH	^{16}OH[b]
ω_e	3724.7360(14)	3737.114(27)
$\omega_e x_e$	83.69032(98)	82.264(17)
$\omega_e y_e$	0.31789(18)	0.3243(28)
B_e	18.78580(11)	18.9091(22)
α_e	0.71643(32)	0.7197(62)
γ_e x10^2	0.657(21)	0.42(34)
δ_e x10^3	0.425(37)	
D_e x10^2	0.19052(43)	0.1930(21)
β_e x10^4	-0.32(12)	-0.32(57)
H_e x10^6	0.174(48)	0.142(51)
A_0	-138.9427(11)	-139.09(31)
A_1	-0.2634(32)	-0.25(85)
p_0	0.20028(39)	0.225(59)
p_1 x10^2	-0.93(11)	
p'_0 x10^4	-0.102(98)	
q_0 x10^1	-0.39121(75)	-0.398(21)
q_1 x10^2	0.168(21)	0.16(54)
q'_0x10^4	0.135(14)	0.144(70)
q'_1x10^5	0.15(39)	
γ_0 x10^1	-0.2101(30)	
γ_1 x10^2	0.101(84)	

[a]cm^{-1} unit. The numbers in parentheses denote one standard deviation, and apply to the last significant digits.

[b]Determined from the molecular constants determined by Maillard, Chauville, and Mantz (1976).

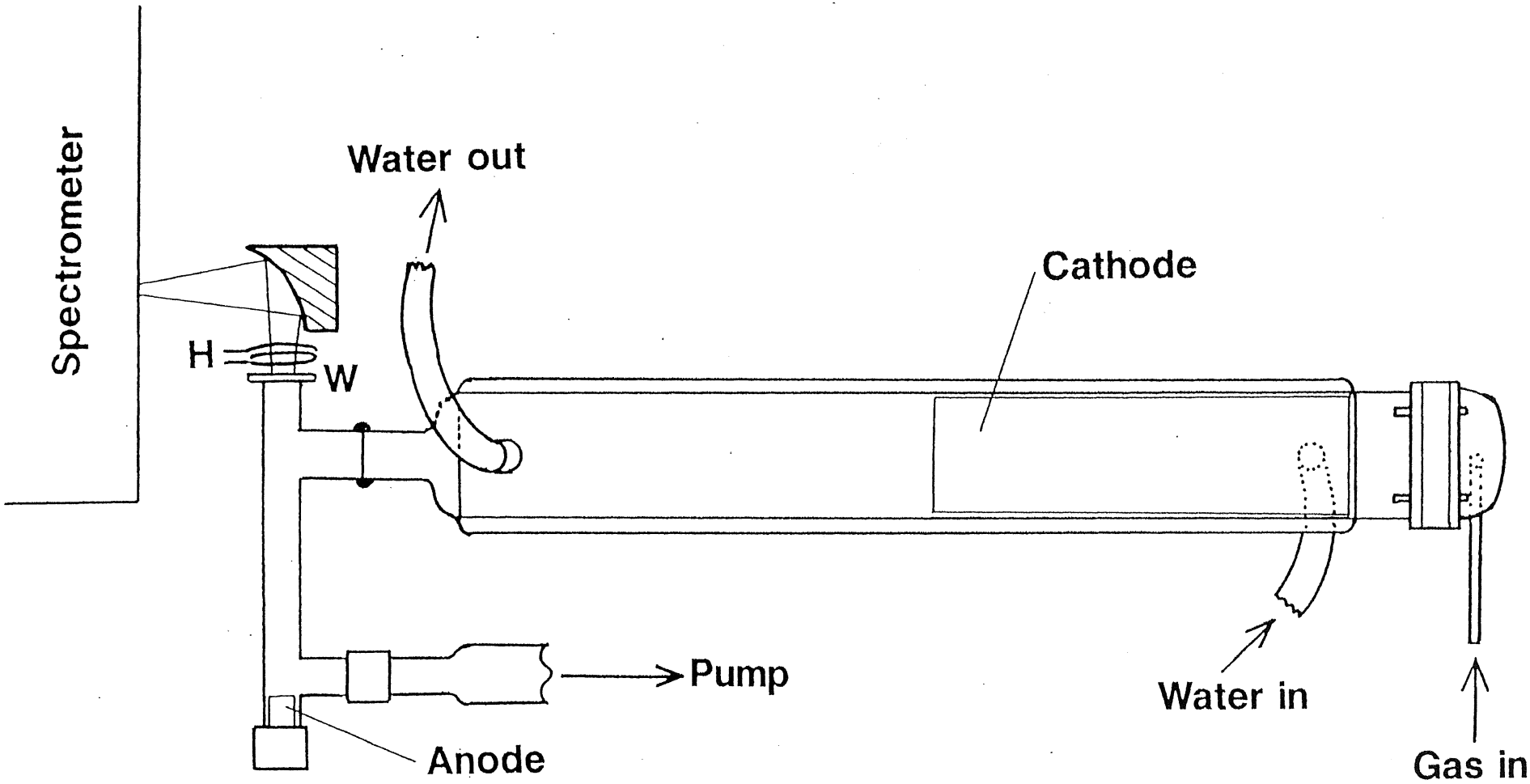

Figure 4 - 2 - 1. Schematic diagram of the emission dc discharge cell. H is a Heater, and W is CaF_2 window.

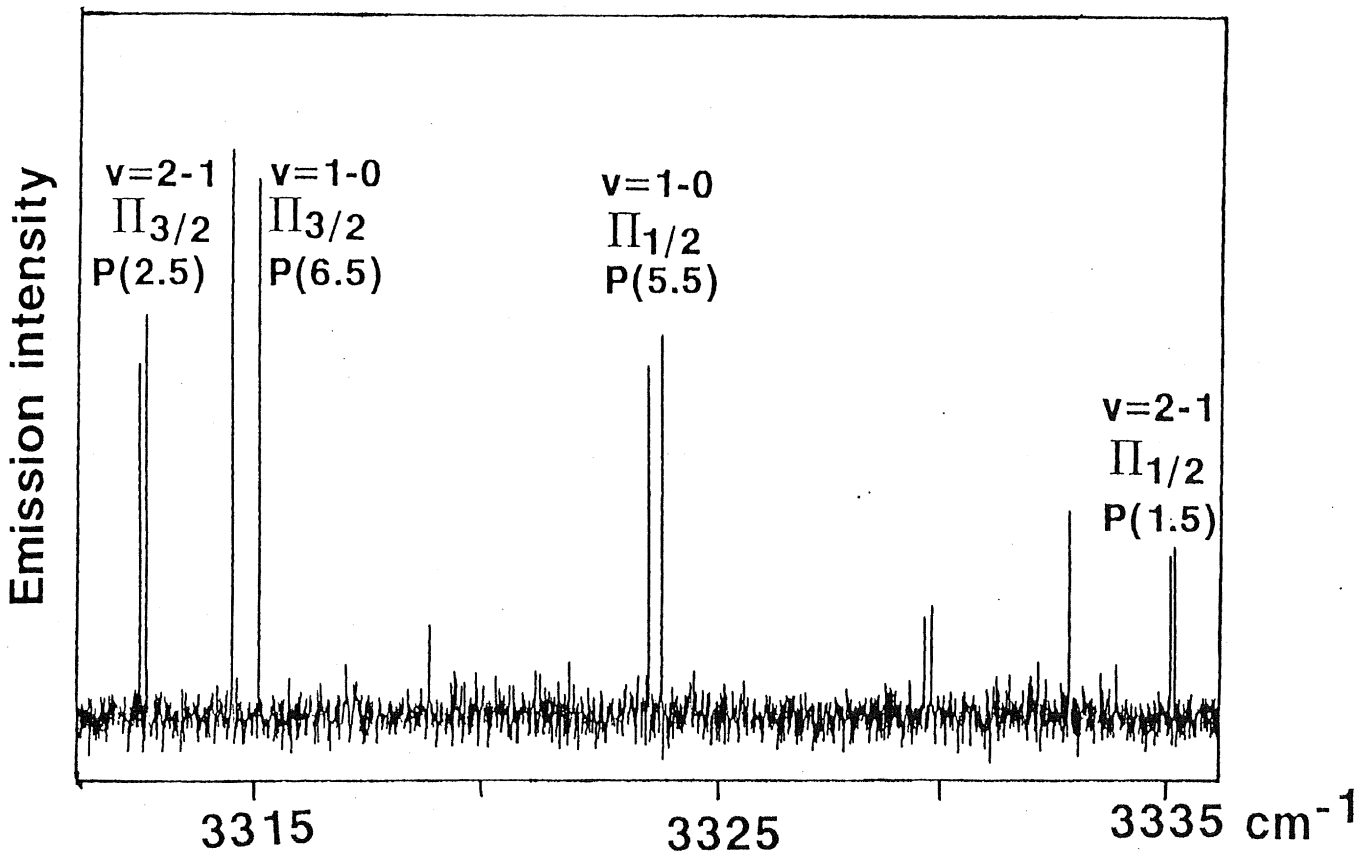

Figure 4 - 2 - 2. Observed emission spectrum of *P*-branch transitions of the ^{18}OH radical in the $X^2\Pi$ state.

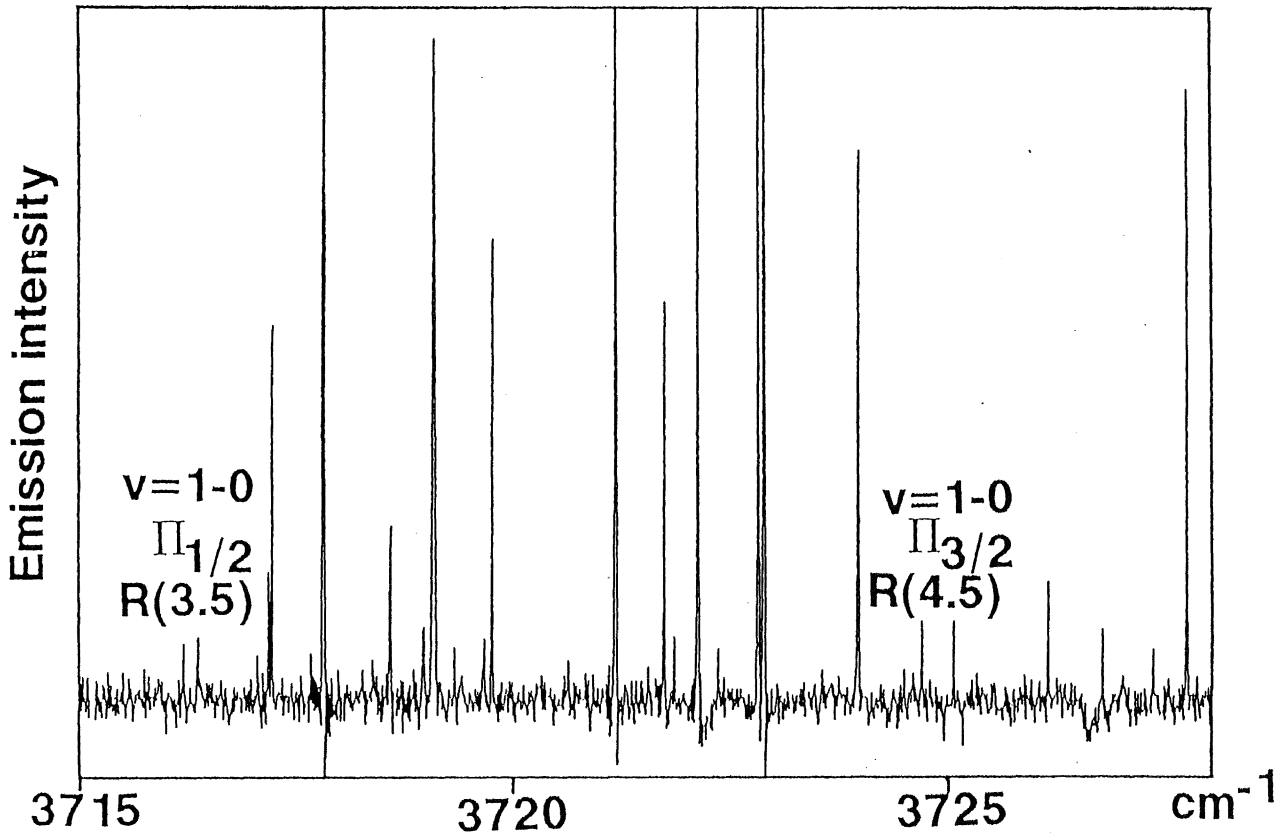

Figure 4 - 2 - 3. Observed emission spectrum of *R*-branch transitions of the ^{18}OH radical in the $X^2\Pi$ state. Strong emission lines are due to $H_2{}^{18}O$, and broad absorption is due to $H_2{}^{16}O$ in air between a discharge cell and a Fourier transform spectrometer.

Chapter 5. Application to Astronomical observations

Abstract

The SH $J = 1.5 - 0.5$ transition was not found in the observed spectrum toward Orion-KL using the Caltech Submillimeter Observatory 10.4 m telescope combined with a Fourier transform spectrometer. The upper limit of the column density was estimated from the observed spectral data to be $< 5.5 \times 10^{18}$ cm^{-2}. The column density of CH in the C-type late star TX Psc was derived by using the vibrational transition moment determined in the present study. The rotational lines of NHD were not found in the observed spectral line survey data in the 70 - 115, 150 - 160, 247 - 273, and 330 - 360 GHz toward Orion-KL and in the 70 - 143 and 330 - 355 GHz toward Sgr B2. The upper limit of the column density was estimated to be $< 2.6 \times 10^{17}$ cm^{-2} in Sgr B2.

5 - 1. Investigation of SH in Submillimeter Wave Spectrum Observed toward Orion-KL

It is important to search for the rotational spectrum of the SH radical to understand hydrogen sulfide chemistry, as already described in Chapter 1. Far-infrared (FIR) Fourier transform (FT) measurement of SH is described in Chapter 3, and it makes possible to predict the submillimeter transition frequencies accurately.

Based on the present study, Klisch *et al.* (1995) recently measured the rotational spectrum of the $J = 1.5 - 0.5$ transition in the $^2\Pi_{1/2}$ state using a BWO spectrometer. The observed frequencies measured by them are listed in Table 5 - 1 with calculated frequencies using the molecular constants in the present study. The agreement is within a standard deviation, and this indicates that the measurement and analysis of SH by the FIR-FT study are accurate enough for prediction of submillimeter wave transition frequencies.

There is an atmospheric window around 850 GHz region open to astronomical observations. Figure 5 - 1 shows the millimeter and submillimeter zenith atmospheric transmission at Mauna Kea at an altitude of about 4200 m, with 1 mm precipitable water (Serabyn and Weisstein, 1995). In the 850 GHz region the transmission is about 46 % and search for the rotational transition of SH seems to be more suitable than in other frequency region. The energy level diagram of the lower rotational levels of SH is shown in Figure 5 - 2. Although the transition in 850 GHz region is not the best one because of the small numbers of population compared with the other $^2\Pi_{3/2}$ transitions, the lowest transition frequency of the $^2\Pi_{3/2}$ state in 1400 GHz region is impossible to observe from the ground based telescopes because of strong water vapor absorption.

Recently, Serabyn and Weisstein (1995) observed the millimeter and submillimeter emission spectrum of the Orion molecular cloud core using the Caltech Submillimeter Observatory (CSO) 10.4 m telescope combined with a FT spectrometer. The spectrum covers the region from 190 to 900 GHz, with some discontinuity due to strong absorption by water. The frequency resolution is 206 MHz that corresponds to a velocity resolution of about 70 km/s at 850 GHz. The beam size (FWHM) is about 30" at 850

GHz. The scan length of the FT spectrometer is about 1 m, and millimeter and submillimeter radiation is detected by a bolometer with the equivalent heterodyne noise temperature of 26,000 K, which is roughly 2 order of magnitude higher than current SIS receiver. The position observed by them is IRc 2($\alpha = 5^h32^m47^s$, δ = -5°24'24"), the core of the well-known Orion molecular cloud. Toward this position, Minh *et al.* (1990) observed the $1_{10} - 1_{01}$ transition (168 GHz) of H_2S with $T_A^* \sim 0.39$ K , which gives the column density of 5 x 10^{18} cm^{-2}, FHWM of 12 km/s, and $T_{rot} \sim 200$ K. Its source diameter was found to be $\theta_s \sim 3$". In the FT spectrum of CSO, the $J = 1.5 - 0.5$ transition of SH was not found, as shown in Figure 5 - 3, and the upper limit of the column density of SH was determined from the noise level of $T_A^* \sim 0.2$ K.

In the estimation of the column density of SH, the local thermodynamic equilibrium (LTE) approximation was adopted. The observed temperature was analyzed using the following formula (Rohlfs, 1990):

$$T_R = [J_\nu(T_{ex}) - J_\nu(T_{bg})][1 - \exp(-\tau)], \quad (1)$$

where $J_\nu(T) = (h\nu/k)[\exp(h\nu/kT) - 1]^{-1}$, T_{ex} and T_{bg} are the excitation temperature and the cosmic background temperature (2.7 K), respectively, and ν the transition frequency. The optical depth τ is related to the column density as follows,

$$\tau = \frac{8\pi^3\mu^2 SN}{3h\Delta\nu Q}\left[\exp(h\nu / kT_{ex}) - 1\right]\exp(-E_U / kT_{ex}), \quad (2)$$

where μ is the dipole moment, S the line strength, N column density, $\Delta\nu$ the line width, E_U the upper state energy of the transition, and Q the partition function. Eq. (1) was directly used for analysis of the observed antenna temperature, where the antenna temperature (T_A^*) was related to brightness temperature (T_R) of molecular transition in the source as follows,

$$T_A^* = T_R \, \eta \, \eta_{BD} \quad (3)$$

where η was the main beam efficiency of telescope, and η_{BD} was the beam dilution correction for a molecular source. Since the main beam efficiency was calibrated for this observation by FT-spectrometer, η was set to be 1. The η_{BD} value is calculated by

$$\eta_{BD} = \theta_S^2/(\theta_B^2 + \theta_S^2), \quad (4)$$

where θ_B is the antenna beam width (FWHM) and θ_S is the source diameter. Since in these case values of θ_B and θ_S were 30" and 3", respectively, the η_{BD} value of 0.01 was used.

The excitation temperature T_{ex} of SH was assumed to be 100 K, which was almost the same as determined for SO and SO_2 in their observation. Using Eq. (1) and (2), the upper limit of the column density of SH was estimated to be 5.5 x 10^{18} cm^{-2}, where μ = 0.758 Debye (Meerts and Dymanus, 1974) and the line width of 206 MHz equal to the resolution of their observation was used. The 2_{02} - 1_{11} transition of H_2S in 687 GHz was observed with the temperature of T_A^* ~ 0.5 K. But since it was overlapped with the transition of SO, the observed antenna temperature was not very accurate. The column density of H_2S was estimated to be 5.4 x 10^{17} cm^{-2}, where the same Eqs. (1) and (2) in the case of H_2S and, μ = 0.934 Debye were used. This result is roughly consistent with the H_2S abundance of 5 x 10^{18} cm^{-2} derived by Minh *et al.* (1990).

This result was not enough for further discussion about the assumption in Chapter 1 due to the low sensitive observation. If the same abundance of SH as H_2S is produced by gas-phase reactions and H_2S in Orion-KL is thought to be produced by dust surface reaction, the column density of SH is expected to be 10^{15} cm^{-2}, which is over three orders of magnitude lower than the upper limit in the FT-observation.

5 - 2. Application to Infrared Absorption Spectrum in TX Psc

In Chapter 4, the vibrational transition moment of the v = 1 - 0 band of CH was determined by intensity analysis using the Herman-Wallis effect. In this Section, the author shows an example of the application to astronomical infrared observation.

Ridgway *et al.* (1984) made an atlas of late-type stellar spectra in the region between 2400 and 2778 cm^{-1}. The observations were carried out using the Kitt Peak National Observatory 4 m telescope combined with a FT spectrometer. The integration time was typically 30 min. They got the atlas of α Ori, α Tau, o Cet, R And, and TX Psc. In TX Psc the vibration rotation spectra of CH and CS were detected, and in other

objects, OH, NH, SiO, and HCl were identified. PX Psc is one of the well studied C-type stars and has a cool envelope. The effective temperature is determined to be 3100 K from a number of lunar occultation and infrared photometry.

In TX Psc, the $N = 3 - 4$ and $2 - 3$ transitions of the CH $v = 1 - 0$ band were observed with absorption of about 30(10) % with three standard deviations in parentheses. The line width (FWHM) was about 0.125 cm^{-1}. Figure 5 - 4 shows the absorption spectrum of the $N = 3 - 4$ transition. From the $v = 1 - 0$ band, the author determined the column density of CH.

The transmission of radiation through a homogenous gas sample is described as follows,

$$I(\nu) = I_0 \exp[-k(\nu)l], \tag{5}$$

where $I(\nu)$ and I_0 are radiation intensity after absorption by gas and source intensity from star, respectively, and l the optical path length. $k(\nu)$ denotes the absorption coefficient and expressed by,

$$k(\nu) = S \cdot f(\nu - \nu_0), \tag{6}$$

S is the line strength for vibration rotation transition, and is given as follows,

$$S = \frac{8\pi^3}{3hc}\frac{N}{Q}\nu\mu^2 S_R F(m)\left[1-\exp(-h\nu / kT)\right]\exp(-E_L / kT), \tag{7}$$

where N is the total number of molecules of the absorbing gas, Q the partition function, ν the transition frequency, μ the vibrational transition moment, S_R Hönl-London factor, E_L the lower state energy of the transition, $F(m)$ the Herman-Wallis factor that is already described in Chapters 1 and 4, and T rotational temperature of molecule. The part of $\left[1-\exp(-h\nu / kT)\right]$ represents the effect of induced emission. In most case, this is equal to be 1. The part of $\exp(-E_L / kT)$ denotes the Boltzmann distribution. The column density N is expressed by $N = nl$, where n is the volume density. The function $f(\nu - \nu_0)$ is the line shape function, which is normalized and in infrared region the Doppler profile is assumed.

The rotational temperature of CH was estimated to be 604 ± 160 K by a Boltzmann plot of the observed 8 vibration-rotation transitions in the $v = 1 - 0$ band. The column density, N of CH in TX Psc was estimated to be $1.3(3) \times 10^{14}$ cm^{-2} with three standard

deviations, adopting the vibration transition moment of -0.190 Debye, as described in Chapter 4.

On the other hand, van Dishoeck and Black (1989) observed the electronic absorption spectrum of the $A^2\Delta$ - $X^2\Pi$ 0 - 0 band of CH in visible region toward diffuse clouds, and determined column density of about 10^{15} cm^{-2} in most diffuse clouds. They used the calculated transition moment, which may have larger uncertainty than that determined by experiment. It is noted that in envelope of the C-type late star CH exists with almost the same column density as diffuse clouds. The rotational excitation temperature is high in the envelope, and the formation of CH seems to be due to chemical equilibrium reaction (Gustafsson, 1989). It is different from that in diffuse cloud where CH is mainly produced by ion-molecule reactions.

5 - 3. Comparison with Spectral Line Survey Data in Orion-KL and Sgr B2 for NHD

Chapter 3 described the observation of far-infrared absorption spectrum of the NHD radical and analysis to obtain molecular constants. Although NHD has not been detected in interstellar space, very strong line intensity of NH_2 and high abundance of deuterated species in interstellar space will make it possible to detect NHD. The author calculated the frequencies of the *a*- and *b*-type transitions. The *a*-type transitions are about an order of magnitude weaker than the *b*-type transitions; the μ_a dipole moment along with the *a*-axis is one third of that of *b*-axis.

It is found that no NHD lines have been detected in the observed spectral line survey data for Orion-KL (Johansson *et al.* 1984; Sutton *et al.* 1985, 1995; Blake *et al.* 1986, 1987; Jewell *et al.* 1989; Turner, 1989, 1991; Greaves and White, 1991; Ziurys and McGonagle, 1993; Harris *et al.* 1995; Serabyn and Weisstein, 1995) and Sgr B2(Cummins, Linke, and Thaddeus, 1986; Turner, 1989, 1991; Sutton *et al.* 1991). The upper limit of the column density of NHD was estimated to be 2.6 x 10^{17} cm^{-2} from noise level T_R ~ 0.5 K in the 3_{30} - 4_{23} 2.5 - 3.5 transition in 355 GHz (Sutton *et al.* 1991), where μ_0 = 1.694 Debye, T_{ex} ~ 100 K, and the line width of 100 MHz were

used. Unfortunately there are no data in 430 GHz region, where the same 1_{10} -1_{01} transition as NH_2 is expected with strong intensity.

If the abundance ratio of [NHD]/[NH_2] is assumed to be equal to that of [HNH_2D]/[NH_3] = 1.7 x 10^{-2} in Sgr B2 (Turner *et al.* 1978), the brightness temperature of the $1_{1\,0}$ -$1_{0\,1}$ transition of NHD in 430 GHz region is estimated to be -0.17 K, which is high enough for detection. Similarly, in Orion hot core the estimated brightness temperature is roughly 1.1 K.

5 - 4. Interstellar Molecules in Future Submillimeter and Infrared Astronomy

At present, submillimeter astronomical observations up to 1000 GHz are carried out using ground based 10 m class telescopes such as the Caltech Submillimeter Observatory (CSO) 10.4 m telescope at Mauna Kea that is applied for detection of new interstellar molecules like as NH_2 (van Dishoeck *et al.* 1993). A 0.9 m telescope of Kuiper Airborne Observatory (KAO) is using for observations in higher frequency region than 1000 GHz. Recently, high sensitive submillimeter interferometers such as Large Millimeter and Submillimeter Array (LMSA) (Ishiguro, 1995) are proposed to construct. If submillimeter observations using a LMSA become possible, identifications of new light molecules such as hydrides will be greatly improved in interstellar space. They provide complimentary information to interstellar chemistry obtained in millimeter-wave observations. For example, the following molecules have pure rotational transitions below 1000 GHz and are expected to have detectable abundances in space, but not yet observed so far: AlH (Goto and Saito, 1995), CaH (Frum *et al.* 1993; Barclay, Anderson, and Ziurys, 1993), MgH (Zink *et al.* 1990; Ziurys, Barclay, and Anderson, 1993), NaH (Sastry, Herbst, and De Lucia, 1981; Leopold *et al.* 1987), PH (Goto and Saito, 1993), SH (this work; Klisch *et al.* 1995), and SiH (Brown, Curl, and Evenson, 1985).

Infrared astronomical observations are carried out using ground based 3 - 4 m class telescopes and more than 20 species of interstellar molecules were discovered in

absorption through vibration-rotation transitions. Recently, larger telescopes with 8 - 10 m diameter are under construction, and by infrared observations many molecules will be identified. Especially molecules with no permanent dipole moment such as H_2, CH_4, and C_2H_2 can be observed through vibration-rotation transitions. Infrared observations also provide deeper understanding of chemistry and physics in relatively warmer interstellar space.

However, information about frequency and intensity of molecules of astronomical interest are limited. Although ion-molecule reactions and neutral-neutral reactions are relatively well studied in laboratory, branching ratios in recombination reactions with electron and roles of dust surface in molecular formation mechanisms are not still clear (Irvine, Goldsmith, and Hjalmarson, 1986). Rate coefficients of molecular formation reactions in conditions with very low temperature and density are should be studied deeply. Laboratory experiments and quantum chemical calculations are needed for clarifying these molecular reaction mechanism.

References

Barclay, Jr. W. L., Anderson, M. A., and Ziurys, L. M. 1993, Astrophys. J. **408,** L65.

Blake, G. A., Sutton, E. C., Masson, C. R., and Phillips, T. G. 1986, Astrophys. J. Suppl. **60,** 357.

_____. 1987, Astrophys. J. **315,** 621.

Brown, J. M., Curl, R. F., and Evenson, K. M. 1985, Astrophys. J. **292,** 188.

Cummins, S. E., Linke, R. A., and Thaddeus, P. 1986, Astrophys. J. Suppl. **60,** 819.

Frum, C. I., Oh, J. J., Cohen, E. A., and Pickett, H. M. 1993, Astrophys. J. **408,** L61.

Goto, M. and Saito, S. 1993, Chem. Phys. Lett. **211,** 443.

_____. 1995, Astrophys. J. **452,** L147.

Greaves, J. S. and White, G. J. 1991, Astron. Astrophys. Suppl. **91,** 237.

Gustafsson, B. 1989, Annu. Rev. Astron. Astrophys. **27,** 701.

Harris, A. I., Avery, L. W., Schuster, K. -F., Tacconi, L. J., and Genzel, R. 1995, Astrophys. J. **446,** L85.

Irvine, W. M., Goldsmith, P. F., and Hjalmarson, Å. 1986, "*Interstellar Processes,*" D. Reidel Publishing Co. Vol. **134,** P. 561.

Ishiguro, M., 1995, "*CO: Twenty-five Years of Millimeter-wave Spectroscopy,*" the Proceedings of the IAU Symposium No. 170, Tucson, Arizona, USA.

Jewell, P. R., Hollis, J. M., Lovas, F. J. and L. E. Snyder, 1989, Astrophys. J. Suppl. **70,** 833.

Johansson, L. E. B., Andersson, C., Elldér, J., Friberg, P., Hjalmarson, Å., Högund, B., Irvine, W. M., Olofsson, H., and Rydbeck, G. 1984, Astron. Astrophys. **130,** 227.

Klisch, E., Klaus, Th, Belov, S. P., Winnewisser, G., and Herbst, E. 1995, in preparation.

Leopold, K. R., Zink, L. R., Evenson, K. M., and Jennings, D. A. 1987, J. Mol. Spectrosc. **122,** 150.

Mattila, K. 1986, Astron. Astrophys. **160,** 157.

Meerts, W. L. and Dymanus, A.1974, Astrophys. J. **187,** L45.

Minh, Y. C., Irvine, W. M., and Ziurys, L. M. 1989, Astrophys. J. **345,** L63.

Minh, Y. C., Ziurys, L. M., Irvine, W. M., and McGonagle, D. 1990, Astrophys. J. **360,** 136.

_____. 1991, Astrophys. J. **366,** 192.

Ridgway, S. T., Carbon, D. F., Hall, D. N. B., and Jewell, 1984, J. Astrophys. J. Suppl. **54,** 177.

Rohlfs, K. 1990, "*Tools of Radio Astronomy*," Springer, Berlin.

Sastry, K. V. L. N., Herbst, E., and De Lucia, F. C., 1981, Astrophys. J. **248,** L53.

Serabyn, E. and Weisstein, E. W. 1995, Astrophys. J. **451,** 238.

Sutton, E. C., Jaminet, P. A., Danchi, W. C., and Blake, G. A. 1991, Astrophys. J. **77,** 255.

Sutton, E. C., Peng, R., Danchi, W. C., Jaminet, P. A., Sandell, G., and Russell, A. P. G. 1995, Astrophys. J. Suppl. **97,** 455.

Sutton, E. C., Blake, G. A., Masson, C. R., and Phillips, T. G. 1985, Astrophys. J. Suppl. **58,** 341.

Turner, B. E. 1989, Astrophys. J. Suppl. **70,** 539.

_____. 1991, Astrophys. J. Suppl. **76,** 617.

Turner, B. E., Zuckerman, B., Morris, M., and Palmer, P. 1978, Astrophys. J. **219,** L43.

van Dishoeck, E. F., Jansen, D. J., Schilke, P., and Phillips, T. G. 1993, Astrophys. J. **416,** L83.

van Dishoeck, E. F. and Black, J. H. 1989, Astrophys. J. **340,** 273.

Zink. L. R., Jennings, D. A., Evenson, K. M. and Leopold, K. R., 1990, Astrophys. J. **359,** L65.

Ziurys, L. M., Barclay, Jr., W. L., and Anderson. M. A. 1993, Astrophys. J. **402,** L21.

Ziurys, L. M. and McGonagle, D. 1993, Astrophys. J. Suppl. **89,** 155.

Table 5 - 1

Observed and calculated frequencies of the $J = 1.5 - 0.5$ transition of the SH radical[a]

Parity	Observed with BWO[b]	Calculated from this work
- ← +	866949.93(87)[c]	866949.3(4.5)[d]
+ ← -	875266.727(80)	875268.8(4.5)

[a]MHz unit.

[b]Observed by Klisch *et al.* (1995) and corrected for the hyperfine structure.

[c]The numbers in parentheses denote uncertainty in units of the last quoted digits.

[d]The numbers in parentheses denote calculated uncertainty in units of the last quoted digits.

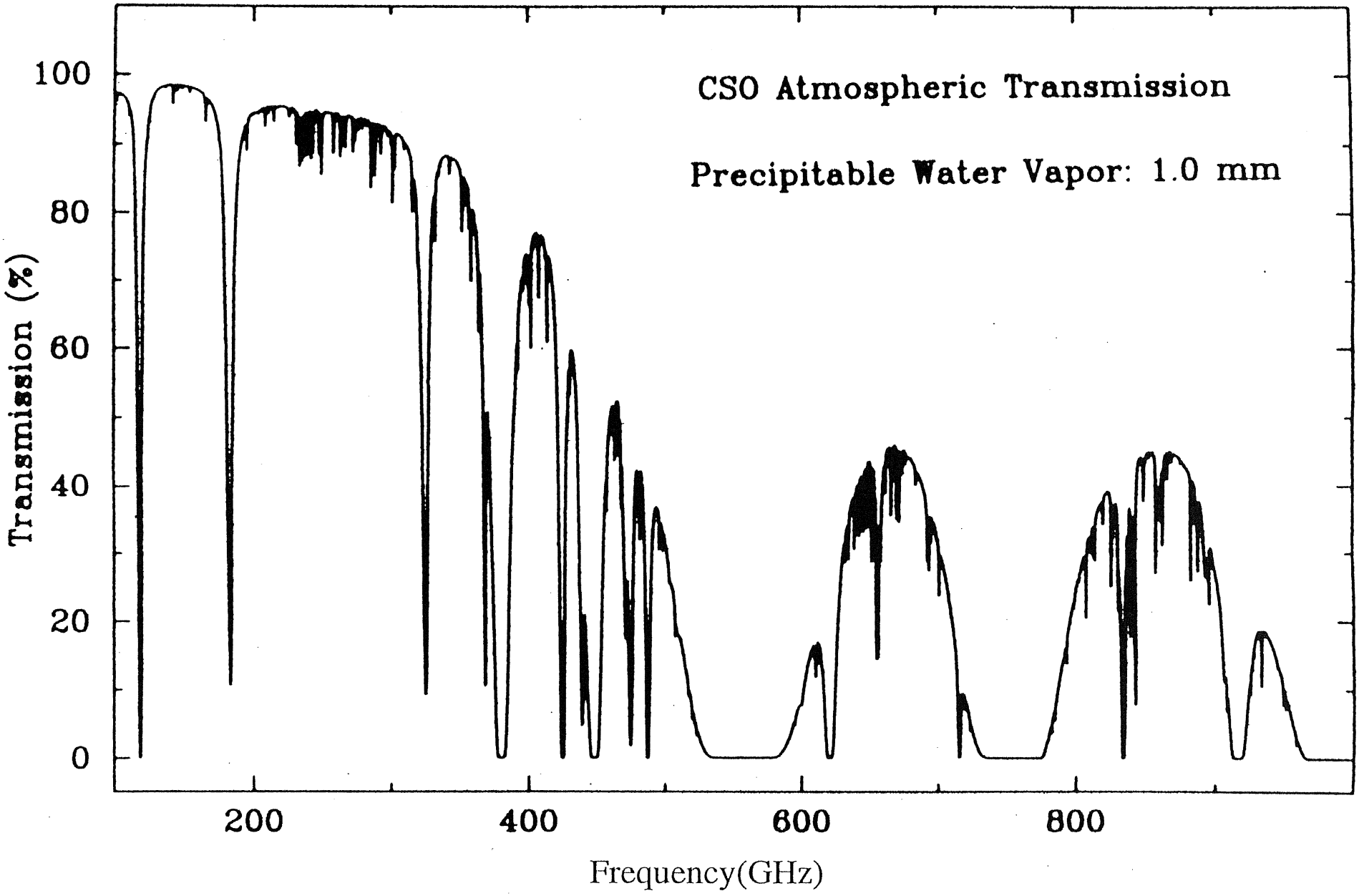

Figure 5 - 1. Theoretical zenith atmospheric transmission at Mauna Kea from Serabyn and Weisstein (1995).

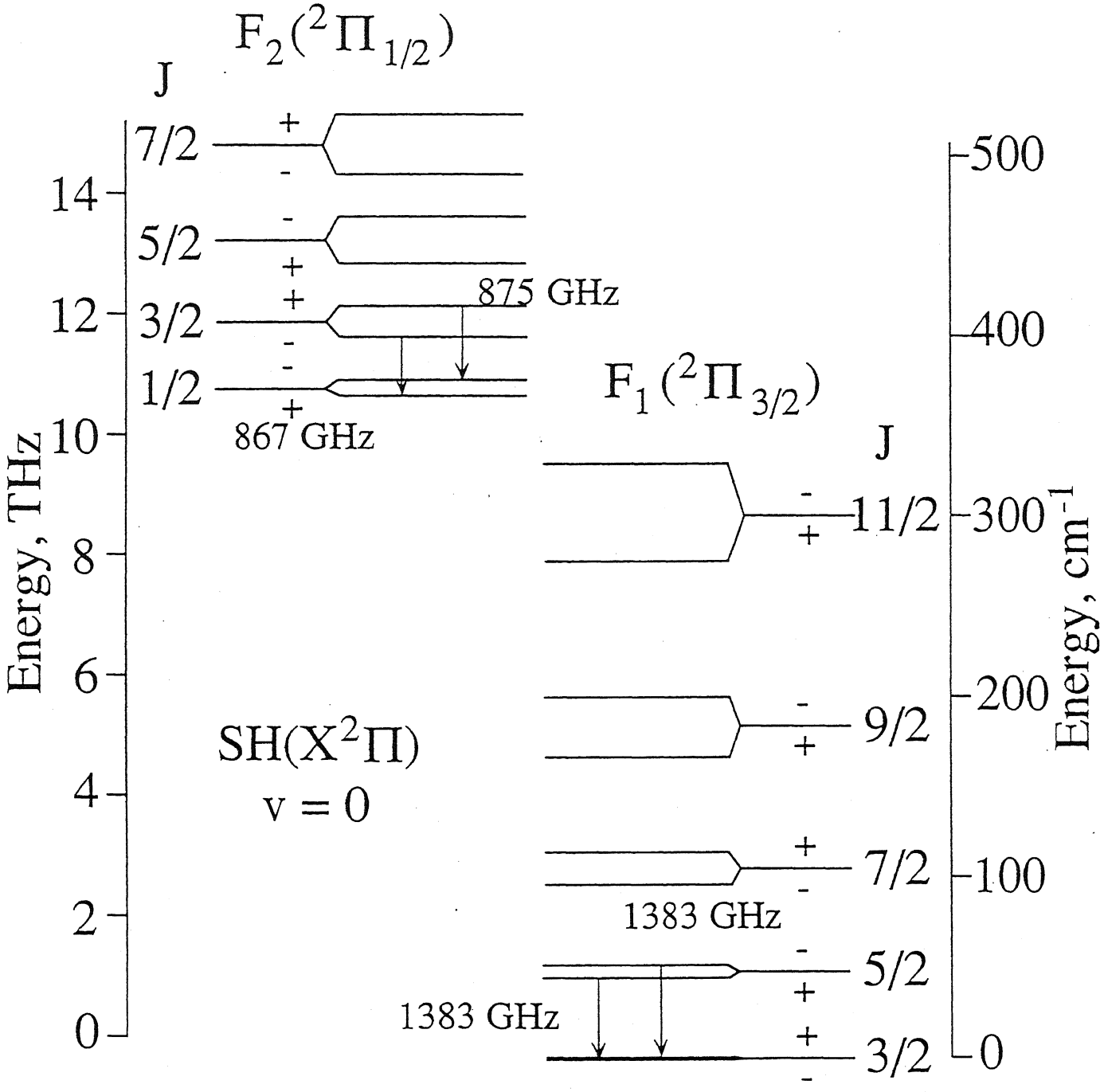

Figure 5 - 2. Energy diagram showing the lower rotational levels of the SH radical in the $X^2\Pi$ state. The Λ-type doubling is exaggerated by a factor 4000 for the F_1 state and 300 for F_2 for clarity.

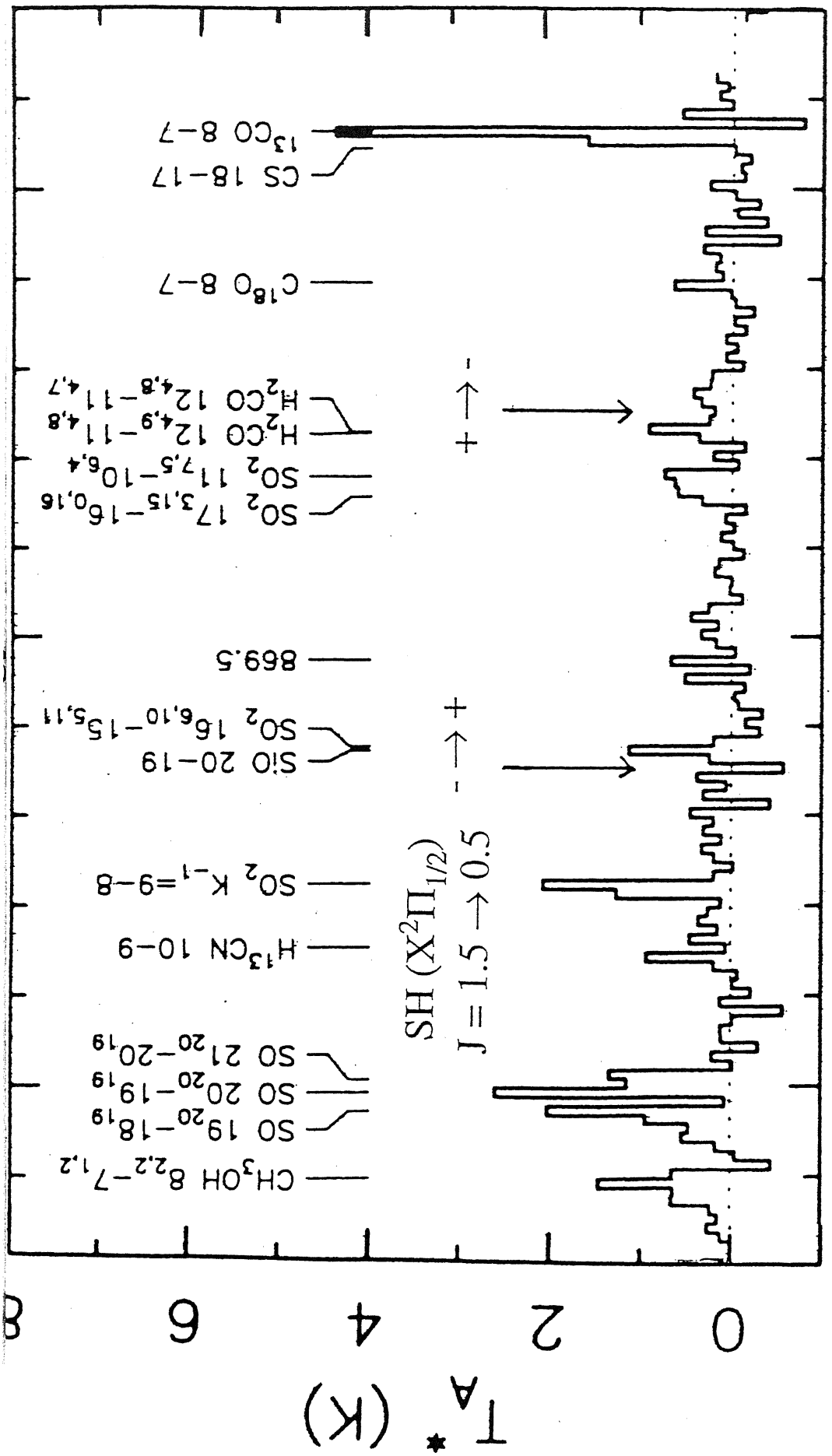

Figure 5 - 3. Observed spectrum in Orion IRc2 between 854 and 884 GHz, with lines identification from Serabyn and Weisstein (1995). The spectrum was observed by the CSO 10.4 m telescope combined with a FT spectrometer.

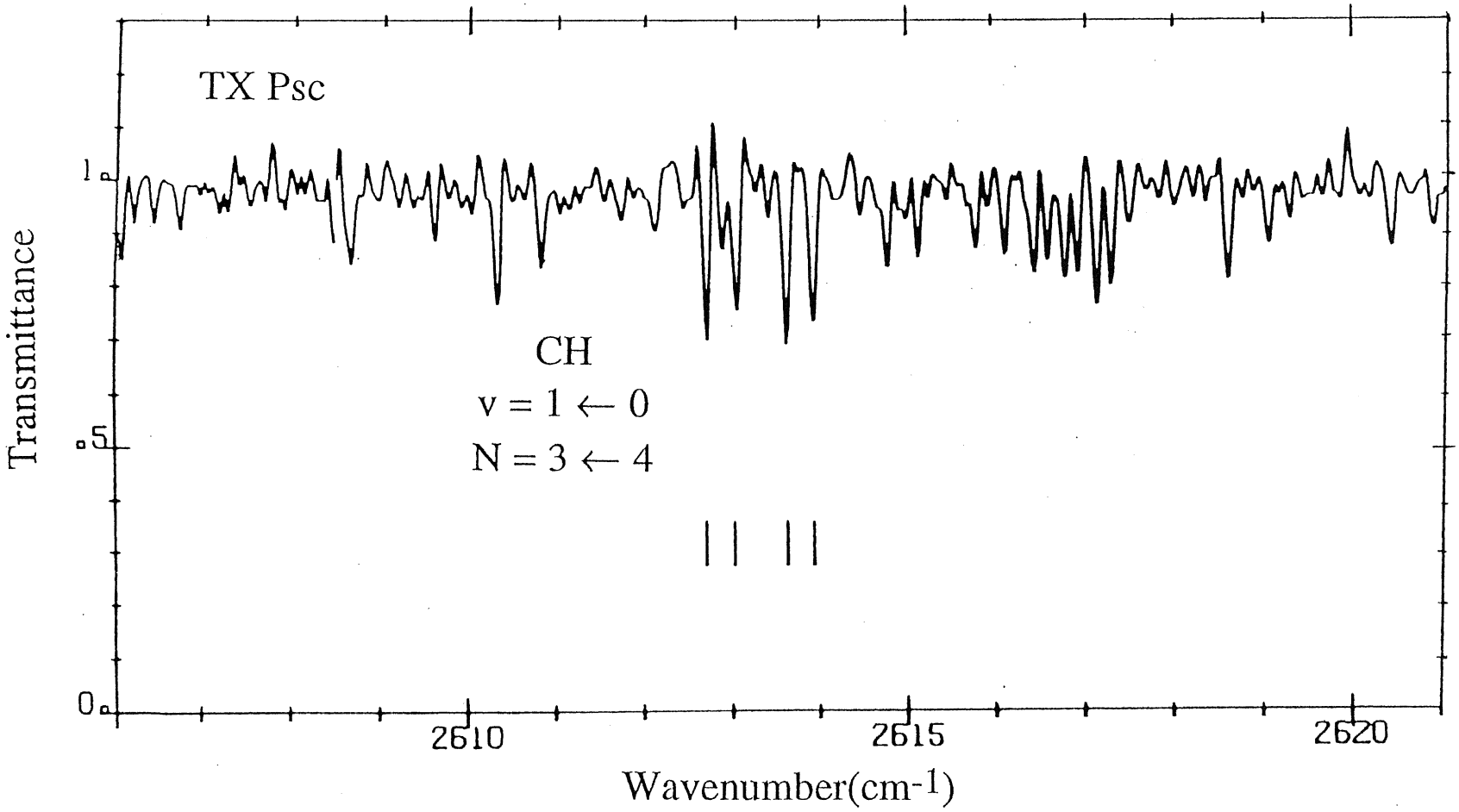

Figure 5 - 4. Observed infrared absorption spectrum in TX Psc, corrected for telluric transmission (Ridgway *et al.* 1984). The spectrum was observed by the Kitt Peak 4 m telescope combined with a FT spectrometer and the integration time of 30 min.

Summary

Since molecular observations in interstellar space have very important role to understand physical conditions - density and temperature - and production mechanisms of molecules, many molecules are studied in laboratory and in astronomical observation. A lot of information in interstellar space has been mainly obtained by millimeter-wave astronomical observations, but in millimeter wave region relatively heavy molecules have their rotational transitions. Observations of small molecules such as hydrides are limited, although they are important to understand the production mechanism related hydrogen compounds. Most of hydrides have rotational transitions in submillimeter-wave or far-infrared region. Recently, the astronomical observation techniques in submillimeter-wave, far-infrared, and infrared regions are greatly developed, and the observations in these regions become possible. However, there are a few laboratory data for molecules in these regions. In the present study, far-infrared and infrared Fourier transform spectroscopy was applied to measure transient molecules of astronomical interest in laboratory and the results were applied to astronomically observed data.

The dc discharge cell with multi-reflection system was constructed for far-infrared absorption measurement. The author applied to observe the pure rotational spectra of the SH, NH_2, NHD, and ND_2 radicals and the vibration rotation spectrum of NH_2OH. The measurement of SH was the first application of far-infrared Fourier transform spectroscopy to transient molecules, and detection limit of this measurement system was estimated. About 600 rotational lines of NH_2, NHD, ND_2 and about 5000 rovibrational lines of NH_2OH were observed in high-resolution and wide frequency coverage. By the analysis of the observed spectra, precise molecular parameters were obtained. The information obtained by these measurements is very useful for sub-millimeter and far-infrared astronomical observation.

The positive column discharge cell was constructed for infrared emission observation. The author applied to measure the vibration rotational spectra of the CD and ^{18}OH radicals. By analysis, precise molecular constants in the vibrationally excited states

were obtained. From intensity analysis using Herman-Wallis effect, the vibration transition moment of CH was determined, and applied to determination of column density in infrared astronomical observation. The observed intensity of ^{18}OH was discussed.

Some result of laboratory spectroscopy were applied to astronomical observational results. The upper limit of column density of SH was estimated from the submillimeter-wave emission spectrum in Orion-KL. For clarifying the production mechanism of SH_n, it is clear that more deep search for SH is necessary. Using the transition moment of CH in this study, the column density of CH was determined from infrared absorption spectrum in late-type star TX Psc. The author found that the column density in envelope of C-type late star was almost same as diffuse cloud. The rotational spectrum of NHD was not found in the published millimeter and submillimeter line survey data in Orion-KL and Sgr B2.

Acknowledgments

The author would like to express his science and technical gratitude to Associate Professor Dr. Kentarou Kawaguchi for his helpful guidance and suggestion about this thesis. The author also thanks Professor Drs. Junji Inatani and Norio Kaifu for their helpful suggestions. Without their kind helpfulness, this study would have never been achieved.

The author is also very grateful to Professor Dr. Keiji Matsumura of Seinan Gakuin University, Dr. Benjamin Hanoune of Universite des Sciences et Techniques de Lille, and Professor Dr. Kojiro Takagi of Toyama University for helpful discussions for this study. The author expresses to thank to Professor Dr. Takayosihi Amano of Ibaraki University for discussion for observed spectrum of the SH radical. The author thanks Professor Dr. Gisbert Winnewisser of Universität zu Köln for information of the measured frequencies of SH using a BWO spectrometer. The author is grateful to Dr. Masatoshi Ohishi for helpful suggestion.

He thanks Mr. Tetsuya Mori of Bruker Japan Co. Ltd. for his terrible support throughout Fourier transform spectrometer, Dr. Hiroshi Matsuo for a helpful suggestion with regard to the adjustment of the Si composite bolometer, and Associate Professor Dr. Fusakazu Matsushima and Dr. Hitoshi Odashima of Toyama University for an offer of polypropylene sheet as far-infrared window. Also, thanks have been appeared to all members of Nobeyama Radio Observatory for great support and encouragement.

The author gives his applicant to his parents for encouragement, care, and support for this study.